PTN COL 2.5-2

Table 2.5.2-224 (Sheet 2 of 3) Percent Contribution to Deaggregation

Percent Contribution to Low-Frequency Deaggregation for 1E-05								
	Percent Contribution By Moment Magnitude [M] — Distance [R, km] Bin							
R \ M	5.25	5.75	6.25	6.75	7.25	7.75	8.25	8.75
0–20	12.15	3.879	1.943	0.2549	0.08261	9.658E-3	1.464E-19	1.464E-19
20–40	3.472	3.102	2.368	0.4021	0.1452	0.01803	1.866E-19	1.866E-19
40–60	0.7056	1.364	1.664	0.3581	0.1528	0.01961	2.652E-19	2.652E-19
60–80	0.2055	0.5543	0.9977	0.2854	0.1481	0.02069	2.418E-19	2.418E-19
80–100	0.08325	0.3335	0.6990	0.2373	0.1433	0.02116	2.153E-19	2.153E-19
100–210	0.1133	0.6144	1.742	0.7683	0.6158	0.1023	4.922E-19	4.922E-19
210–330	6.898E-3	0.1182	1.198	5.745	4.268	0.04352	2.548E-19	2.548E-19
>330	1.738E-4	7.247E-3	0.1672	3.428	28.87	15.48	0.8831	8.244E-3

Percent Contribution to High-Frequency Deaggregation for 1E-05								
	Percent Contribution By Moment Magnitude [M] — Distance [R, km] Bin							
R \ M	5.25	5.75	6.25	6.75	7.25	7.75	8.25	8.75
0–20	40.80	6.066	2.324	0.2676	0.08196	9.276E-3	1.094E-19	1.094E-19
20–40	15.35	5.979	3.210	0.4532	0.1469	0.01742	1.475E-19	1.475E-19
40–60	3.048	2.545	2.122	0.3819	0.1490	0.01923	2.246E-19	2.246E-19
60–80	0.8306	0.9665	1.146	0.2708	0.1341	0.01861	2.141E-19	2.141E-19
80–100	0.3785	0.6072	0.8052	0.2195	0.1229	0.01816	1.993E-19	1.993E-19
100–210	0.5505	1.159	1.927	0.6413	0.4498	0.07458	4.284E-19	4.284E-19
210–330	0.01752	0.1130	0.6067	1.879	1.253	0.02071	1.728E-19	1.728E-19
>330	2.546E-4	3.359E-3	0.03420	0.3020	2.390	0.09811	8.617E-4	6.446E-7

PTN COL 2.5-2

Table 2.5.2-224 (Sheet 3 of 3) Percent Contribution to Deaggregation

Percent Contribution to Low-Frequency Deaggregation for 1E-06								
	Percent Contribution By Moment Magnitude [M] — Distance [R, km] Bin							
R \ M	5.25	5.75	6.25	6.75	7.25	7.75	8.25	8.75
0–20	19.29	13.59	10.37	1.814	0.7091	0.08862	1.680E-18	1.680E-18
20–40	1.613	4.002	6.005	1.678	0.9085	0.1309	1.744E-18	1.744E-18
40–60	0.1375	0.8059	2.227	0.8867	0.6630	0.1078	2.006E-18	2.006E-18
60–80	0.02297	0.1897	0.8379	0.4697	0.4684	0.08811	1.618E-18	1.618E-18
80–100	6.569E-3	0.08325	0.4397	0.2939	0.3611	0.07376	1.354E-18	1.354E-18
100–210	6.415E-3	0.1091	0.7689	0.6570	1.050	0.2427	2.846E-18	2.846E-18
210–330	1.432E-4	7.221E-3	0.1538	1.234	1.759	0.06449	1.203E-18	1.203E-18
>330	1.425E-6	2.598E-4	0.01353	0.9716	21.14	3.306	0.1628	7.440E-4

Percent Contribution to High-Frequency Deaggregation for 1E-06								
	Percent Contribution By Moment Magnitude [M] — Distance [R, km] Bin							
R \ M	5.25	5.75	6.25	6.75	7.25	7.75	8.25	8.75
0–20	53.64	17.36	9.988	1.553	0.5884	0.07252	1.248E-18	1.248E-18
20–40	3.143	3.754	4.109	1.060	0.5958	0.08899	1.408E-18	1.408E-18
40–60	0.1753	0.4668	0.9073	0.3421	0.3022	0.05753	1.586E-18	1.586E-18
60–80	0.02240	0.07983	0.2270	0.1166	0.1499	0.03383	1.176E-18	1.176E-18
80–100	6.819E-3	0.03427	0.1105	0.06464	0.09602	0.02359	9.290E-19	9.290E-19
100–210	6.744E-3	0.04374	0.1743	0.1210	0.2085	0.05592	1.688E-18	1.688E-18
210–330	5.549E-5	9.710E-4	9.667E-3	0.03550	0.05705	6.170E-3	4.768E-19	4.768E-19
>330	1.102E-7	1.140E-5	2.378E-4	2.641E-3	0.1054	8.841E-4	3.100E-19	3.100E-19

PTN COL 2.5-2

Table 2.5.2-225
Controlling Magnitudes and Distances from Deaggregation

Struct. Frequency	Annual Freq. Exceed.	Overall Hazard		Hazard from R > 100 km	
		M	R, km	M	R, km
1 & 2.5 Hz	1E-04	7.1	400	7.3	570
5 & 10 Hz	1E-04	5.9	110	6.5	290
1 & 2.5 Hz	1E-05	6.7	190	7.2	560
5 & 10 Hz	1E-05	5.5	31	6.7	250
1 & 2.5 Hz	1E-06	6.3	61	7.2	600
5 & 10 Hz	1E-06	5.5	17	6.9	180

Notes:
Shaded cells indicate values used to construct UHRS
"M" is moment magnitude; "R" is epicentral distance

PTN COL 2.5-2

Table 2.5.2-226
Assigned Strong Motion Durations in P-SHAKE

Set of Runs	Description	Recurrence	Input Rock Spectra	
			Moment Magnitude	Duration [sec]
LF4	Low Freq.	1E-04	7.3	13
HF4	High Freq.	1E-04	5.9	6
LF5	Low Freq.	1E-05	7.2	13
HF5	High Freq.	1E-05	5.5	6

PTN COL 2.5-3

Table 2.5.2-227 (Sheet 1 of 2)
HF and LF horizontal 1E-05 Rock Spectra, Amplification Factors, Site Spectra, and Raw and Smoothed Envelope Spectra

Horizontal 1E-05 Rock and Site Spectra UHRS (g)								
Freq,	Rock UHRS		Transfer Function		Surface UHRS		Raw Envelope	Smooth Spectrum
Hz	LF SA(g)	HF SA(g)	LF Amp	HF Amp	LF SA(g)	HF SA(g)	SA(g)	SA(g)
100	1.47E-01	1.47E-01	0.767	0.646	1.13E-01	9.49E-02	1.13E-01	1.13E-01
90	1.63E-01	1.63E-01	0.694	0.584	1.13E-01	9.55E-02	1.13E-01	1.13E-01
80	1.89E-01	1.90E-01	0.601	0.507	1.13E-01	9.65E-02	1.13E-01	1.14E-01
70	2.29E-01	2.31E-01	0.501	0.427	1.14E-01	9.85E-02	1.14E-01	1.15E-01
60	2.80E-01	2.84E-01	0.415	0.361	1.16E-01	1.02E-01	1.16E-01	1.16E-01
50	3.33E-01	3.39E-01	0.360	0.323	1.20E-01	1.09E-01	1.20E-01	1.20E-01
45	3.56E-01	3.62E-01	0.347	0.322	1.23E-01	1.17E-01	1.23E-01	1.24E-01
40	3.75E-01	3.82E-01	0.346	0.338	1.30E-01	1.29E-01	1.30E-01	1.32E-01
35	3.91E-01	3.98E-01	0.359	0.376	1.40E-01	1.50E-01	1.50E-01	1.50E-01
30	4.04E-01	4.09E-01	0.384	0.426	1.55E-01	1.74E-01	1.74E-01	1.73E-01
25	4.14E-01	4.14E-01	0.394	0.436	1.63E-01	1.80E-01	1.80E-01	1.79E-01
20	3.85E-01	3.93E-01	0.407	0.426	1.57E-01	1.68E-01	1.68E-01	1.67E-01
15	3.42E-01	3.52E-01	0.448	0.453	1.53E-01	1.59E-01	1.59E-01	1.58E-01
12.5	3.14E-01	3.20E-01	0.481	0.483	1.51E-01	1.54E-01	1.54E-01	1.54E-01
10	2.78E-01	2.78E-01	0.588	0.606	1.64E-01	1.68E-01	1.68E-01	1.67E-01
9	2.63E-01	2.64E-01	0.647	0.665	1.70E-01	1.75E-01	1.75E-01	1.76E-01
8	2.47E-01	2.47E-01	0.732	0.757	1.81E-01	1.87E-01	1.87E-01	1.86E-01
7	2.29E-01	2.29E-01	0.813	0.822	1.86E-01	1.88E-01	1.88E-01	1.88E-01
6	2.08E-01	2.08E-01	0.903	0.908	1.88E-01	1.89E-01	1.89E-01	1.91E-01
5	1.84E-01	1.84E-01	1.118	1.131	2.06E-01	2.08E-01	2.08E-01	2.07E-01
4	1.60E-01	1.51E-01	1.271	1.228	2.03E-01	1.86E-01	2.03E-01	2.05E-01
3	1.29E-01	1.14E-01	1.919	1.925	2.48E-01	2.20E-01	2.48E-01	2.42E-01
2.5	1.10E-01	9.37E-02	2.005	1.855	2.21E-01	1.74E-01	2.21E-01	2.19E-01
2	9.82E-02	7.11E-02	1.734	1.588	1.70E-01	1.13E-01	1.70E-01	1.69E-01
1.5	8.51E-02	4.77E-02	1.852	1.744	1.58E-01	8.33E-02	1.58E-01	1.57E-01
1.25	7.66E-02	3.64E-02	2.221	2.119	1.70E-01	7.72E-02	1.70E-01	1.70E-01
1	6.63E-02	2.58E-02	2.844	2.742	1.89E-01	7.09E-02	1.89E-01	1.91E-01
0.9	6.60E-02	2.19E-02	3.292	3.230	2.17E-01	7.07E-02	2.17E-01	2.13E-01
0.8	6.45E-02	1.81E-02	3.360	3.223	2.17E-01	5.84E-02	2.17E-01	2.13E-01
0.7	6.17E-02	1.46E-02	3.041	2.859	1.88E-01	4.17E-02	1.88E-01	1.90E-01
0.6	5.76E-02	1.13E-02	3.036	2.862	1.75E-01	3.23E-02	1.75E-01	1.74E-01
0.5	5.19E-02	8.26E-03	2.784	2.645	1.44E-01	2.19E-02	1.44E-01	1.41E-01
0.4	4.15E-02	6.61E-03	2.073	1.948	8.61E-02	1.29E-02	8.61E-02	8.74E-02
0.3	3.11E-02	4.96E-03	1.866	1.753	5.81E-02	8.69E-03	5.81E-02	5.83E-02
0.2	2.08E-02	3.30E-03	1.882	1.767	3.91E-02	5.84E-03	3.91E-02	3.90E-02
0.15	1.56E-02	2.48E-03	1.602	1.523	2.49E-02	3.78E-03	2.49E-02	2.51E-02
0.125	1.29E-02	2.06E-03	1.423	1.377	1.84E-02	2.83E-03	1.84E-02	1.82E-02

PTN COL 2.5-3

Table 2.5.2-227 (Sheet 2 of 2)
HF and LF horizontal 1E-05 Rock Spectra, Amplification Factors, Site Spectra, and Raw and Smoothed Envelope Spectra

Horizontal 1E-05 Rock and Site Spectra UHRS (g)								
Freq, Hz	Rock UHRS		Transfer Function		Surface UHRS		Raw Envelope	Smooth Spectrum
	LF SA(g)	HF SA(g)	LF Amp	HF Amp	LF SA(g)	HF SA(g)	SA(g)	SA(g)
0.1	8.30E-03	1.32E-03	1.324	1.268	1.10E-02	1.68E-03	1.10E-02	1.10E-02

UHRS = Uniform hazard response spectra
LF = Low frequencies
HF = High frequencies
SA = Spectral acceleration
Amp = Amplitude

PTN COL 2.5-3

Table 2.5.2-228
Horizontal 1E-04 and 1E-05 Site Spectra, Values of A_R and DF, and GMRS

Freq. Hz	Horizontal 1E-04 (g)	Horizontal 1E-05 (g)	A_R	DF	Horizontal GMRS (g)
100	5.20E-02	1.13E-01	2.17	1.11	5.79E-02
90	5.21E-02	1.13E-01	2.17	1.11	5.81E-02
80	5.23E-02	1.14E-01	2.17	1.11	5.83E-02
70	5.28E-02	1.15E-01	2.17	1.11	5.89E-02
60	5.37E-02	1.16E-01	2.17	1.11	5.98E-02
50	5.51E-02	1.20E-01	2.18	1.12	6.16E-02
45	5.65E-02	1.24E-01	2.19	1.12	6.35E-02
40	5.86E-02	1.32E-01	2.25	1.15	6.72E-02
35	6.18E-02	1.50E-01	2.43	1.22	7.53E-02
30	6.55E-02	1.73E-01	2.64	1.30	8.54E-02
25	6.65E-02	1.79E-01	2.69	1.33	8.82E-02
20	6.43E-02	1.67E-01	2.60	1.29	8.28E-02
15	6.29E-02	1.58E-01	2.51	1.25	7.88E-02
12.5	6.28E-02	1.54E-01	2.45	1.23	7.72E-02
10	6.71E-02	1.67E-01	2.49	1.24	8.35E-02
9	6.99E-02	1.76E-01	2.52	1.26	8.78E-02
8	7.32E-02	1.86E-01	2.53	1.26	9.25E-02
7	7.52E-02	1.88E-01	2.50	1.25	9.38E-02
6	7.84E-02	1.91E-01	2.44	1.22	9.59E-02
5	8.63E-02	2.07E-01	2.40	1.21	1.04E-01
4	8.69E-02	2.05E-01	2.36	1.19	1.04E-01
3	1.11E-01	2.42E-01	2.18	1.12	1.24E-01
2.5	1.02E-01	2.19E-01	2.15	1.11	1.13E-01
2	8.07E-02	1.69E-01	2.10	1.08	8.75E-02
1.5	8.02E-02	1.57E-01	1.96	1.03	8.24E-02
1.25	8.84E-02	1.70E-01	1.92	1.01	8.94E-02
1	1.05E-01	1.91E-01	1.83	1.00	1.05E-01
0.9	1.15E-01	2.13E-01	1.85	1.00	1.15E-01
0.8	1.12E-01	2.13E-01	1.91	1.01	1.12E-01
0.7	9.72E-02	1.90E-01	1.95	1.03	9.96E-02
0.6	8.86E-02	1.74E-01	1.96	1.03	9.11E-02
0.5	7.17E-02	1.41E-01	1.97	1.03	7.39E-02
0.4	4.46E-02	8.74E-02	1.96	1.03	4.59E-02
0.3	3.00E-02	5.83E-02	1.95	1.02	3.06E-02
0.2	2.01E-02	3.90E-02	1.94	1.02	2.05E-02
0.15	1.29E-02	2.51E-02	1.95	1.02	1.32E-02
0.125	9.37E-03	1.82E-02	1.95	1.02	9.58E-03
0.1	5.65E-03	1.10E-02	1.95	1.02	5.78E-03

Notes:
A_R and DF are defined in Equations 2.5.2-14 and 2.5.2-15, respectively.
GMRS = Ground motion response spectrum

PTN COL 2.5-3

Table 2.5.2-229
Smooth 1E-04, 1E-05, and 1E-06 Spectra at GMRS Elevation

Freq, Hz	Smooth Spectra (g)		
	1E-04	1E-05	1E-06
100	5.20E-02	1.13E-01	2.50E-01
90	5.21E-02	1.13E-01	2.51E-01
80	5.23E-02	1.14E-01	2.53E-01
70	5.28E-02	1.15E-01	2.56E-01
60	5.37E-02	1.16E-01	2.63E-01
50	5.51E-02	1.20E-01	2.77E-01
45	5.65E-02	1.24E-01	2.92E-01
40	5.86E-02	1.32E-01	3.18E-01
35	6.18E-02	1.50E-01	3.61E-01
30	6.55E-02	1.73E-01	4.19E-01
25	6.65E-02	1.79E-01	4.51E-01
20	6.43E-02	1.67E-01	4.35E-01
15	6.29E-02	1.58E-01	4.19E-01
12.5	6.28E-02	1.54E-01	4.06E-01
10	6.71E-02	1.67E-01	4.36E-01
9	6.99E-02	1.76E-01	4.63E-01
8	7.32E-02	1.86E-01	4.91E-01
7	7.52E-02	1.88E-01	5.06E-01
6	7.84E-02	1.91E-01	5.09E-01
5	8.63E-02	2.07E-01	5.45E-01
4	8.69E-02	2.05E-01	5.20E-01
3	1.11E-01	2.42E-01	5.73E-01
2.5	1.02E-01	2.19E-01	5.12E-01
2	8.07E-02	1.69E-01	3.82E-01
1.5	8.02E-02	1.57E-01	3.02E-01
1.25	8.84E-02	1.70E-01	3.11E-01
1	1.05E-01	1.91E-01	3.34E-01
0.9	1.15E-01	2.13E-01	3.77E-01
0.8	1.12E-01	2.13E-01	4.01E-01
0.7	9.72E-02	1.90E-01	3.78E-01
0.6	8.86E-02	1.74E-01	3.52E-01
0.5	7.17E-02	1.41E-01	2.93E-01
0.4	4.46E-02	8.74E-02	1.79E-01
0.3	3.00E-02	5.83E-02	1.17E-01
0.2	2.01E-02	3.90E-02	7.78E-02
0.15	1.29E-02	2.51E-02	5.05E-02
0.125	9.37E-03	1.82E-02	3.67E-02
0.1	5.65E-03	1.10E-02	2.21E-02

GMRS = Ground motion response spectrum

PTN COL 2.5-3

Table 2.5.2-230
V/H Ratios, Vertical 1E-04 and 1E-05 Site Spectra, Values of A_R and DF, and GMRS

Freq. Hz	V/H	Vertical 1E-04 (g)	Vertical 1E-05 (g)	A_R	DF	Vertical GMRS (g)
100	1.000	5.20E-02	1.13E-01	2.17	1.11	5.79E-02
90	1.000	5.21E-02	1.13E-01	2.17	1.11	5.81E-02
80	1.000	5.23E-02	1.14E-01	2.17	1.11	5.83E-02
70	1.000	5.28E-02	1.15E-01	2.17	1.11	5.89E-02
60	1.000	5.37E-02	1.16E-01	2.17	1.11	5.98E-02
50	1.000	5.51E-02	1.20E-01	2.18	1.12	6.16E-02
45	1.000	5.65E-02	1.24E-01	2.19	1.12	6.35E-02
40	1.000	5.86E-02	1.32E-01	2.25	1.15	6.72E-02
35	1.000	6.18E-02	1.50E-01	2.43	1.22	7.53E-02
30	1.000	6.55E-02	1.73E-01	2.64	1.30	8.54E-02
25	1.000	6.65E-02	1.79E-01	2.69	1.33	8.82E-02
20	1.000	6.43E-02	1.67E-01	2.60	1.29	8.28E-02
15	1.000	6.29E-02	1.58E-01	2.51	1.25	7.88E-02
12.5	1.000	6.28E-02	1.54E-01	2.45	1.23	7.72E-02
10	1.000	6.71E-02	1.67E-01	2.49	1.24	8.35E-02
9	1.000	6.99E-02	1.76E-01	2.52	1.26	8.78E-02
8	1.000	7.32E-02	1.86E-01	2.53	1.26	9.24E-02
7	1.000	7.52E-02	1.88E-01	2.50	1.25	9.38E-02
6	0.999	7.84E-02	1.91E-01	2.44	1.22	9.59E-02
5	0.999	8.62E-02	2.07E-01	2.40	1.21	1.04E-01
4	0.999	8.68E-02	2.05E-01	2.36	1.19	1.04E-01
3	0.857	9.53E-02	2.08E-01	2.18	1.12	1.07E-01
2.5	0.715	7.28E-02	1.57E-01	2.15	1.11	8.07E-02
2	0.710	5.73E-02	1.20E-01	2.10	1.08	6.22E-02
1.5	0.704	5.65E-02	1.11E-01	1.96	1.03	5.81E-02
1.25	0.701	6.19E-02	1.19E-01	1.92	1.01	6.27E-02
1	0.696	7.27E-02	1.33E-01	1.83	1.00	7.27E-02
0.9	0.694	7.97E-02	1.47E-01	1.85	1.00	7.97E-02
0.8	0.691	7.72E-02	1.47E-01	1.91	1.01	7.77E-02
0.7	0.689	6.69E-02	1.31E-01	1.95	1.03	6.86E-02
0.6	0.686	6.08E-02	1.19E-01	1.96	1.03	6.25E-02
0.5	0.682	4.89E-02	9.61E-02	1.97	1.03	5.04E-02
0.4	0.678	3.02E-02	5.92E-02	1.96	1.03	3.11E-02
0.3	0.672	2.01E-02	3.92E-02	1.95	1.02	2.06E-02
0.2	0.668	1.34E-02	2.61E-02	1.94	1.02	1.37E-02
0.15	0.668	8.60E-03	1.68E-02	1.95	1.02	8.80E-03
0.125	0.668	6.26E-03	1.22E-02	1.95	1.02	6.40E-03
0.1	0.668	3.78E-03	7.35E-03	1.95	1.02	3.86E-03

Notes:
A_R and DF are defined in Equations 2.5.2-14 and 2.5.2-15, respectively.
GMRS = Ground motion response spectrum

Table 2.5.2-231
Regional Attenuation and Source Parameters Estimated in the Motazedian and Atkinson Study and Used in the Simulation of Ground Motions for the Cuba and Caribbean Region

Parameter	Motazedian and Atkinson (Reference 287) Values	Simulation Values
Stress Parameter	130 bars	65 bars (Low Case) 130 bars (Base Case) 260 bars (High Case)
Geometrical Spreading	1/R for R<75km 1.0 for 75<R<100km 1/SQRT(R) for R>100km	1/R for R<75km 1.0 for 75<R<100km 1/SQRT(R) for R>100km
Anelastic Attenuation Factor (Q) Model	$359\ f^{0.59}$	$241\ f^{0.59}$ (Low Case) $359\ f^{0.59}$ (Base Case) $536\ f^{0.59}$ (High Case)
Path Duration	Atkinson and Boore (Reference 210) Model with hinge points at 75 and 100 km	Atkinson and Boore (Reference 210) Model with hinge points at 75 and 100 km
Site Amplification	Puerto Rico specific for soft rock site (NEHRP C) conditions based on H/V ratio	Chen and Atkinson (Reference 343) CEUS Hard Rock
Kappa	0.03 sec	0.006 sec (Reference 244)
Shear Wave Velocity (Vs) at the Source	3.6 km/sec	3.6 km/sec
Density	2.8 g/cm^3	2.8 g/cm^3

PTN RAI 02.05.02-4

Table 2.5.2-232
Experts Contacted for the SSHAC Level 2 Study in Support of Cuba Hazard Sensitivity Calculations

Expert	Affiliation	Expertise	Response
Coppersmith, Kevin	Coppersmith Consulting	Seismic hazard modeling, seismic source characterization	Email response
Cotilla-Rodríguez, Mario Octavio	Departmento de Fisca de la Tierra y Astrofisica, Facultad de Ciencias Fisicas, Universidad Complutense de Madrid (Madrid, Spain)	Cuba faults and neotectonics	Detailed email response
Garcia, Julio	Centro Nacional de Investigaciones Sismológicas (CENAIS) (Havana, Cuba)	Seismic hazard modeling in Cuba	No response
Hanson, Kathryn	AMEC	Seismic hazard modeling, seismic source characterization	Declined to participate
Ituralde-Vinent, Manuel	Museo Nacional de Historia Natural (Havana, Cuba) and Departamento de Geociencias, Instituto Superior Politécnico J.A. Echeverria (Havana, Cuba)	Geology of Cuba	No response
Moreno, Toiran Bladimir	Inst. of Solid Earth Physics, University of Bergen (Norway) and Centro Nacional de Investigaciones Sismologicas (CENAIS) (Santiago de Cuba, Cuba)	Seismology and geophysics of Cuba	Email response
Slejko, Dario	Istituto Nazionale di Oceanografia e di Geofisica Sperimetale (OGS) (Trieste, Italy)	Seismic hazard modeling in Cuba	Detailed email response
Toscano, Marguerite	Department of Paleobiology, Smithsonian Institute	Marine terrace mapping and dating in northern Cuba	Email response and telephone conversation regarding marine terraces in northern Cuba
Wong, Ivan	URS Corporation	Seismic hazard modeling, seismic source characterization	Detailed email responses
Youngs, Robert	AMEC	Seismic hazard modeling	Declined to participate
Zapata Balanque, Jose Alejandro	Universidad de Oriente (Santiago de Cuba, Cuba)	Cuba faults and neotectonics	Email response regarding plans for future paleoseismic studies in Cuba

Table 2.5.2-233
Cuba Seismic Source Alternatives for Hazard Sensitivity Calculations

PTN RAI 02.05.02-4

		Source Zone Scenarios Increasing Hazard →			
		No Areal Sources	**Z6 Six Areal Sources**	**Z1 Single Areal Source**	**Z11% Elevated Rate Areal Source (+11% Increase in Rate)**
Fault Source Scenarios ←Increasing Hazard	No fault sources	N/A	Z6	Z1	Z11%
	SF Scaled Fault Sources	SF	Z6+SF[(a)]	Z1+SF[(a)]	Z11%+SF[(b)]
	FF Full Fault Sources	FF[(c)]	Z6+FF[(c)]	Z1+FF[(c)]	Z11%+FF[(c)]

(a) Z1+SF was evaluated as a reasonable combination scenario in the hazard sensitivity calculations. As discussed in the text, area source scenario Z6 was found to result in lower hazard than area source scenario Z1. Thus, it is unnecessary to further investigate the combination scenario Z6+SF.

(b) As discussed in the text, source area scenario Z11% is considered a conservative assessment of the seismic hazard derived from the cataloged seismicity. Therefore, the combination scenario Z11%+SF is considered overly conservative for consideration in the hazard sensitivity calculations.

(c) As discussed in the text, fault source scenario FF was determined to be technically indefensible compared to the cataloged seismicity. Therefore, any combination scenarios with FF were similarly eliminated as technically indefensible.

Shaded source scenarios not quantitatively evaluated.

PTN RAI 02.05.02-4

Table 2.5.2-234
Cuba Areal Source Zone and Northern Cuba Subzone Recurrence Parameters

PTN RAI 02.05.02-4

Zone	Zone Area (km^2)	# Events Events[(a)]	a-value[(b)]	b-value	Rate of M_w 5 to 7.3 events per year/km^2
Cuba areal source zone	250,286	152	-2.430	0.839	2.341E-7
Northern Cuba subzone	80,770	46	-2.383[(c)]	0.839[(d)]	2.609E-7

(a) Events ≥ M_w 3.0, filtered for completeness periods
(b) Normalized to events per year/km^2
(c) Value represents the 11 percent increase discussed in text
(d) Fixed to Cuba areal source zone b-value

PTN RAI 02.05.02-4

Table 2.5.2-235
Completeness Periods and Earthquake Counts in Each Bin from the Phase 2 Earthquake Catalog

PTN RAI 02.05.02-4

Magnitude Range (M_W)	Start Date	End Date	Number of Earthquakes from Phase 2 Earthquake Catalog
3.0–4.0	1/1960	3/2008	119
4.0–5.0	1/1940	3/2008	17
5.0–6.0	1/1850	3/2008	14
6.0–7.0	1/1500	3/2008	2

Source: Reference 255

PTN RAI 02.05.02-4

PTN RAI 02.05.02-4

Table 2.5.2-236
Summary of Seismic Source Parameters for Intraplate Cuba Fault Sources for Hazard Sensitivity Calculation

Sensitivity Fault Source	Dip	Rupture Depth Range (km)	Length (km)	Magnitude (M_w) [and weight]	Slip Rate (mm/yr) [and weight]
Baconao SE	90°	0–15	101	7.0 [0.5] 7.3 [0.5]	0.01 [0.1] 0.1 [0.5] 1.0 [0.4]
Baconao NW	90°	0–15	191	7.0 [0.5] 7.3 [0.5]	0.001 [0.33] 0.01 [0.34] 0.1 [0.33]
Camaguey	90°	0–15	131	7.0 [0.5] 7.3 [0.5]	0.001 [0.33] 0.01 [0.34] 0.1 [0.33]
Cochinos	90°	0–15	68	7.0 [0.5] 7.3 [0.5]	0.001 [0.33] 0.01 [0.34] 0.1 [0.33]
Cubitas	90°	0–15	283	7.0 [0.5] 7.3 [0.5]	0.001 [0.33] 0.01 [0.34] 0.1 [0.33]
Guane	90°	0–15	292	7.0 [0.5] 7.3 [0.5]	0.001 [0.33] 0.01 [0.34] 0.1 [0.33]
Habana-Cienfuegos	90°	0–15	269	7.0 [0.5] 7.3 [0.5]	0.001 [0.33] 0.01 [0.34] 0.1 [0.33]
Hicacos	90°	0–15	114	7.0 [0.5] 7.3 [0.5]	0.001 [0.33] 0.01 [0.34] 0.1 [0.33]
La Trocha	90°	0–15	257	7.0 [0.5] 7.3 [0.5]	0.001 [0.33] 0.01 [0.34] 0.1 [0.33]
Las Villas	90°	0–15	197	7.0 [0.5] 7.3 [0.5]	0.001 [0.33] 0.01 [0.34] 0.1 [0.33]
Nipe	90°	0–15	292	7.0 [0.5] 7.3 [0.5]	0.01[0.1] 0.1 [0.5] 1.0 [0.4]
Nortecubana West	30°S	0–15	595	7.0 [0.5] 7.3 [0.5]	0.001 [0.33] 0.01 [0.34] 0.1 [0.33]
Nortecubana Central	30°S	0–15	441	7.0 [0.5] 7.3 [0.5]	0.001 [0.33] 0.01 [0.34] 0.1 [0.33]
Nortecubana East	30°S	0–15	340	7.0 [0.5] 7.3 [0.5]	0.01[0.1] 0.1 [0.5] 1.0 [0.4]
Pinar	90°	0–15	215	7.0 [0.5] 7.3 [0.5]	0.001 [0.33] 0.01 [0.34] 0.1 [0.33]

PTN RAI 02.05.02-4

Table 2.5.2-237 Moment Rates, Ratio of Seismicity-Based Moment Rate to Fault-Based Moment Rates, and Return Periods for M_w 6.5 and 7.0 from Cuba Sensitivity Options

Moment Rate Options	Moment Rate (dyne-cm/yr)	Ratio, Seismicity/ Fault-Based	Return Period for M_w 6.5 (years)	Return Period for M_w 7 (years)
Historical Seismicity[a]	7.7844E+23	Not applicable	81	456
Low Slip Rate Option[b]	6.6686E+22	0.0857	946	5321
Middle Slip Rate Option[b]	6.6686E+23	0.8567	95	532
High Slip Rate Option[b]	6.6686E+24	8.5666	9.5	53
Weighted Mean Slip Rate[c]	2.8535E+24	3.6657	22	124

PTN RAI 02.05.02-4

(a) Moment rate obtained from seismicity catalog and used for Cuba areal source (Z1) and for scaled fault scenario (SF).
(b) Moment rates obtained from low, middle, and high slip rate values presented in Table 2.5.2-236.
(c) Moment rate obtained from weighted mean of slip rate values presented in Table 2.5.2-236 and used for full fault scenario (FF).

PTN RAI 02.05.02-4

Table 2.5.2-238
Summary of Hazard Sensitivity Study Results: Comparison of MAFE

	Base Case Z1		Scenario Z6		Scenario SF		Scenario Z11%		Scenario Z1+SF	
10^{-4} mean annual frequency of exceedance (MAFE)										
Freq	MAFE	Amp[(a)]	MAFE	% Diff	MAFE	% Diff	MAFE	% Diff	MAFE	% Diff
1 Hz	1.00E-04	0.0343	9.499E-05	-5.0%	9.676E-05	-3.2%	1.018E-04	1.8%	1.114E-04	11.4%
10 Hz	1.00E-04	0.0822	9.122E-05	-8.8%	8.798E-05	-12.0%	1.025E-04	2.5%	1.094E-04	9.4%
10^{-5} mean annual frequency of exceedance (MAFE)										
Freq	MAFE	Amp[(a)]	MAFE	% Diff	MAFE	% Diff	MAFE	% Diff	MAFE	% Diff
1 Hz	1.00E-05	0.0663	9.539E-06	-4.6%	1.010E-05	1.0%	1.013E-05	1.3%	1.131E-05	13.1%
10 Hz	1.00E-05	0.278	9.891E-06	-1.1%	9.969E-06	-0.3%	9.992E-06	-0.1%	1.014E-05	1.4%

(a) Rock motion (g)

PTN RAI 02.05.02-4

Table 2.5.2-239
Summary of Hazard Sensitivity Results: Comparison of Rock Motion Amplitudes

PTN RAI 02.05.02-4

	Base Case Z1	Scenario Z6			Scenario SF			Scenario Z11%			Scenario Z1+SF		
Rock motions (g) at 10^{-4} mean annual frequency of exceedance (MAFE)													
Freq	Amp	Amp	Amp Diff	% Diff	Amp	Amp Diff	% Diff	Amp	Amp Diff	% Diff	Amp	Amp Diff	% Diff
1 Hz	0.0343	0.0338	-0.0005	-1.5%	0.0340	-0.0003	-0.9%	0.0345	0.0002	0.6%	0.0354	0.0011	3.2%
10 Hz	0.0822	0.0784	-0.0038	-4.6%	0.0765	-0.0057	-6.9%	0.0832	0.0010	1.2%	0.0858	0.0036	4.4%
Rock motions (g) at 10^{-5} mean annual frequency of exceedance (MAFE)													
Freq	Amp	Amp	Amp Diff	% Diff	Amp	Amp Diff	% Diff	Amp	Amp Diff	% Diff	Amp	Amp Diff	% Diff
1 Hz	0.0663	0.0654	-0.0009	-1.4%	0.0665	0.0002	0.3%	0.0665	0.0002	0.3%	0.0686	0.0023	3.5%
10 Hz	0.278	0.276	-0.0020	-0.7%	0.278	0.0000	0.0%	0.278	0.0000	0.0%	0.280	0.0020	0.7%

PTN COL 2.5-2

Figure 2.5.2-201 Seismicity in the Study Region, Phase 1 and Phase 2

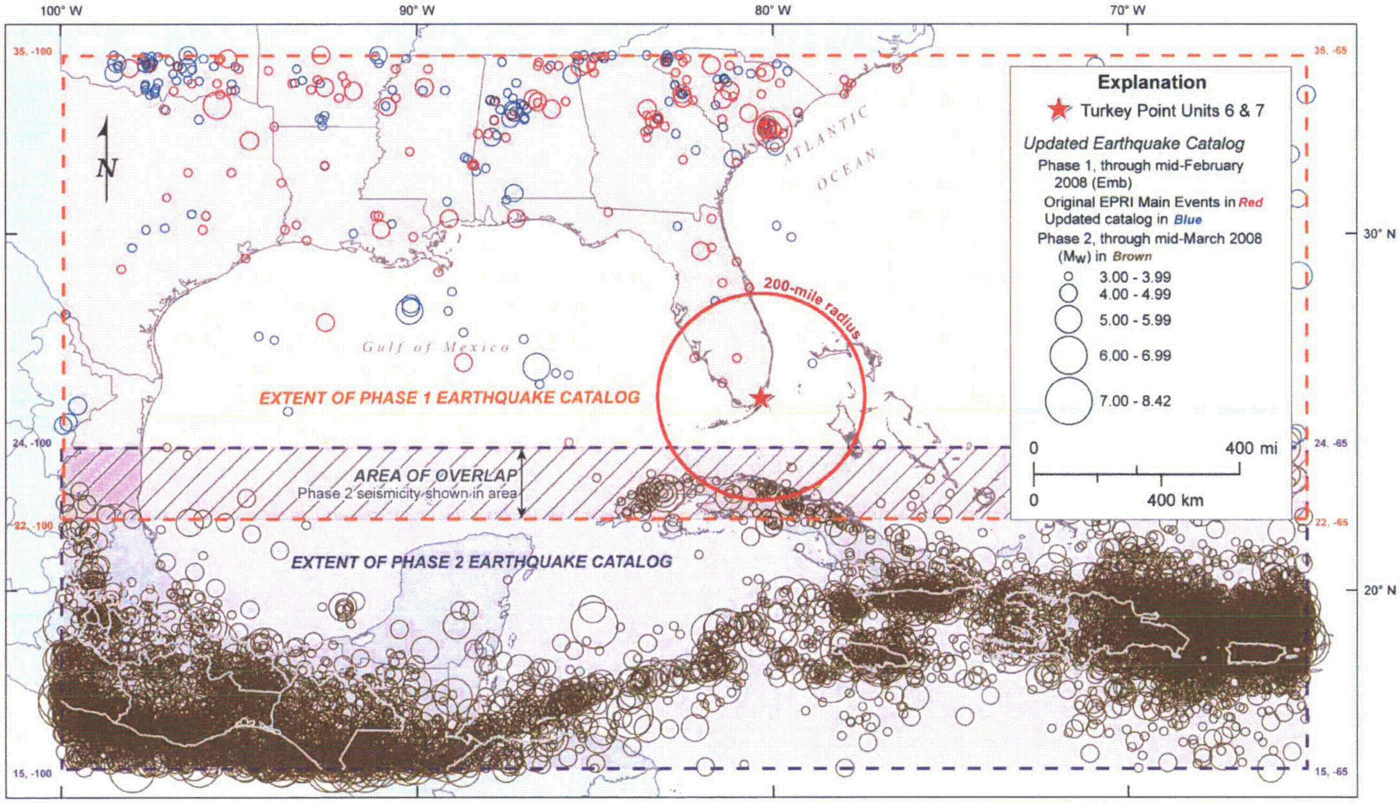

Projection: Equirectangular Plate Carrée (WGS84)

PTN COL 2.5-2

Figure 2.5.2-202 Supplemental Areas of Incompleteness Regions, Gulf of Mexico, Near Florida, and Near Atlantic, South of the Boundary of EPRI Incompleteness Regions

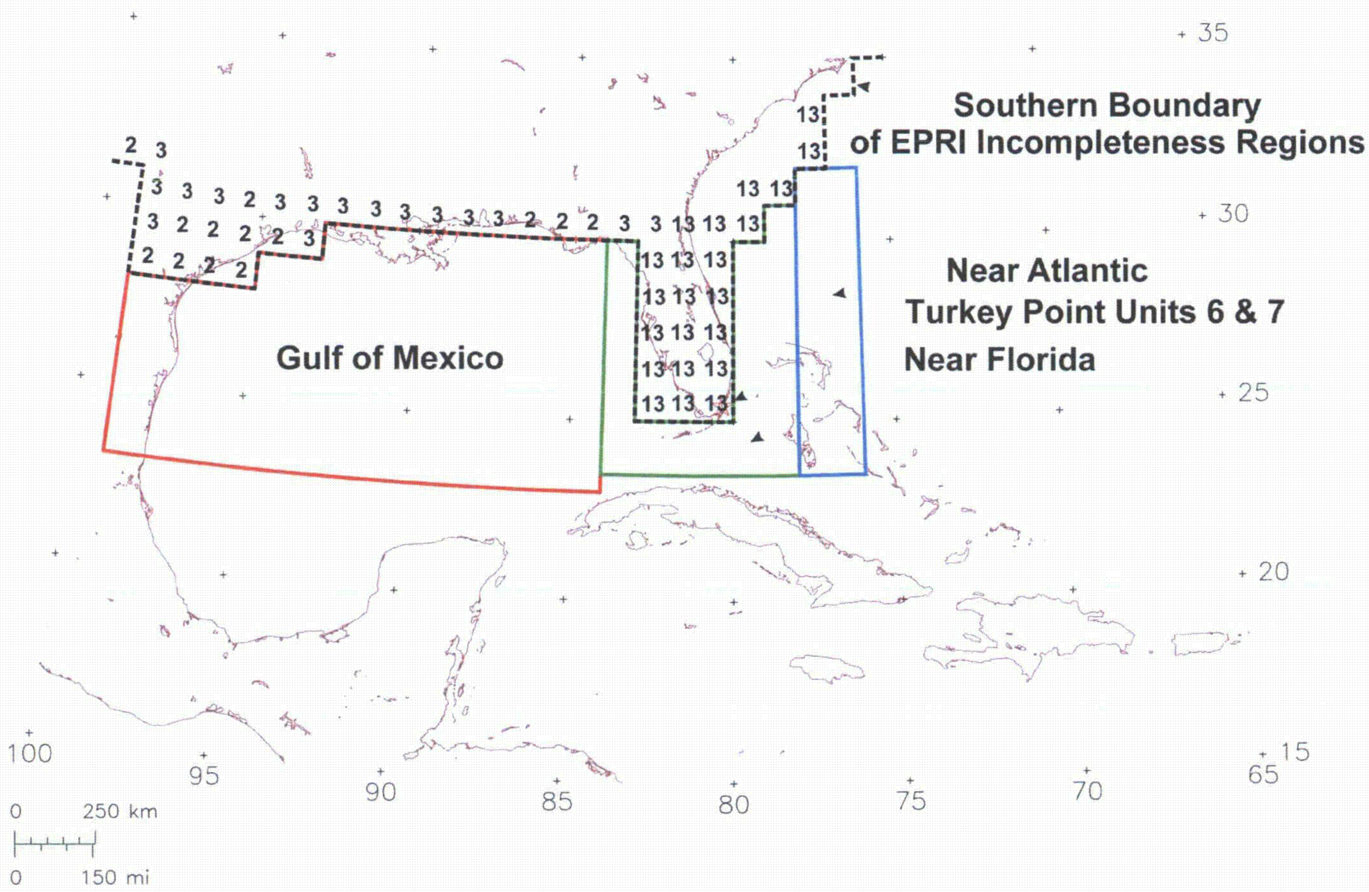

Notes:
See Table 5-1 of EPRI (Reference 243) for EPRI Incompleteness Regions.
Numbers indicate the EPRI 1 degree x 1 degree regions of incompleteness along the southern border of 1989 EPRI-SOG coverage.

PTN COL 2.5-2

Figure 2.5.2-203 EPRI Seismic Source Zones and Updated Charleston Seismic Source (UCSS) Model Sources

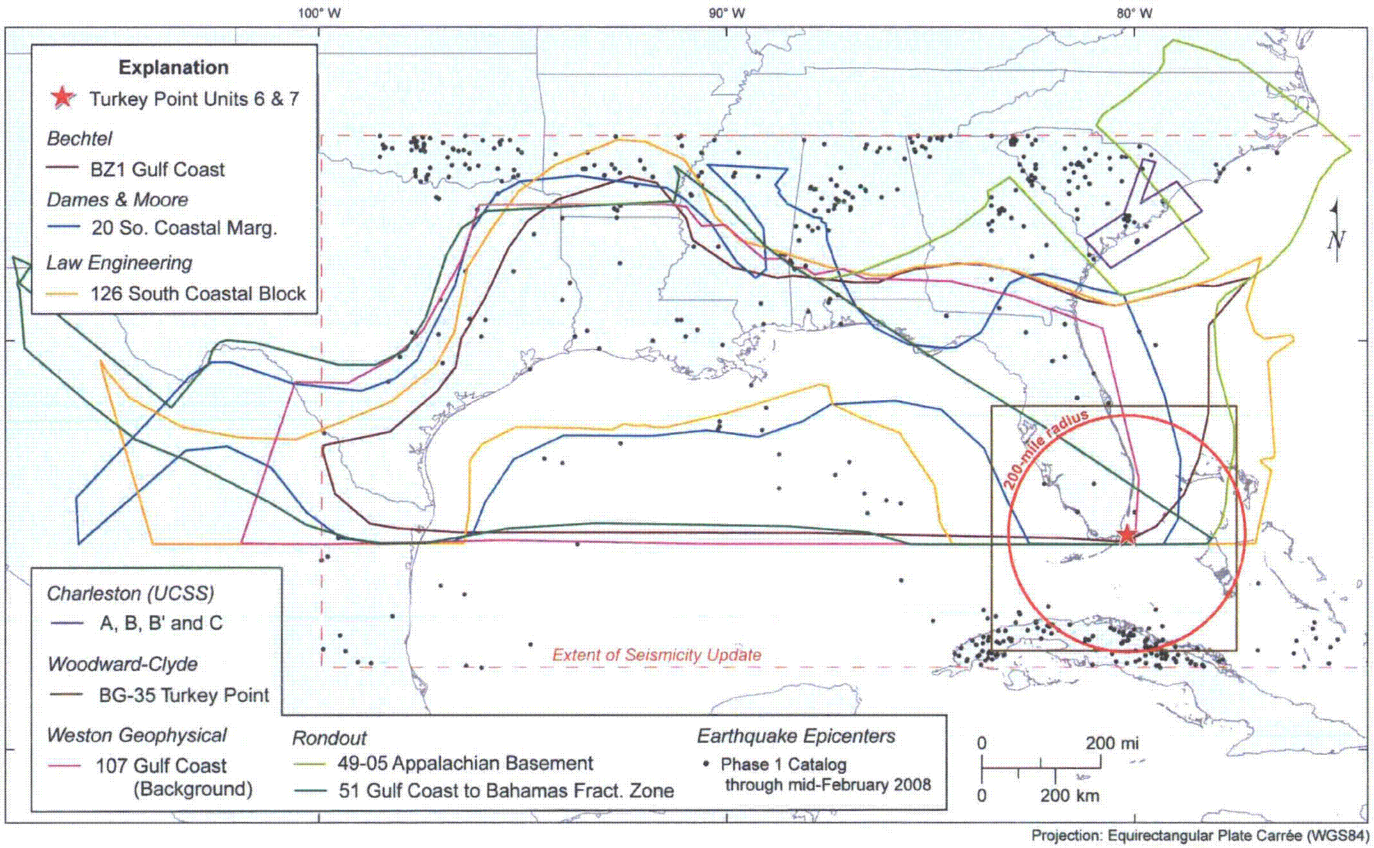

PTN COL 2.5-2

Figure 2.5.2-204 EPRI and Supplemental Source Zones — Bechtel

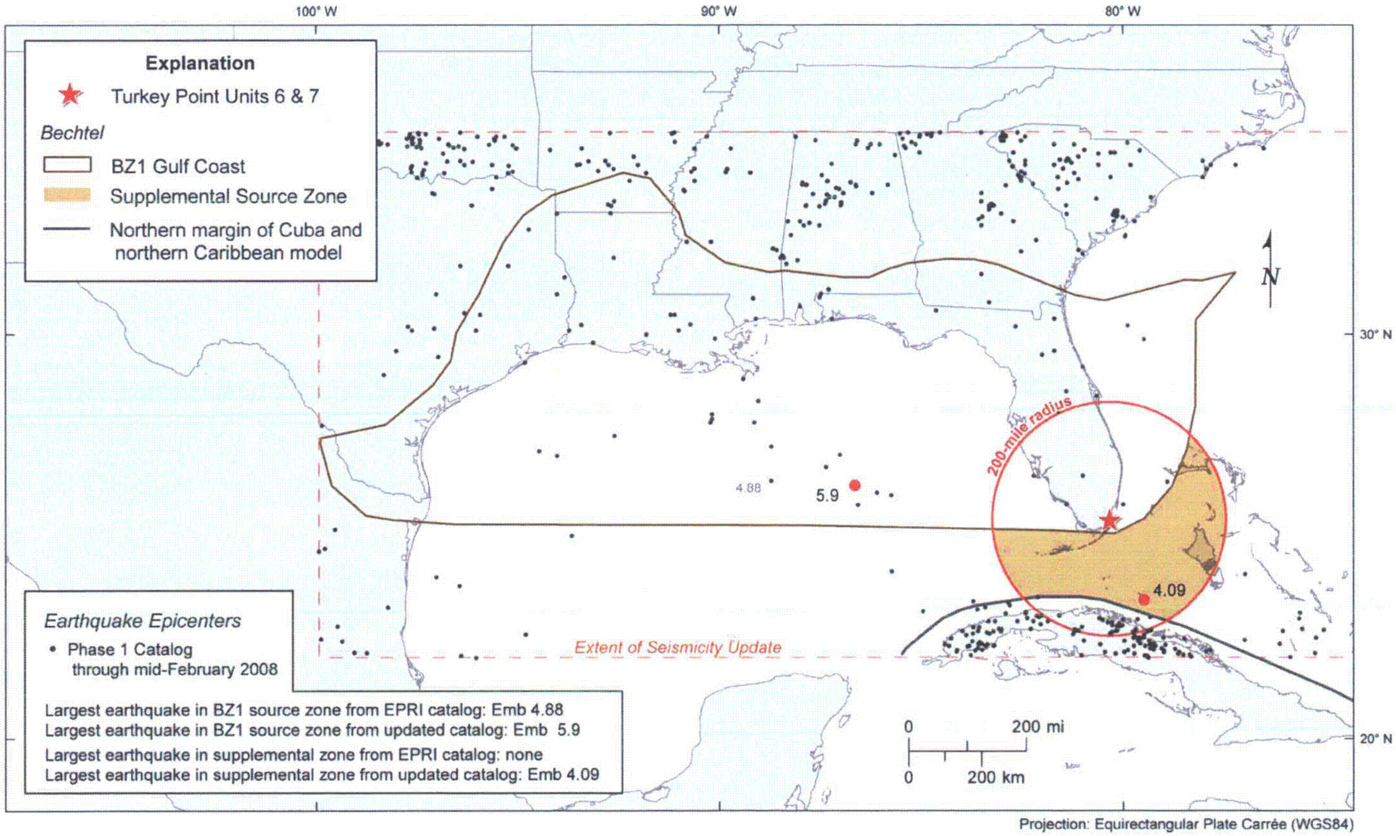

Note: Epicenters of the largest magnitude events in the seismic source zones are highlighted as red dots.

PTN COL 2.5-2

Figure 2.5.2-205 EPRI and Supplemental Source Zones — Dames & Moore

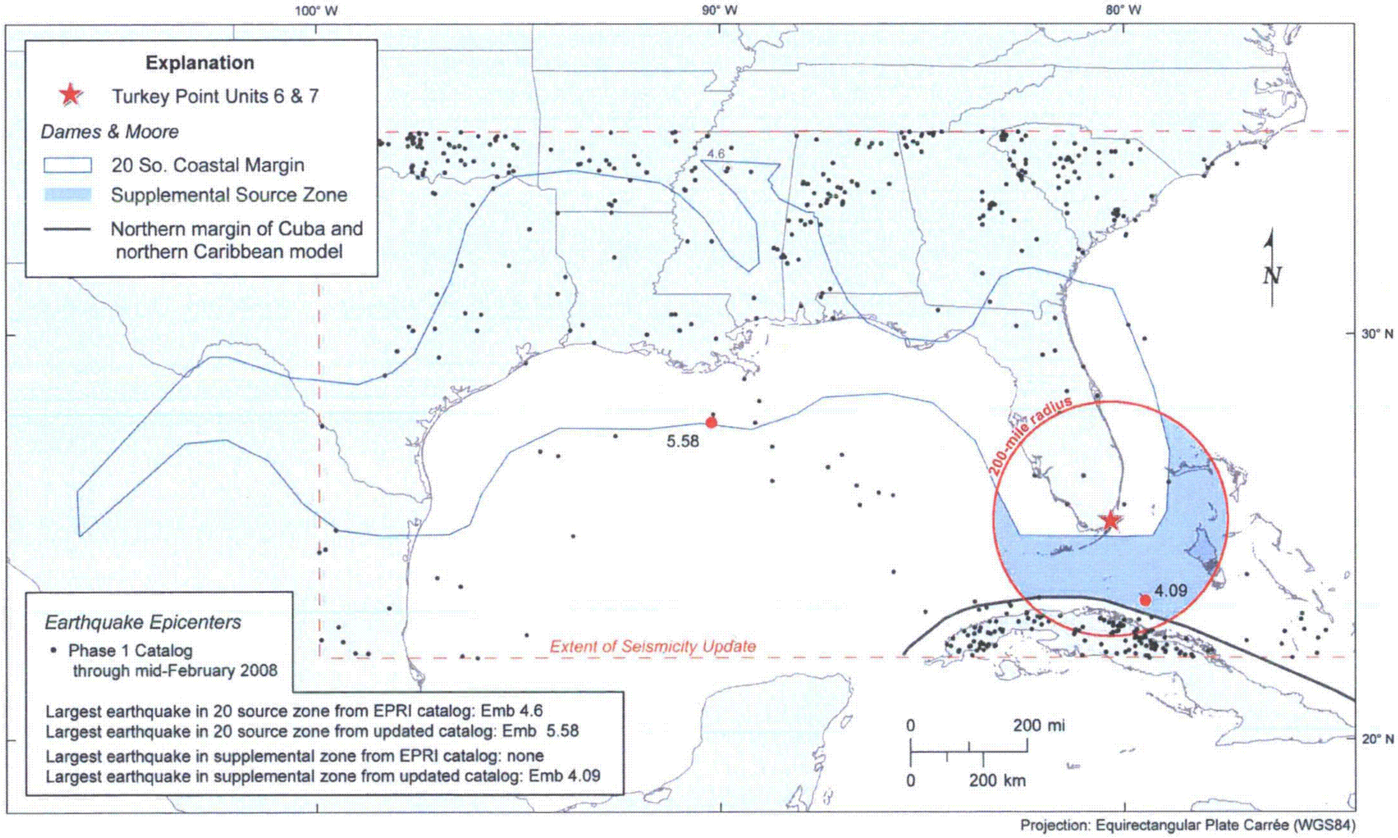

Note: Epicenters of the largest magnitude events in the seismic source zones are highlighted as red dots.

PTN COL 2.5-2

Figure 2.5.2-206 EPRI and Supplemental Source Zones — Law Engineering

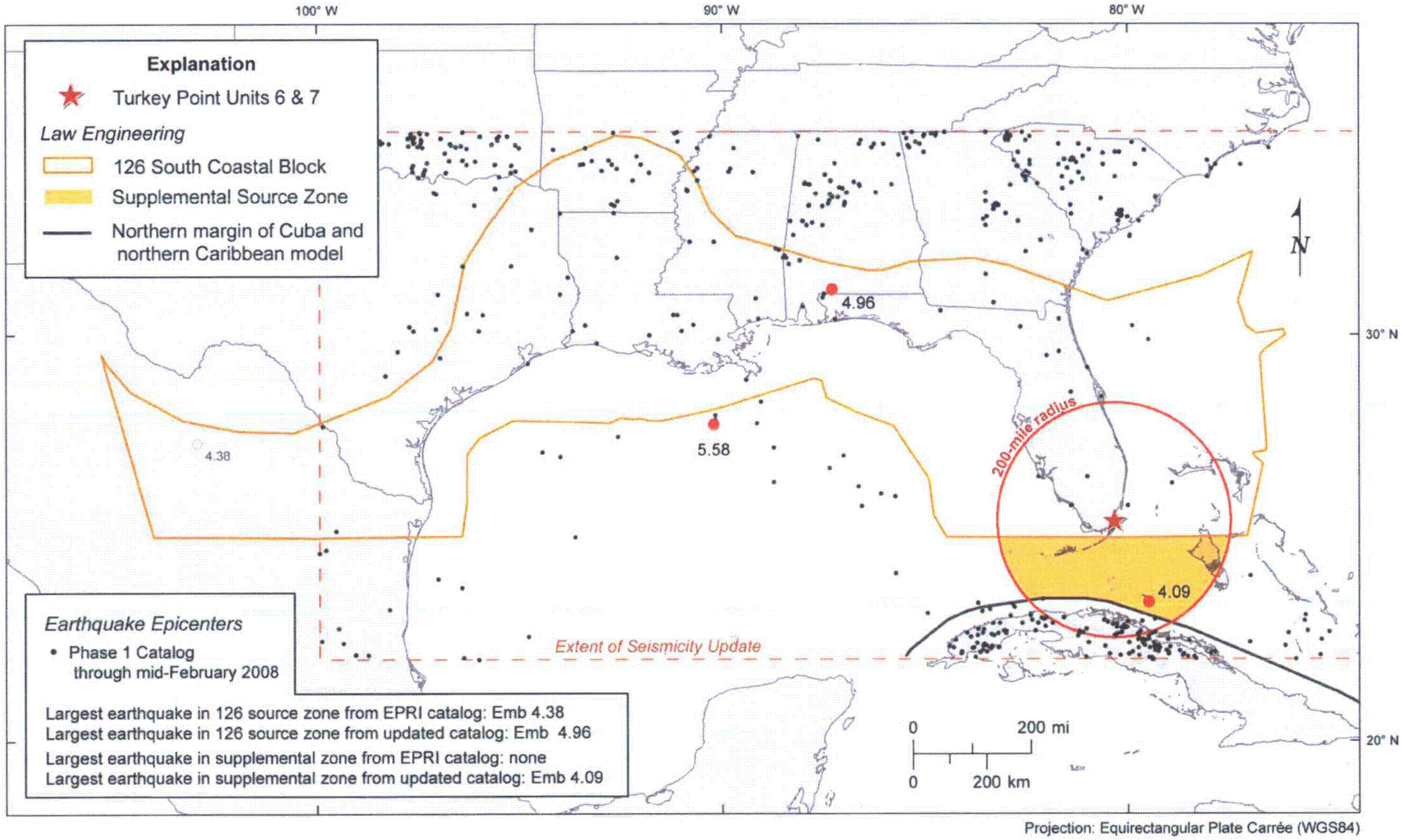

Note: Epicenters of the largest magnitude events in the seismic source zones are highlighted as red dots.

PTN COL 2.5-2

Figure 2.5.2-207 EPRI and Supplemental Source Zones — Rondout Associates

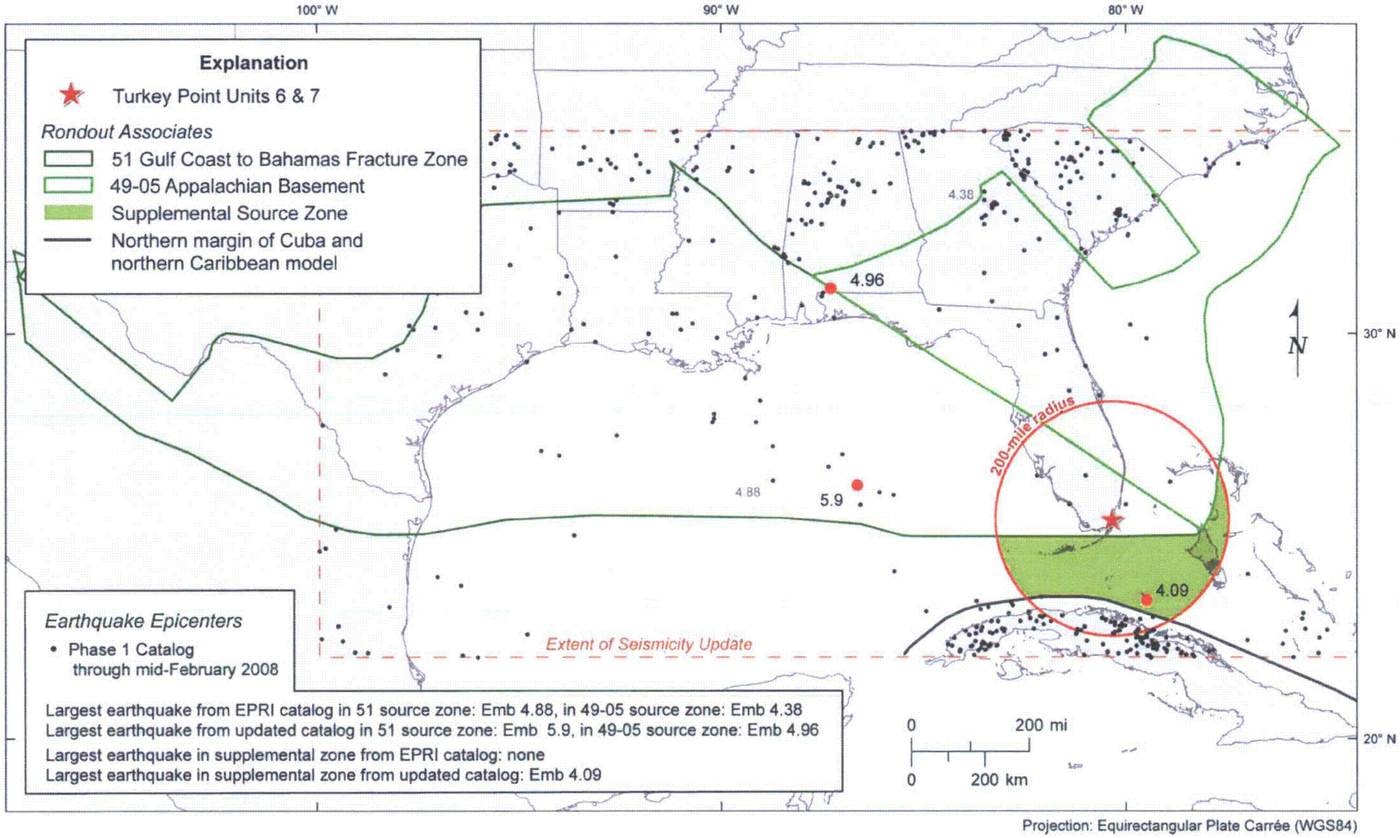

Note: Epicenters of the largest magnitude events in the seismic source zones are highlighted as red dots.

PTN COL 2.5-2

Figure 2.5.2-208 EPRI and Supplemental Source Zones — Weston Geophysical

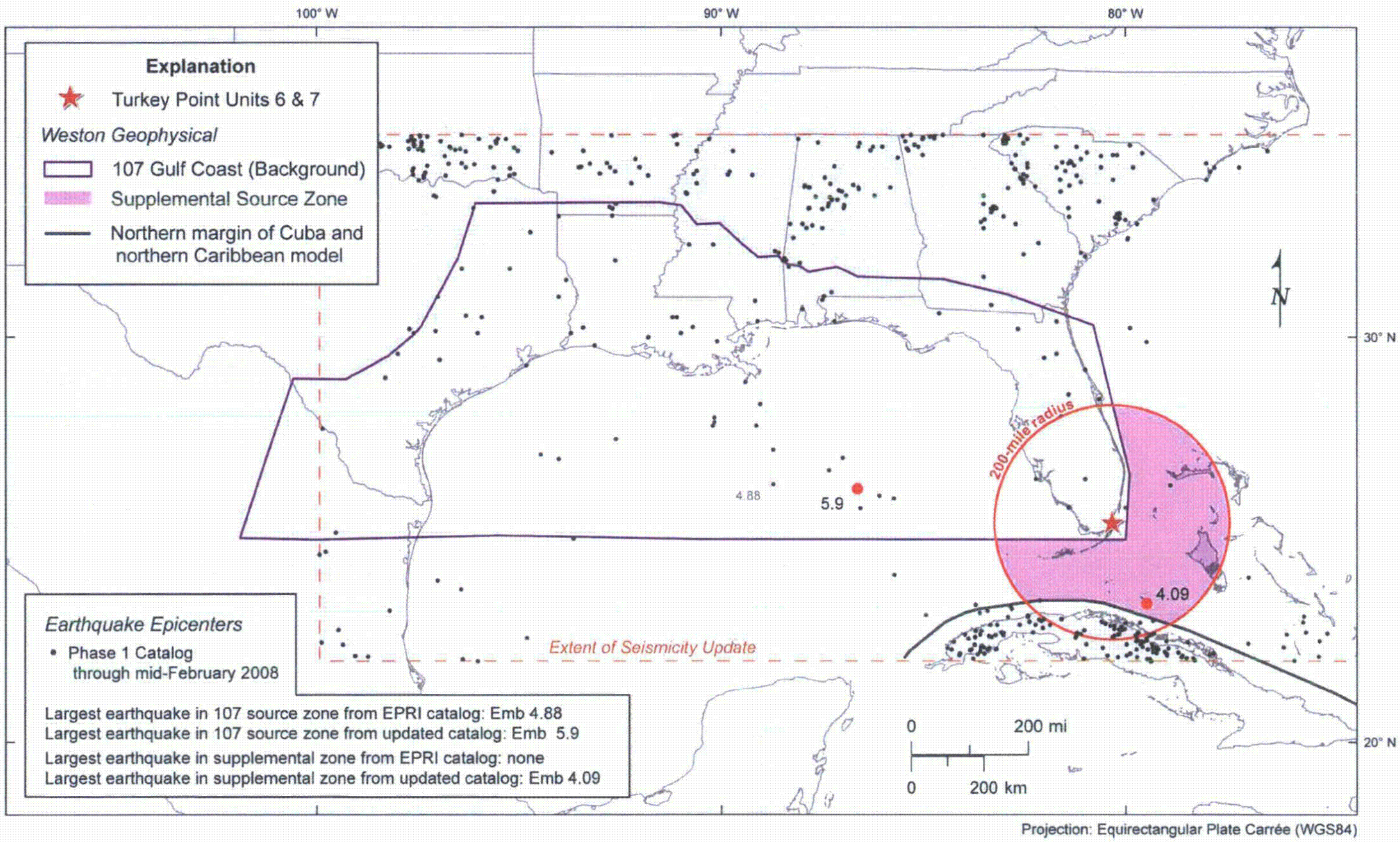

Note: Epicenters of the largest magnitude events in the seismic source zones are highlighted as red dots.

PTN COL 2.5-2

Figure 2.5.2-209 EPRI and Supplemental Source Zones — Woodward-Clyde

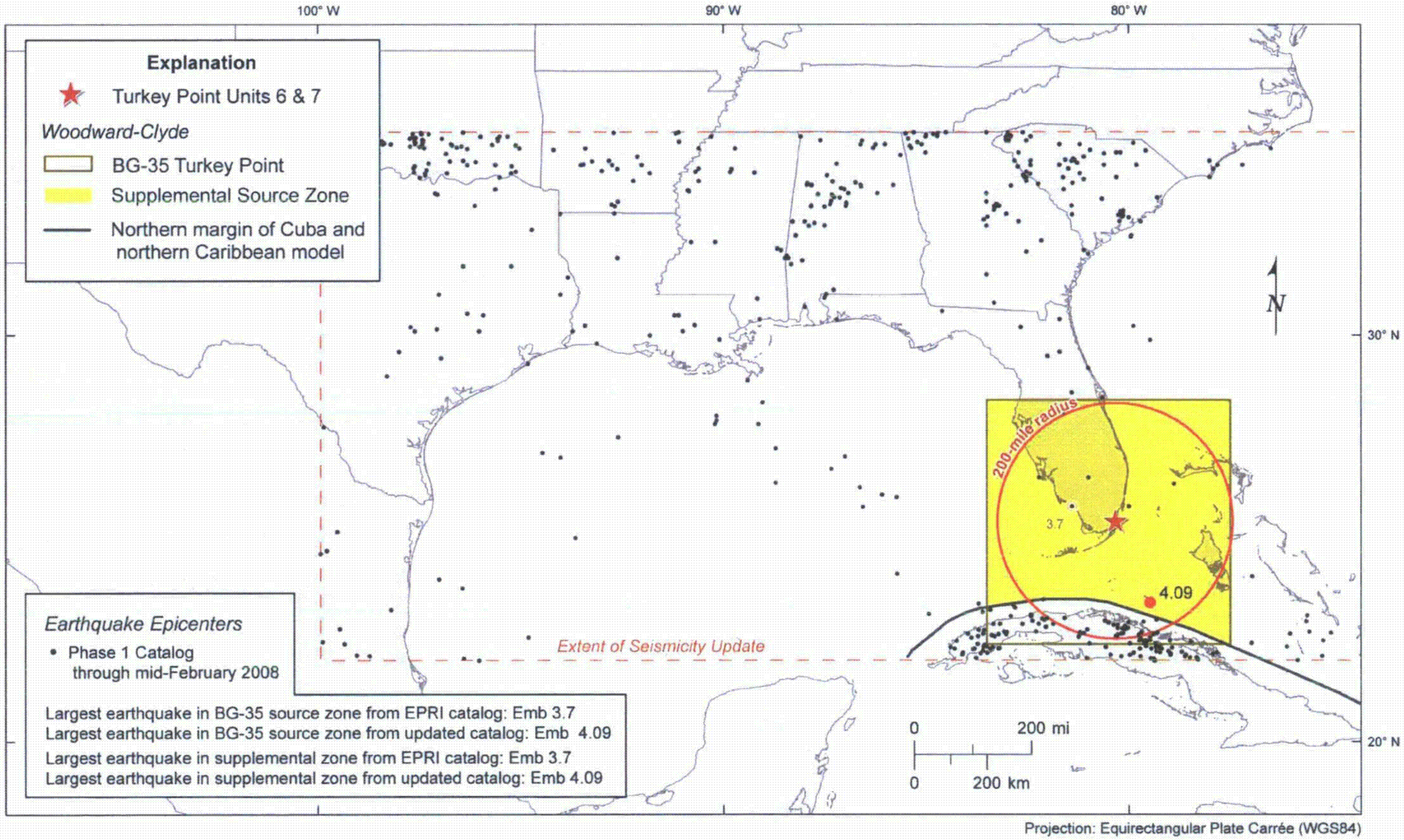

Note: Epicenters of the largest magnitude events in the seismic source zones are highlighted as red dots.

PTN COL 2.5-2

Figure 2.5.2-210 Historical Seismicity from EPRI Earthquake Catalog and from Updated Catalog (Through 2007) in Southeastern United States

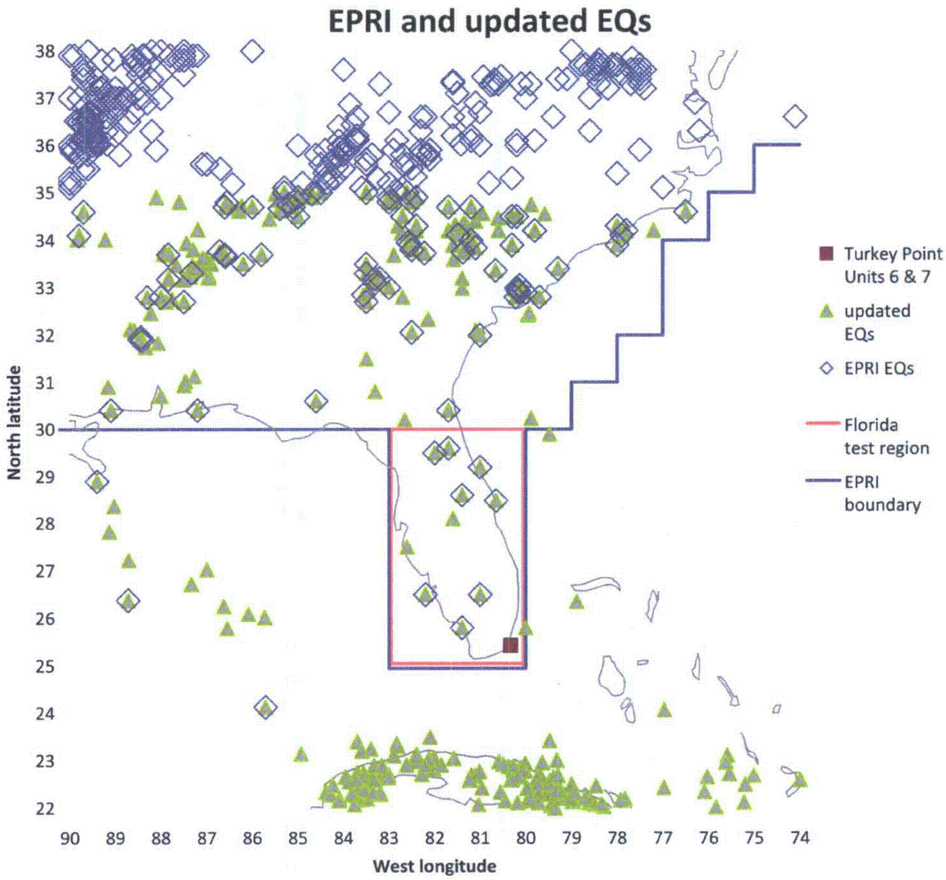

Note: The boundary of the EPRI study region is shown in blue, and the Florida test region used to compare seismicity rates is shown in orange.

PTN COL 2.5-2

Figure 2.5.2-211 Earthquake Occurrence Rates for EPRI Catalog and for Updated Catalog Extended Through 2007 for Florida Test Region

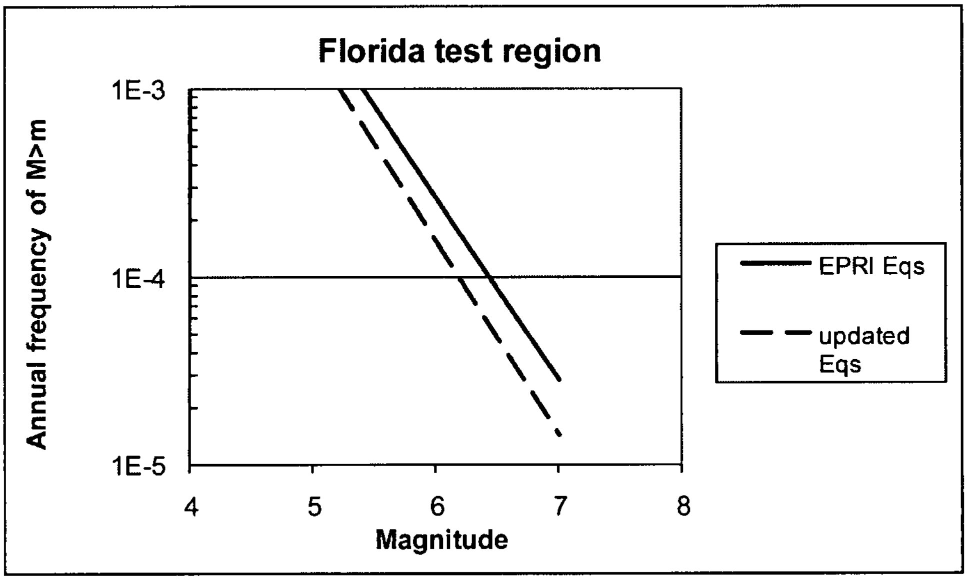

Sources: References 245 and 246

PTN COL 2.5-2

Figure 2.5.2-212 Updated Charleston Seismic Source (UCSS) Model Sources

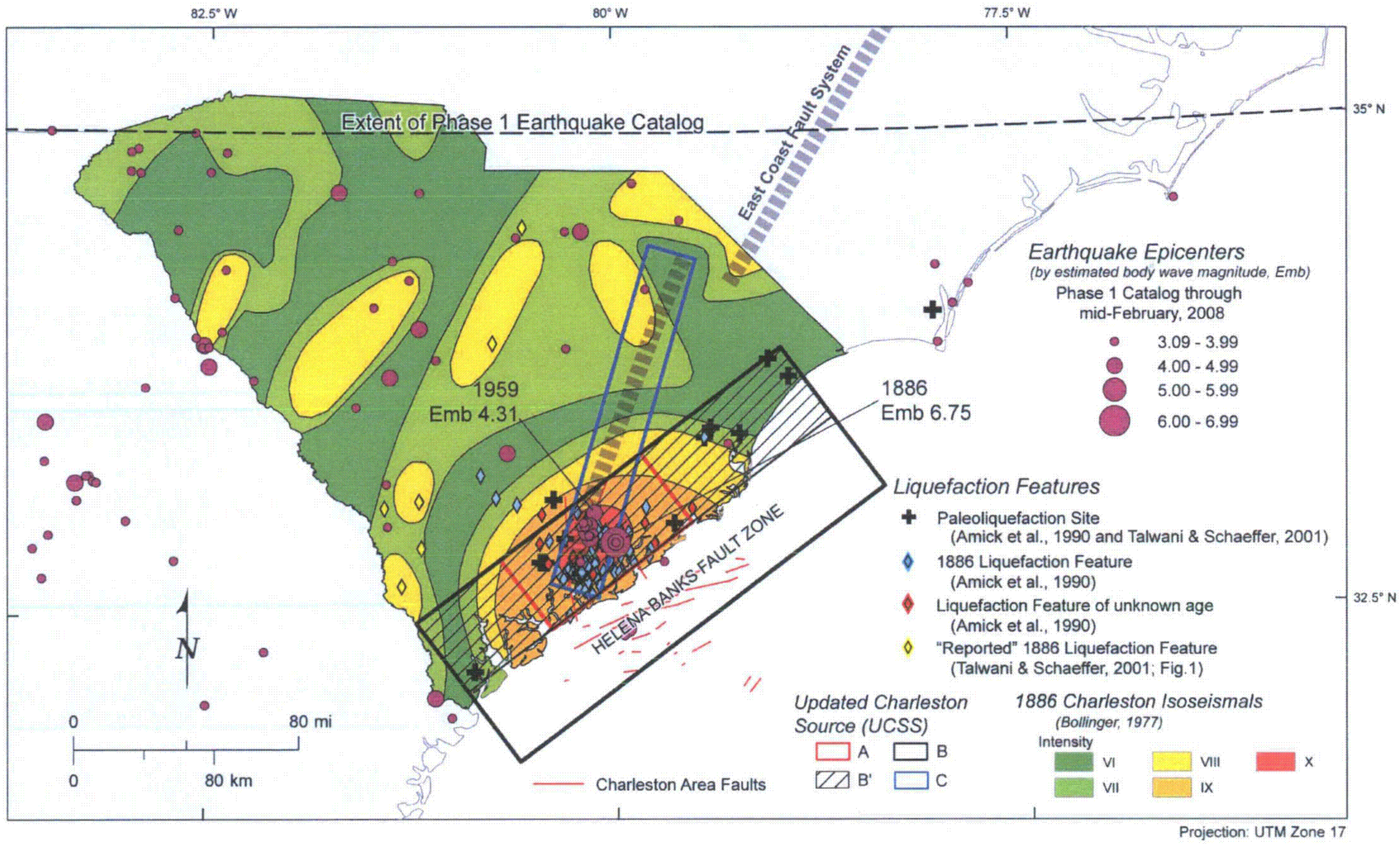

Sources of liquefaction features: References 207, 208, and 323
Source of the 1886 Charleston isoseismals: Reference 216

PTN COL 2.5-2

Figure 2.5.2-213 Updated Charleston Seismic Source (UCSS) Logic Tree with Weights for Each Branch

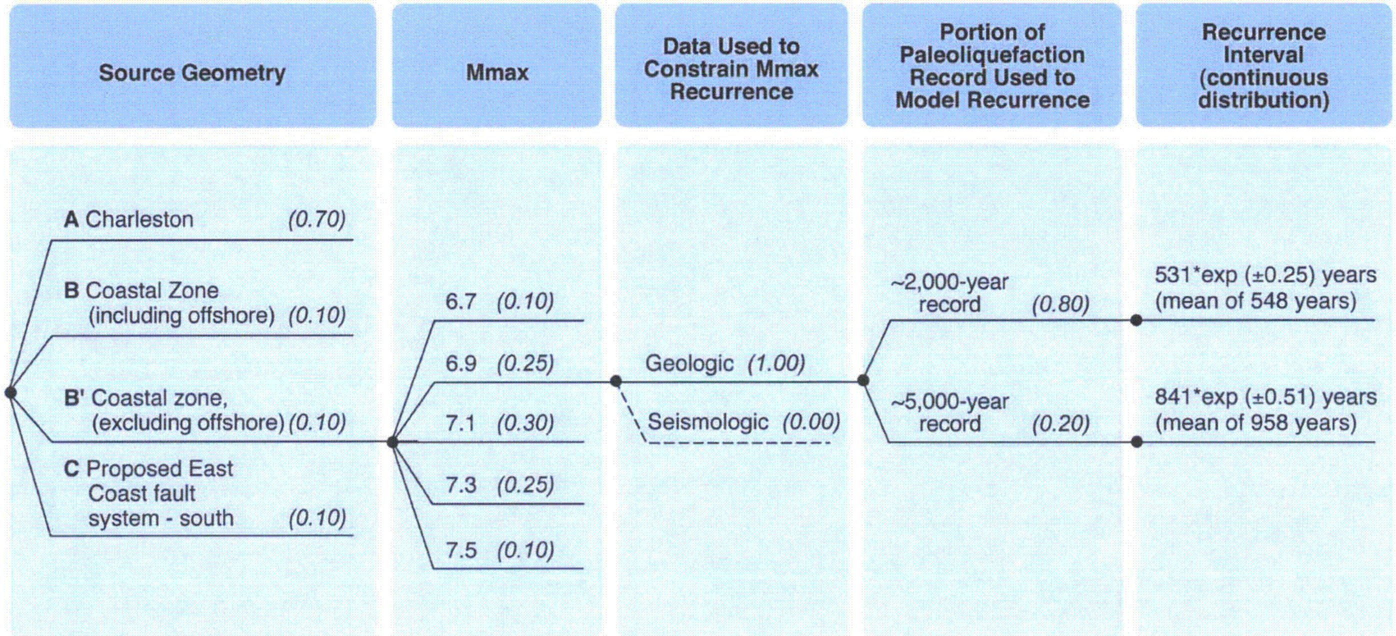

PTN COL 2.5-2

Figure 2.5.2-214 Tectonic Features and Significant Earthquakes of Cuba Area and the North America-Caribbean Plate Boundary Region

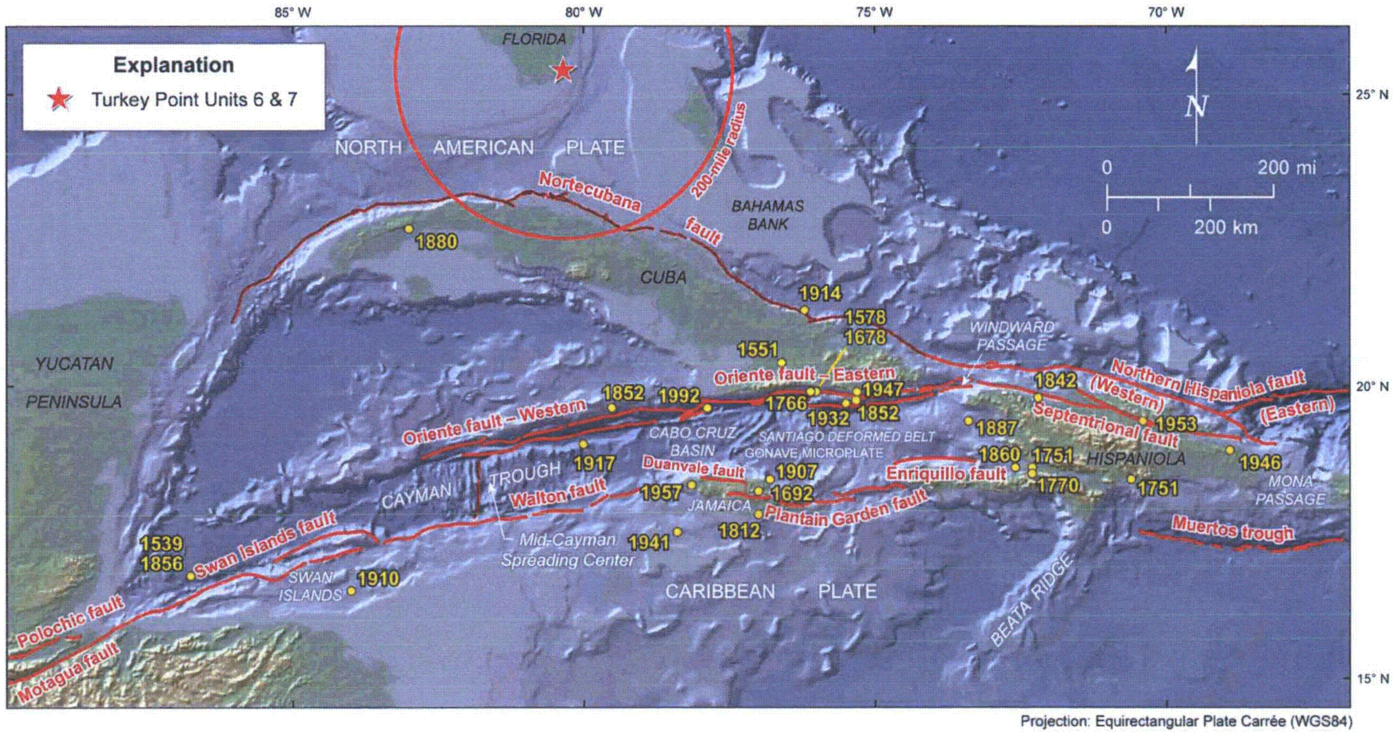

PTN COL 2.5-2

Figure 2.5.2-215 Fault Map of Cuba from Garcia et al.

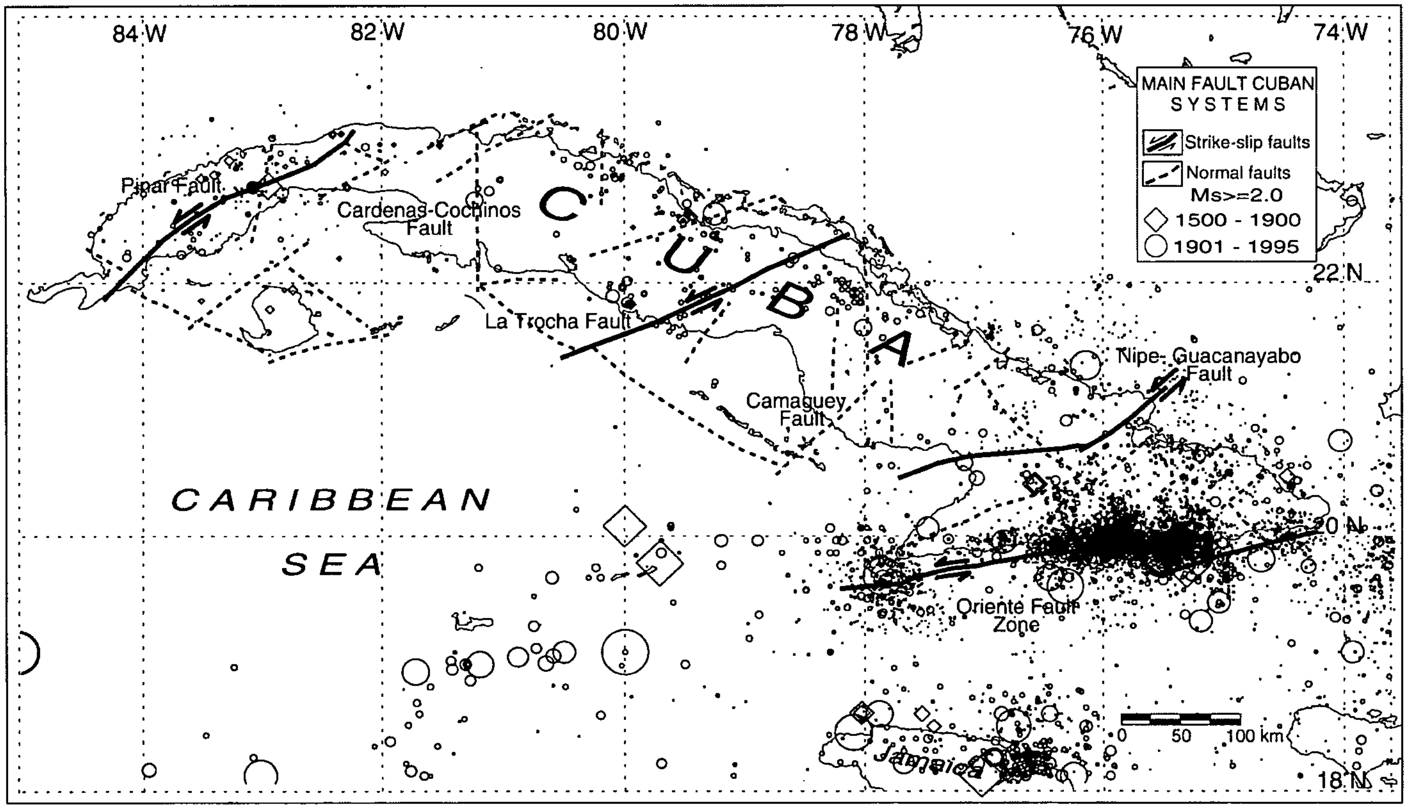

Figure 5. Map of the principal faults in Cuba (modified from Iturralde-Vinent, 1996). Solid lines show strike-slip faults; dashed lines represent normal faults. The epicenters of earthquakes (diamond, pre-1900; circles, during the twentieth century) with magnitude larger than, or equal to, 2 are reported.

Source: Reference 254

PTN COL 2.5-2

Figure 2.5.2-216 Seismicity in the Cuba Area and the North America-Caribbean Plate Boundary Region, 1500–2008

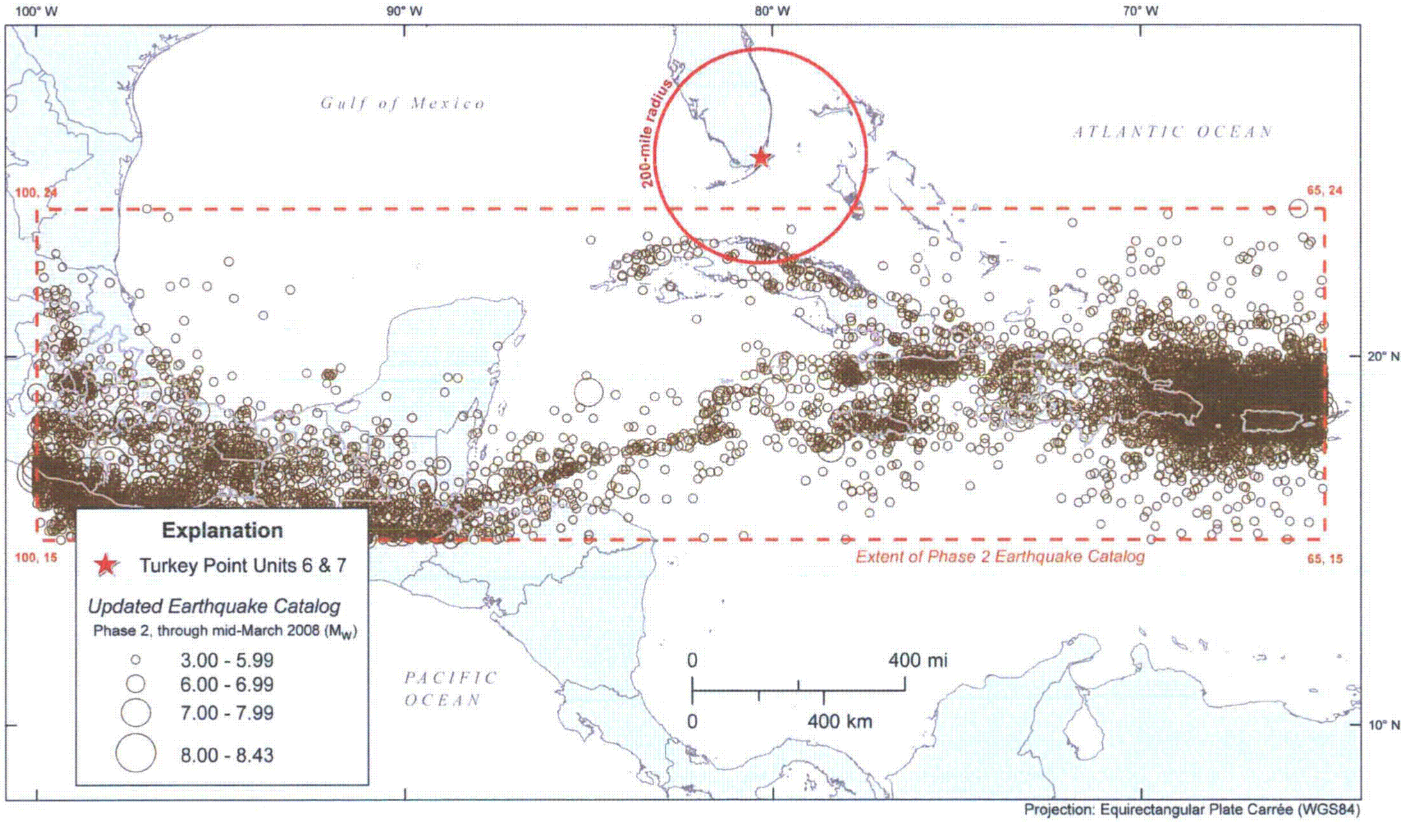

PTN COL 2.5-2

Figure 2.5.2-217 Cuba and Northern Caribbean Seismic Source Model Sources

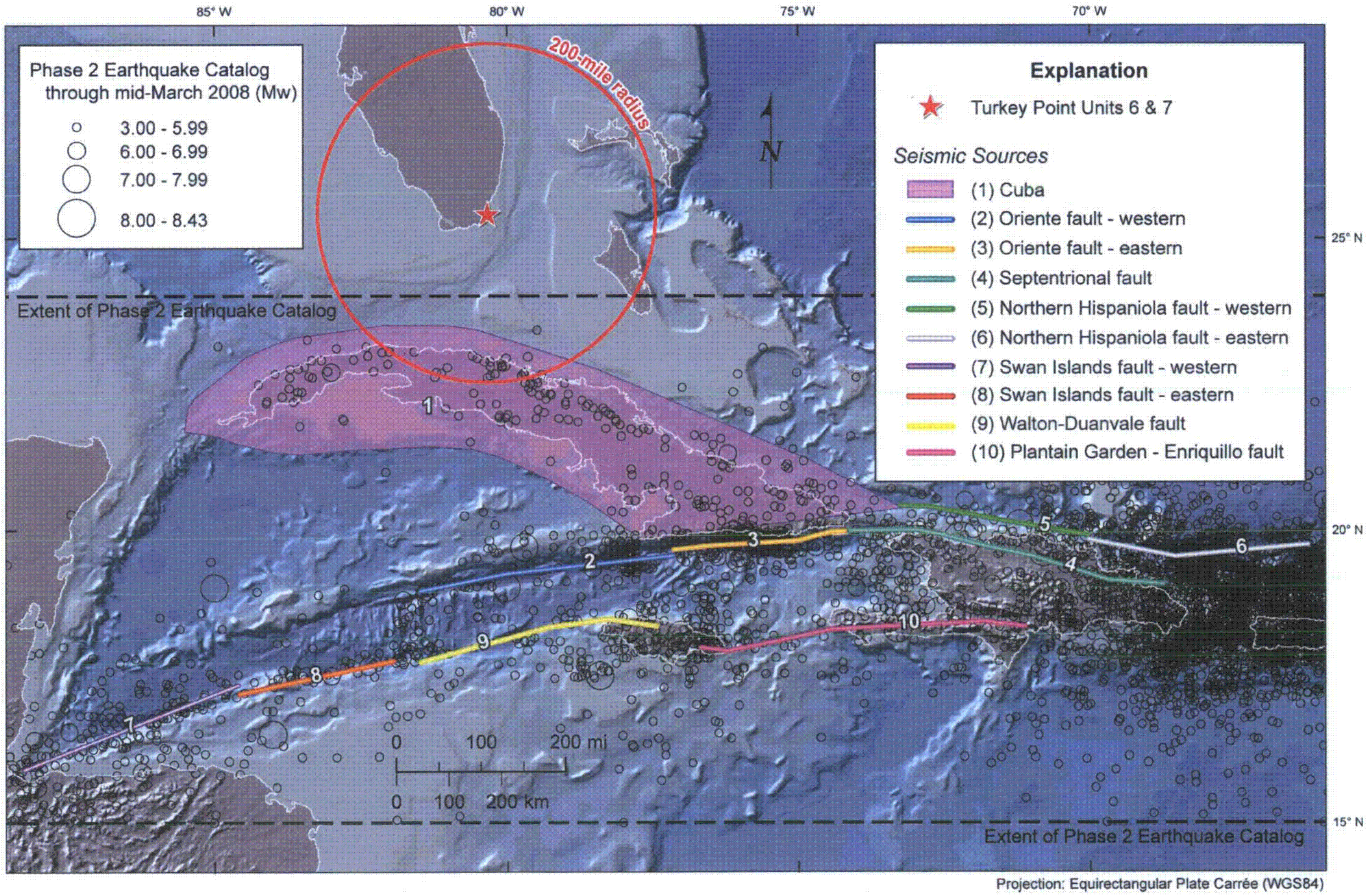

PTN COL 2.5-2

Figure 2.5.2-218 Mean and Fractile Rock PGA Seismic Hazard Curves

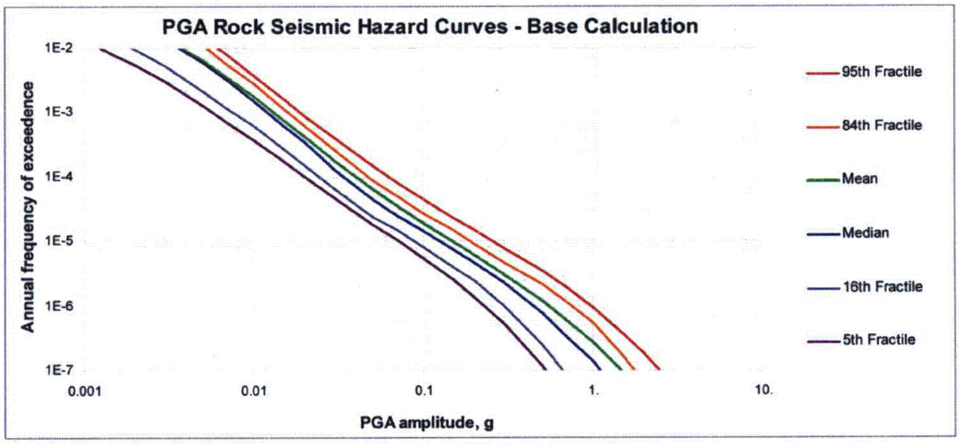

PTN COL 2.5-2

Figure 2.5.2-219 Mean and Fractile Rock 25 Hz Seismic Hazard Curves, Rock

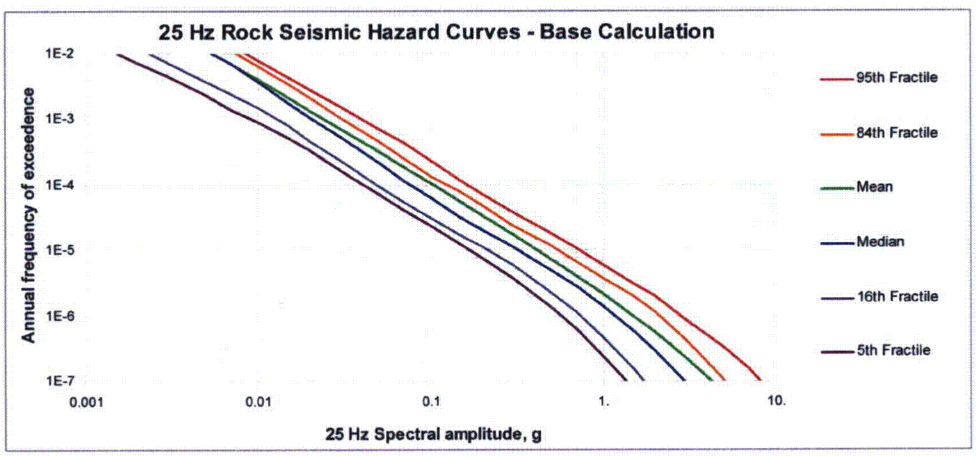

PTN COL 2.5-2

Figure 2.5.2-220 Mean and Fractile Rock 10 Hz Seismic Hazard Curves, Rock

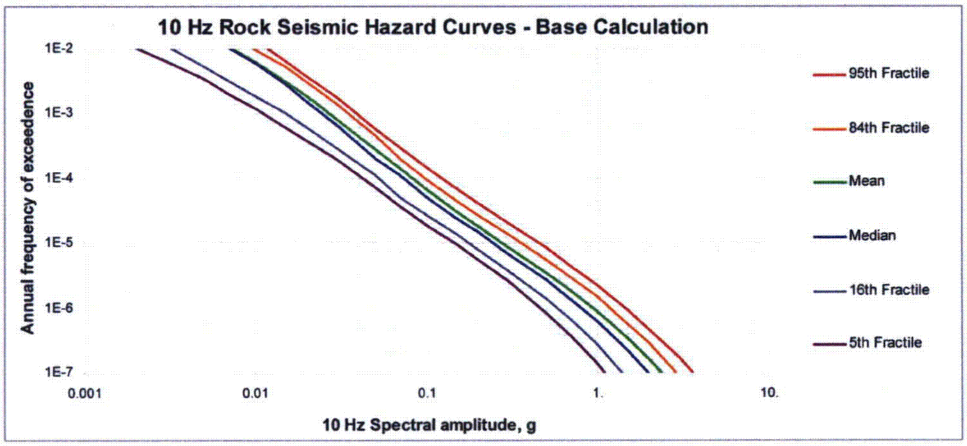

PTN COL 2.5-2

Figure 2.5.2-221 Mean and Fractile Rock 5 Hz Seismic Hazard Curves, Rock

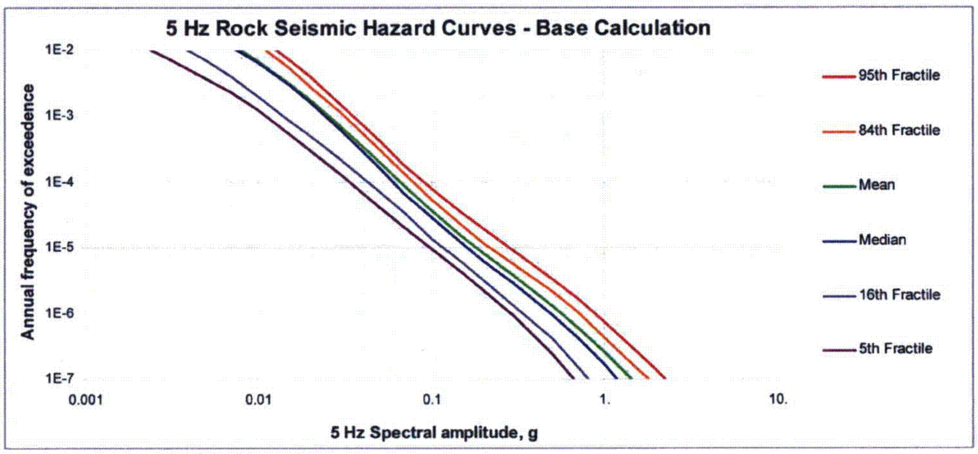

PTN COL 2.5-2

Figure 2.5.2-222 Mean and Fractile Rock 2.5 Hz Seismic Hazard Curves, Rock

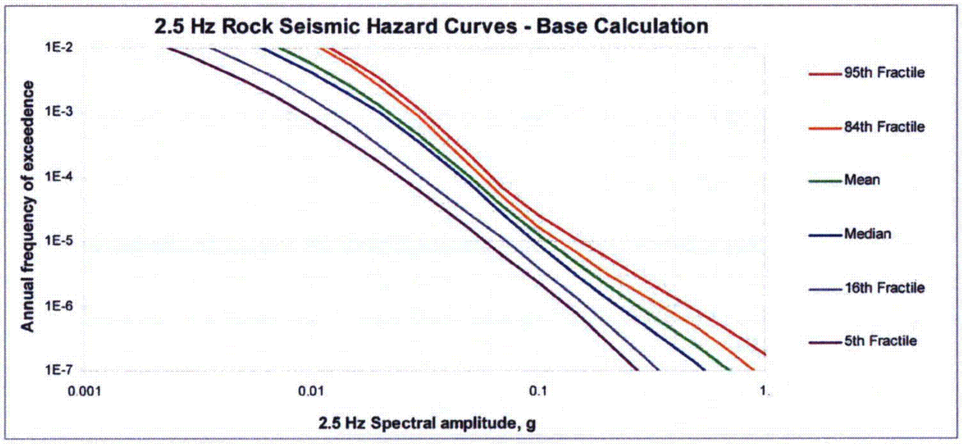

PTN COL 2.5-2

Figure 2.5.2-223 Mean and Fractile Rock 1 Hz Seismic Hazard Curves, Rock

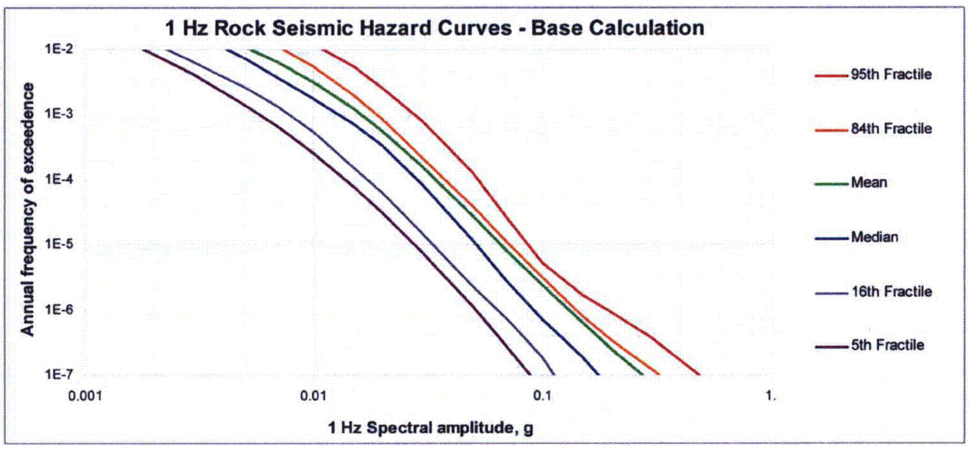

PTN COL 2.5-2

Figure 2.5.2-224 Mean and Fractile Rock 0.5 Hz Seismic Hazard Curves, Rock

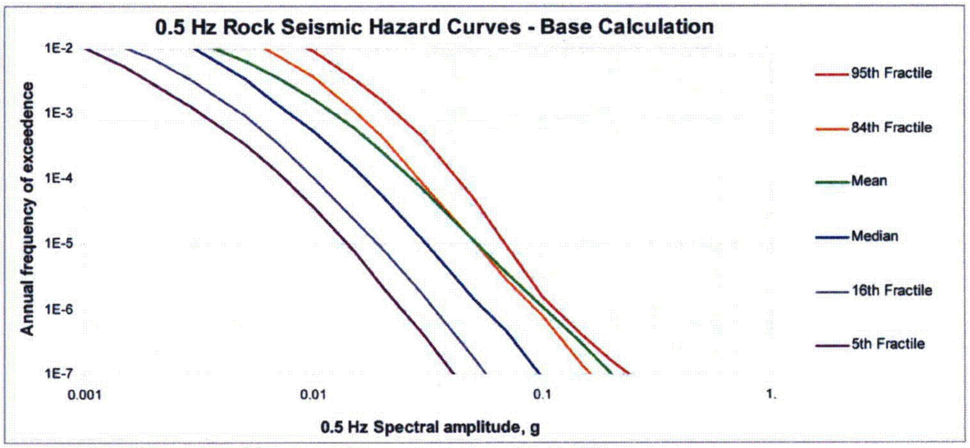

PTN COL 2.5-2

Figure 2.5.2-225 Mean and Median Rock UHRS for 1E-04, 1E-05, and 1E-06

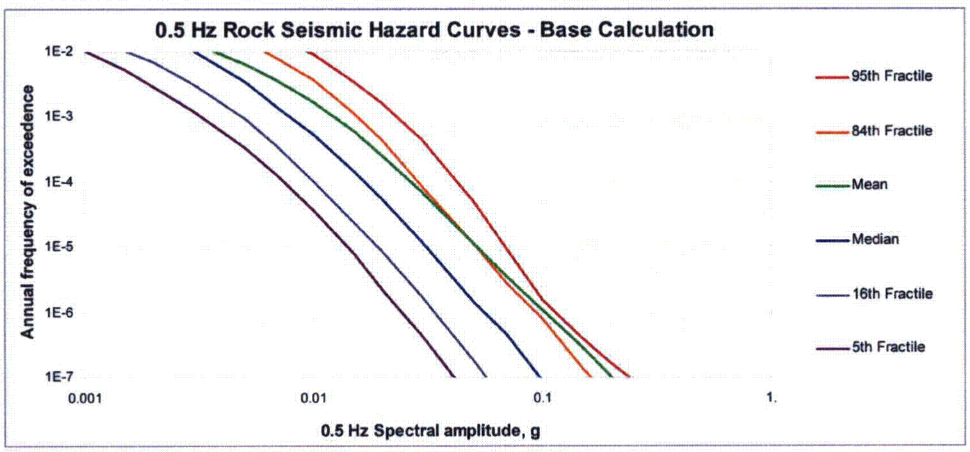

PTN COL 2.5-2

Figure 2.5.2-226 M and R Deaggregation for 1 and 2.5 Hz at 1E-04 Annual Frequency of Exceedence

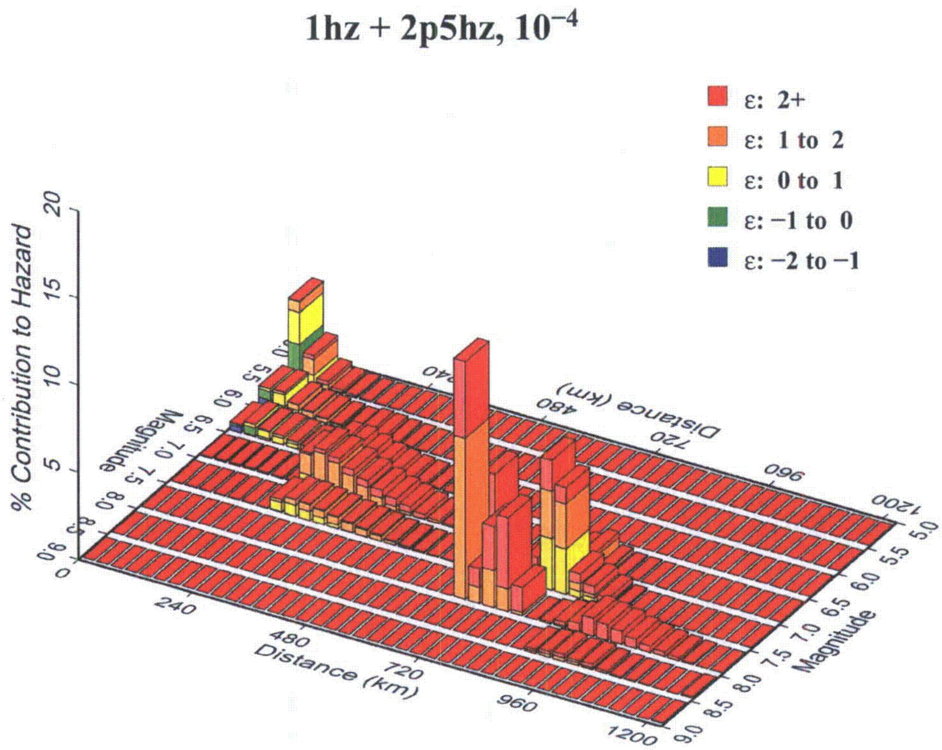

PTN COL 2.5-2

Figure 2.5.2-227 M and R Deaggregation for 5 and 10 Hz at 1E-04 Annual Frequency of Exceedence

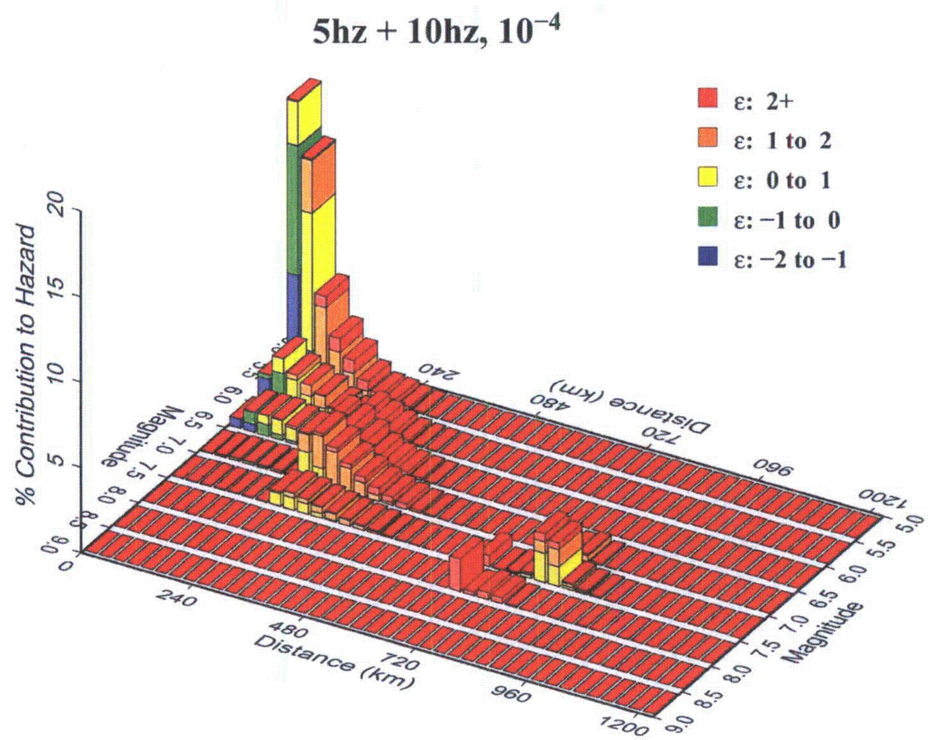

PTN COL 2.5-2

Figure 2.5.2-228 M and R Deaggregation for 1 and 2.5 Hz at 1E-05 Annual Frequency of Exceedence

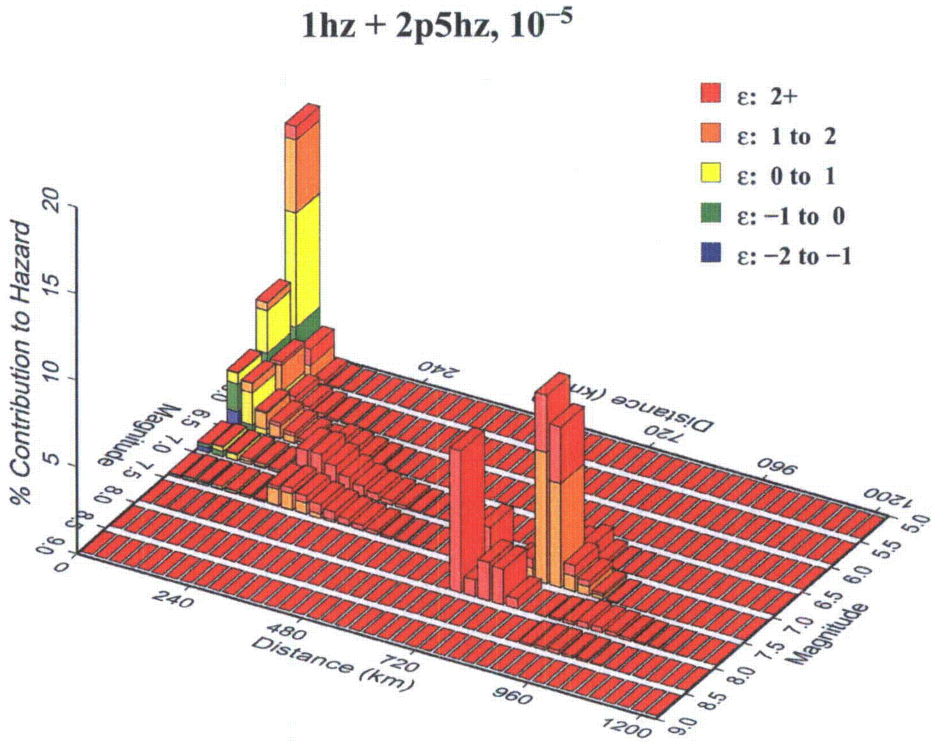

PTN COL 2.5-2

Figure 2.5.2-229 M and R Deaggregation for 5 and 10 Hz at 1E-05 Annual Frequency of Exceedence

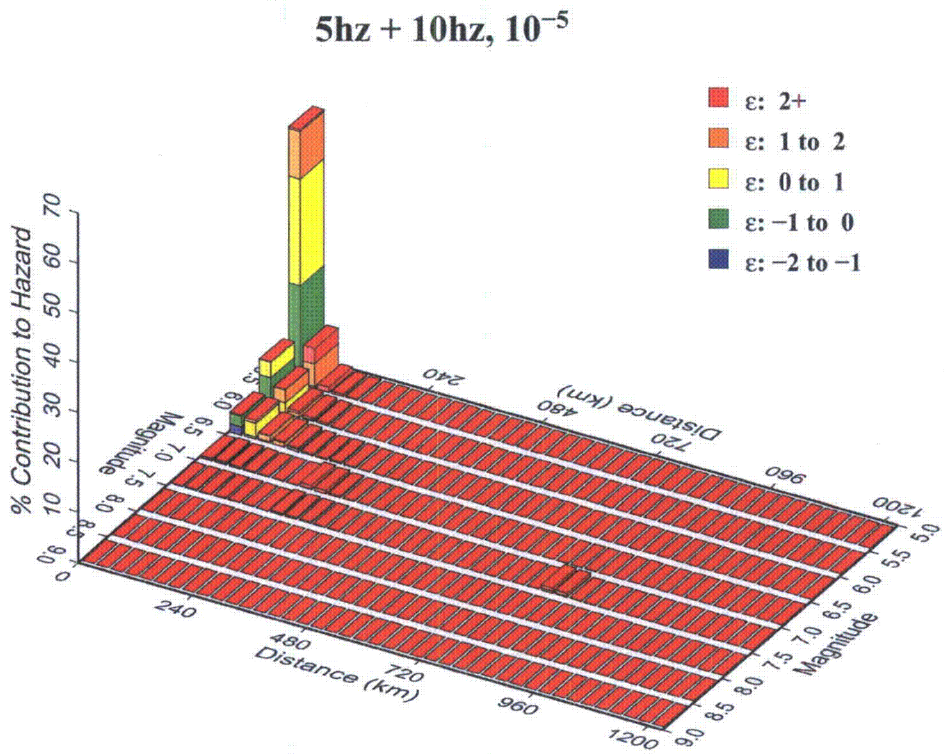

PTN COL 2.5-2

Figure 2.5.2-230 M and R Deaggregation for 1 and 2.5 Hz at 1E-06 Annual Frequency of Exceedence

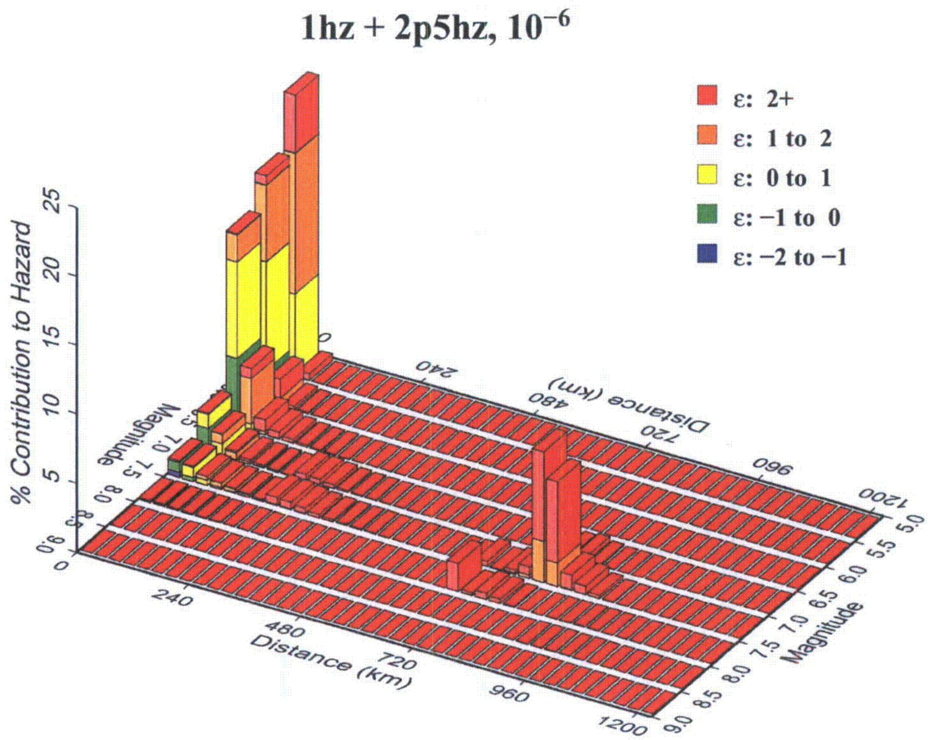

PTN COL 2.5-2

Figure 2.5.2-231 M and R Deaggregation for 5 and 10 Hz at 1E-06 Annual Frequency of Exceedence

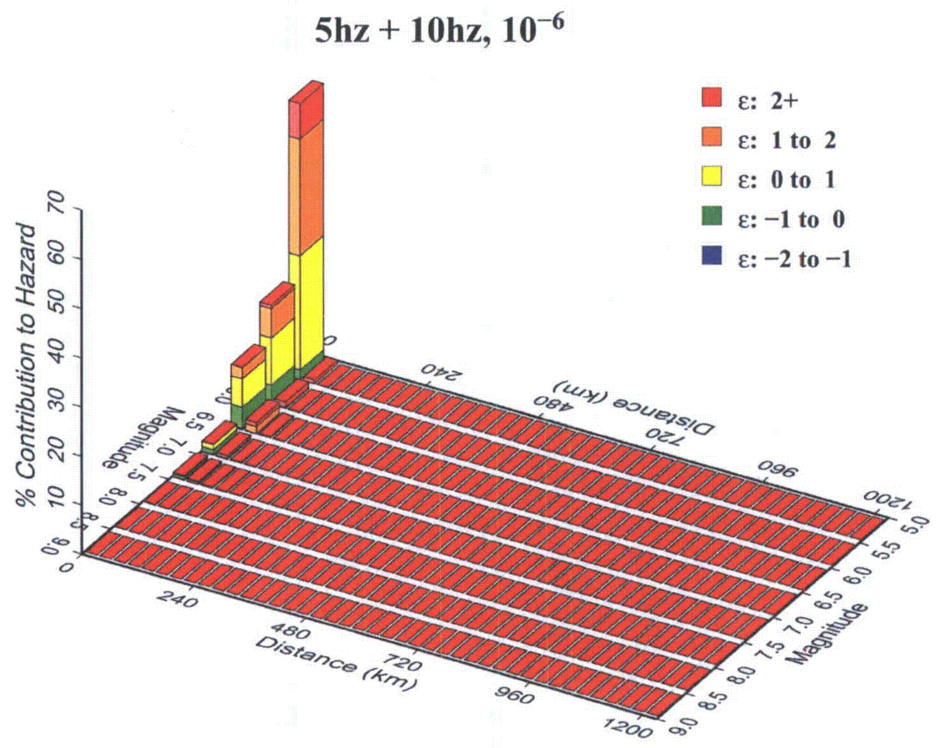

PTN COL 2.5-2

Figure 2.5.2-232 HF and LF Rock Spectra Anchored to Mean UHRS Values from Hazard Calculation for 1E-04 Spectra

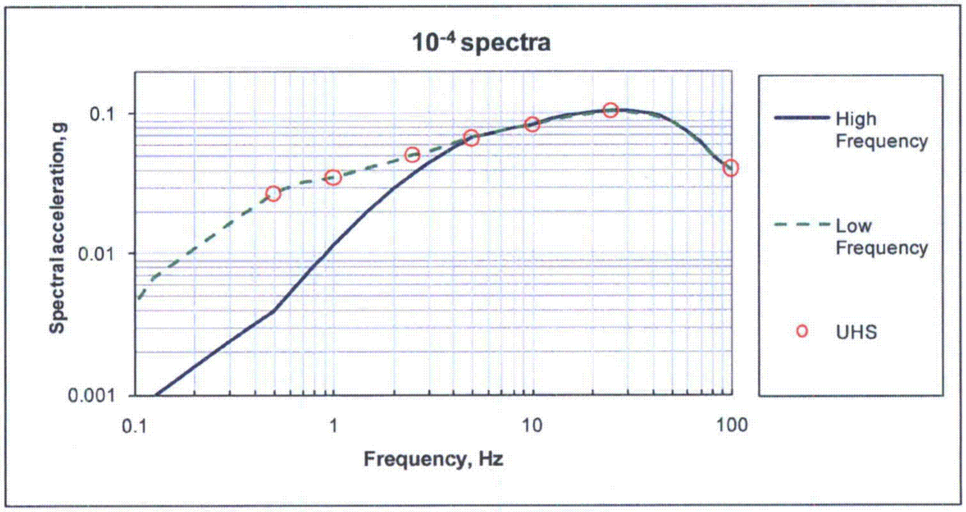

PTN COL 2.5-2

Figure 2.5.2-233 HF and LF Rock Spectra Anchored to Mean UHRS Values from Hazard Calculation for 1E-05 Spectra

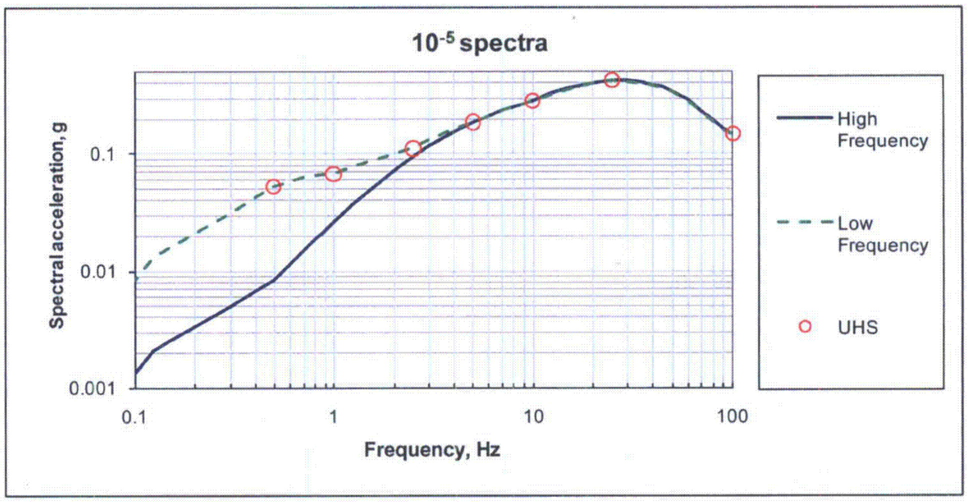

PTN COL 2.5-2

Figure 2.5.2-234 HF and LF Rock Spectra Anchored to Mean UHRS Values from Hazard Calculation for 1E-06 Spectra

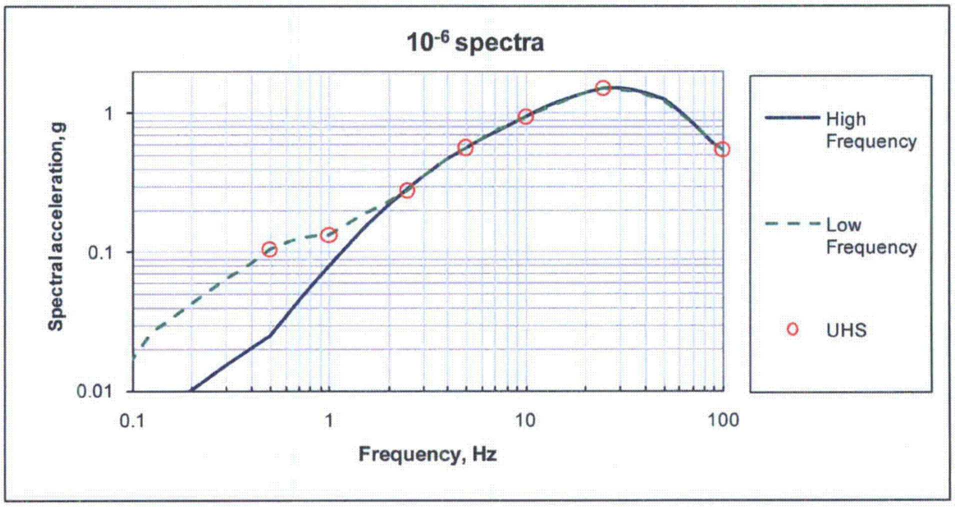

PTN COL 2.5-2

Figure 2.5.2-235 Input Base Case Shear Wave Velocity Profile

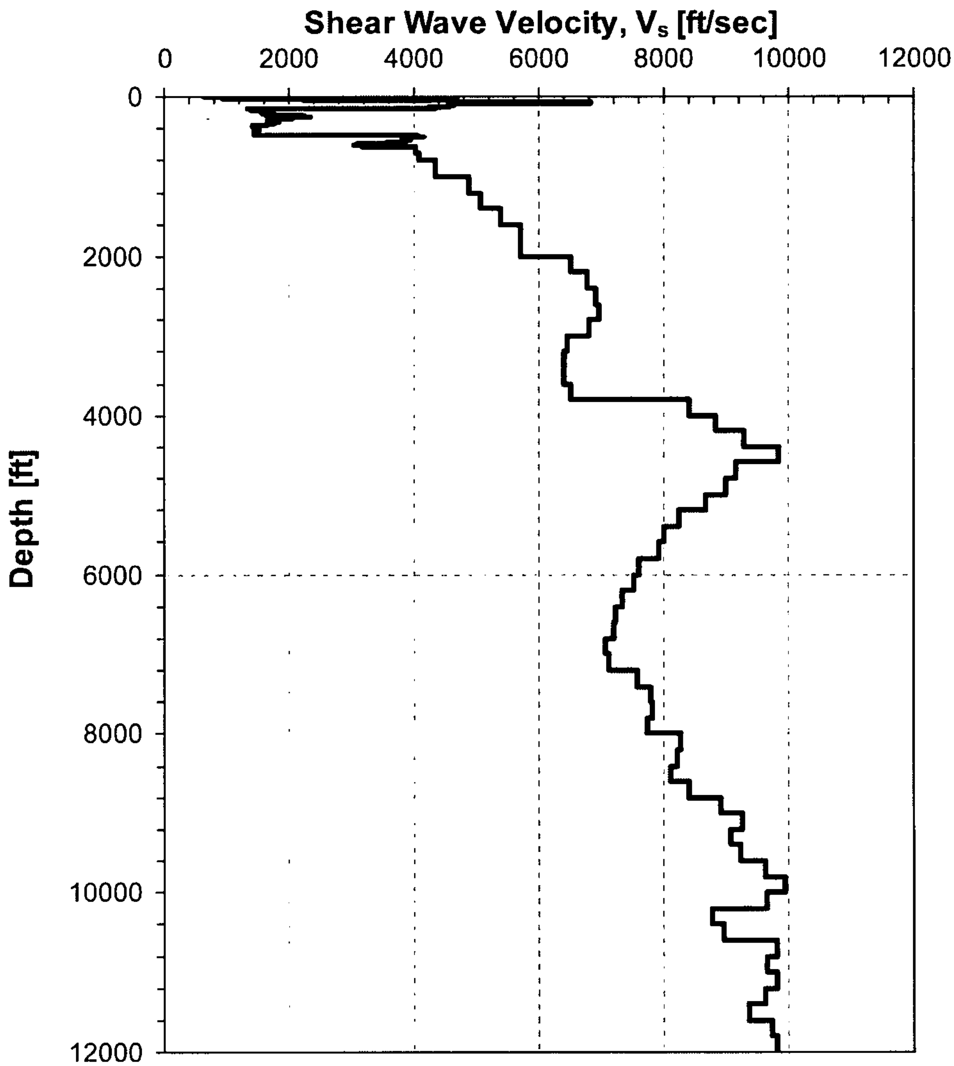

PTN COL 2.5-2

Figure 2.5.2-236 Input Median Shear Wave Velocity Profile (+/- One Standard Deviation) for Randomization Process

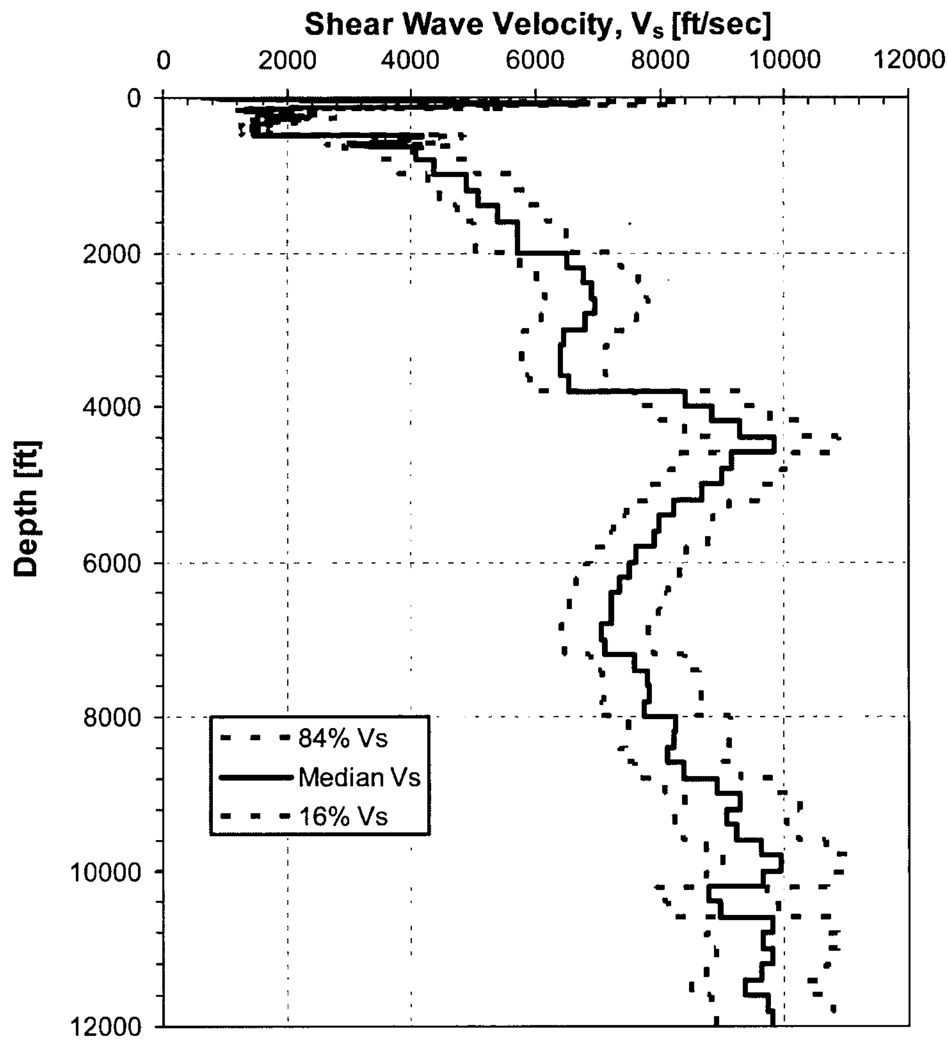

PTN COL 2.5-2

Figure 2.5.2-237 Strain Dependent Degradation Curves for Natural Soils (<150 feet)

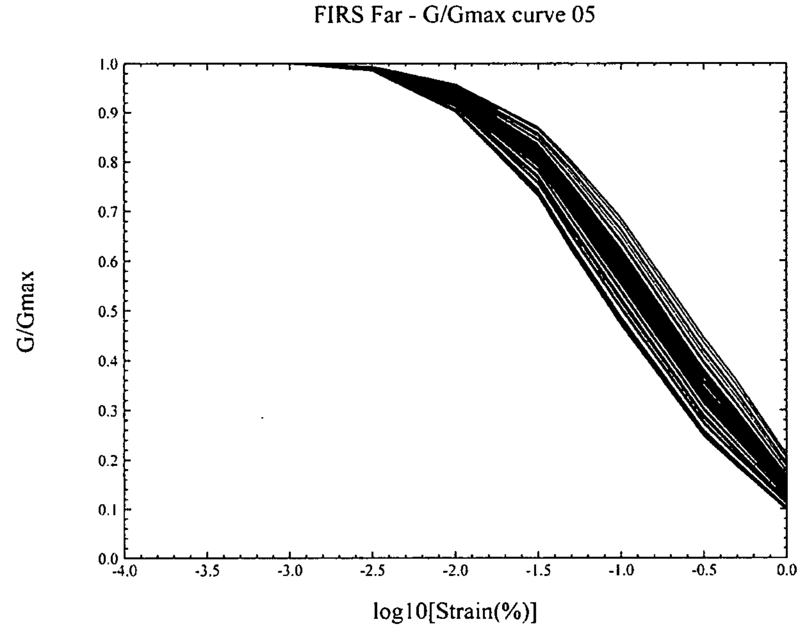

PTN COL 2.5-2

Figure 2.5.2-238 Strain Dependent Damping Ratio Properties for Natural Soils (<150 feet)

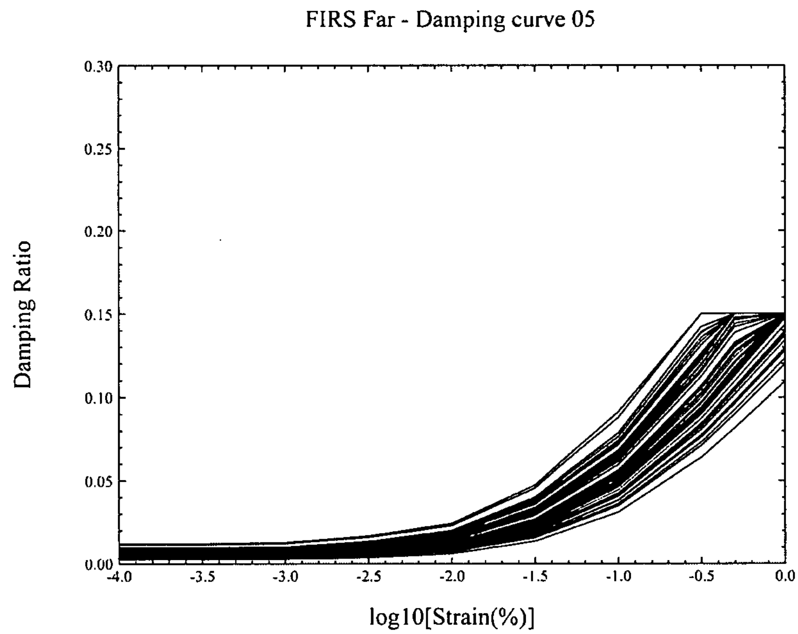

PTN COL 2.5-2

Figure 2.5.2-239 Randomized Shear Wave Velocity Profiles, Median Shear Wave Velocity Profile and the Input Median Profile Used For Randomization

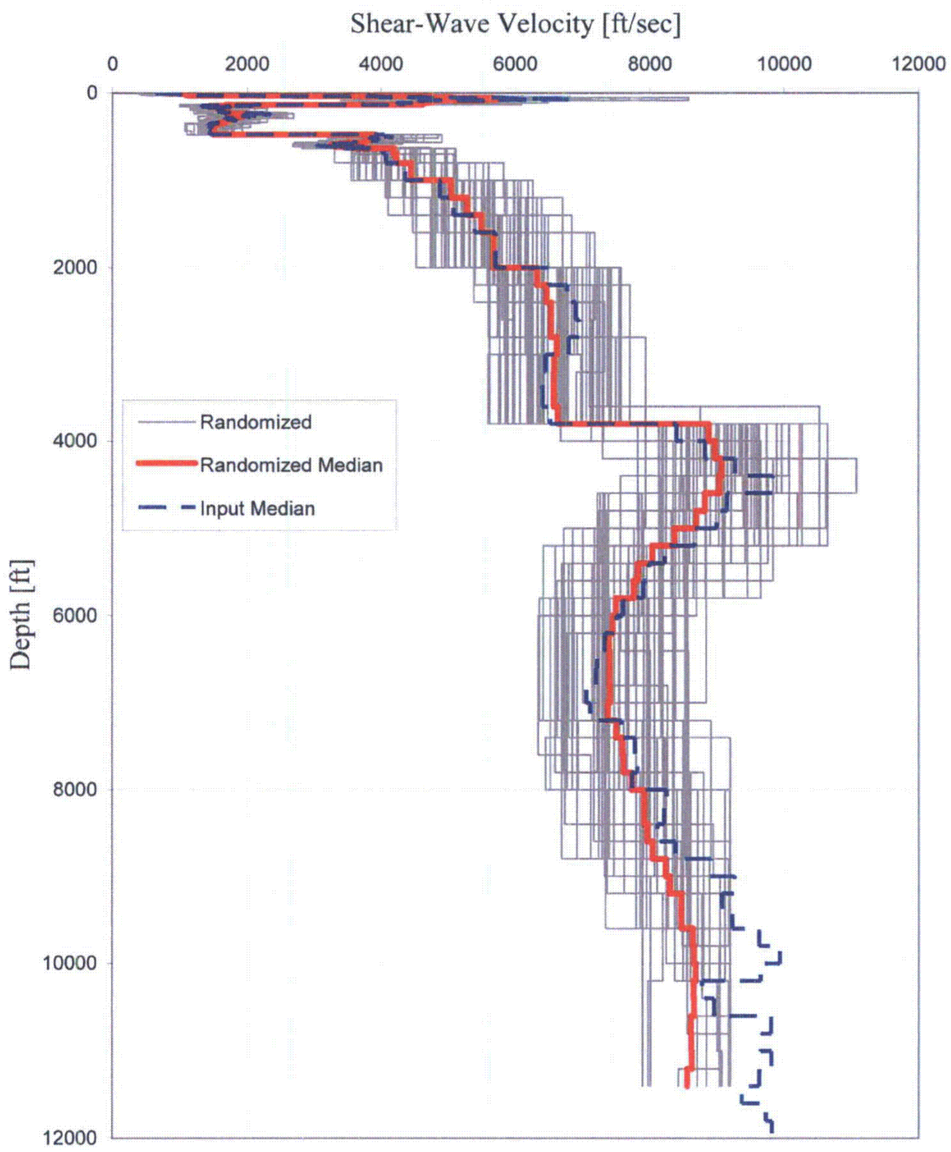

PTN COL 2.5-2

Figure 2.5.2-240 Median of Site Amplification Factors at GMRS Horizon (El. –35 feet) from Analyses of the 60 Random Profiles with the 1E-04 LF Input Motion

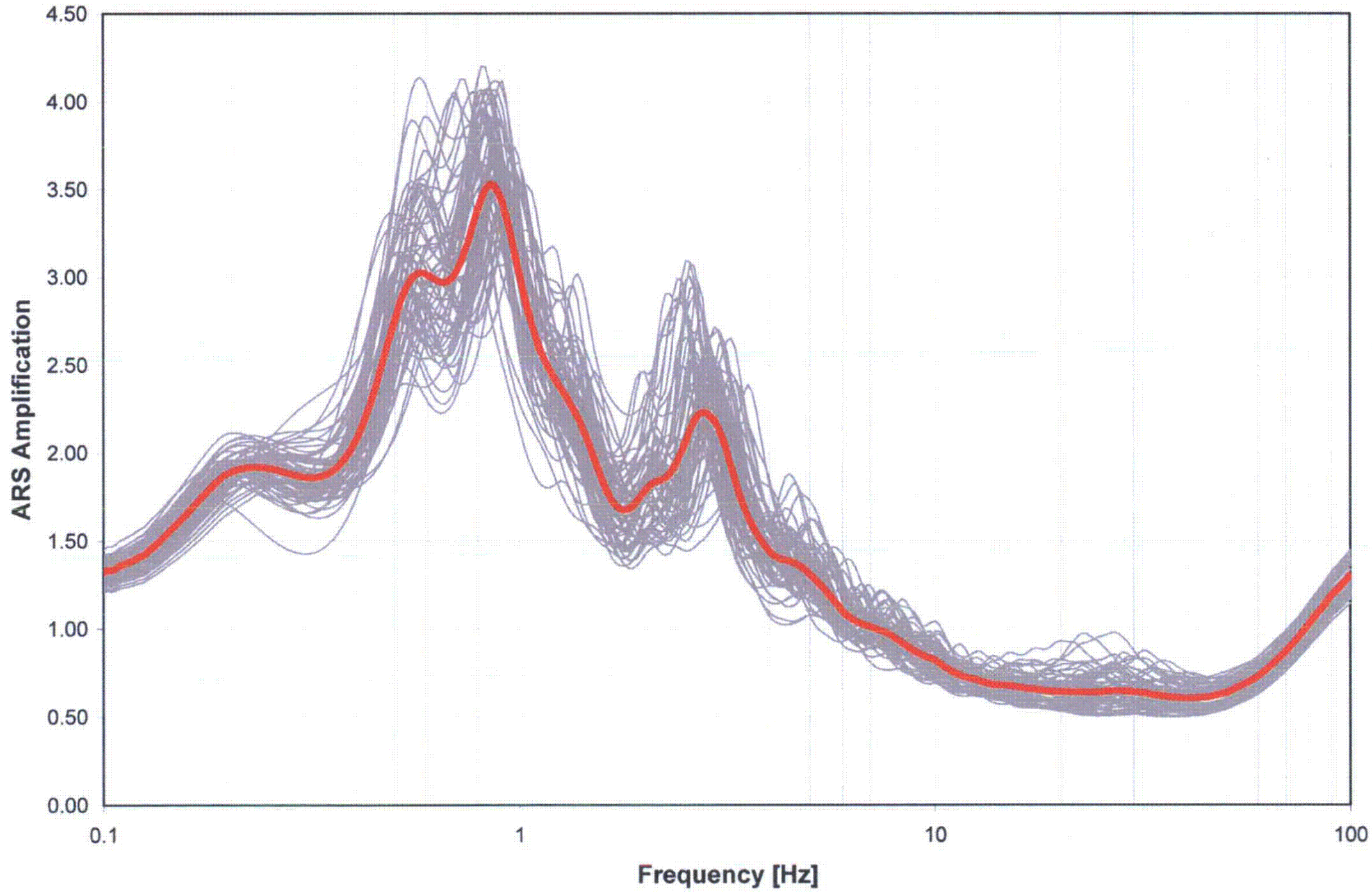

PTN COL 2.5-2

Figure 2.5.2-241 Maximum Strains Versus Depth that are Calculated for the 60 Profiles and their Median (Thick Red Line) with the 1E-04 LF Input Motion

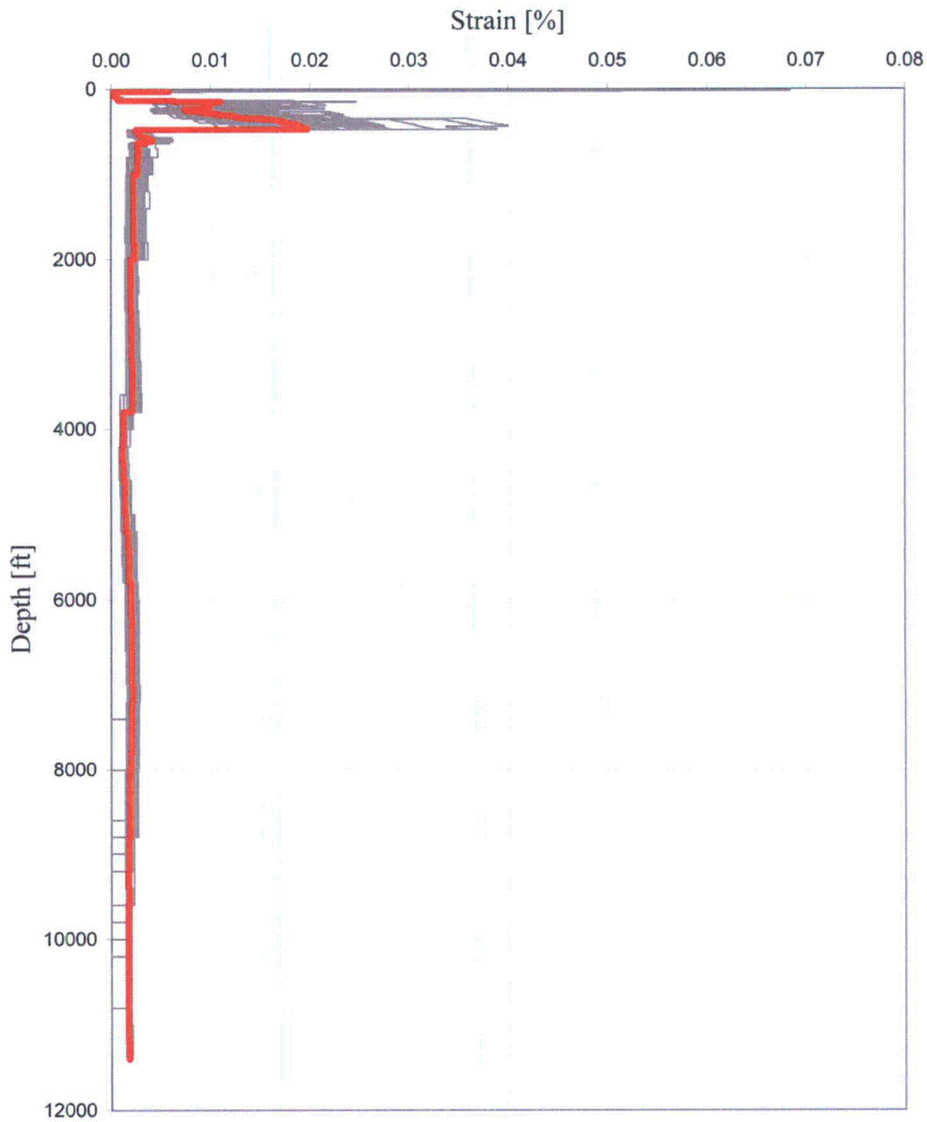

PTN COL 2.5-2

Figure 2.5.2-242 Median of Site Amplification Factors at GMRS Horizon (El. –35 feet) from Analyses of the 60 Random Profiles with the 1E-04 HF Input Motion

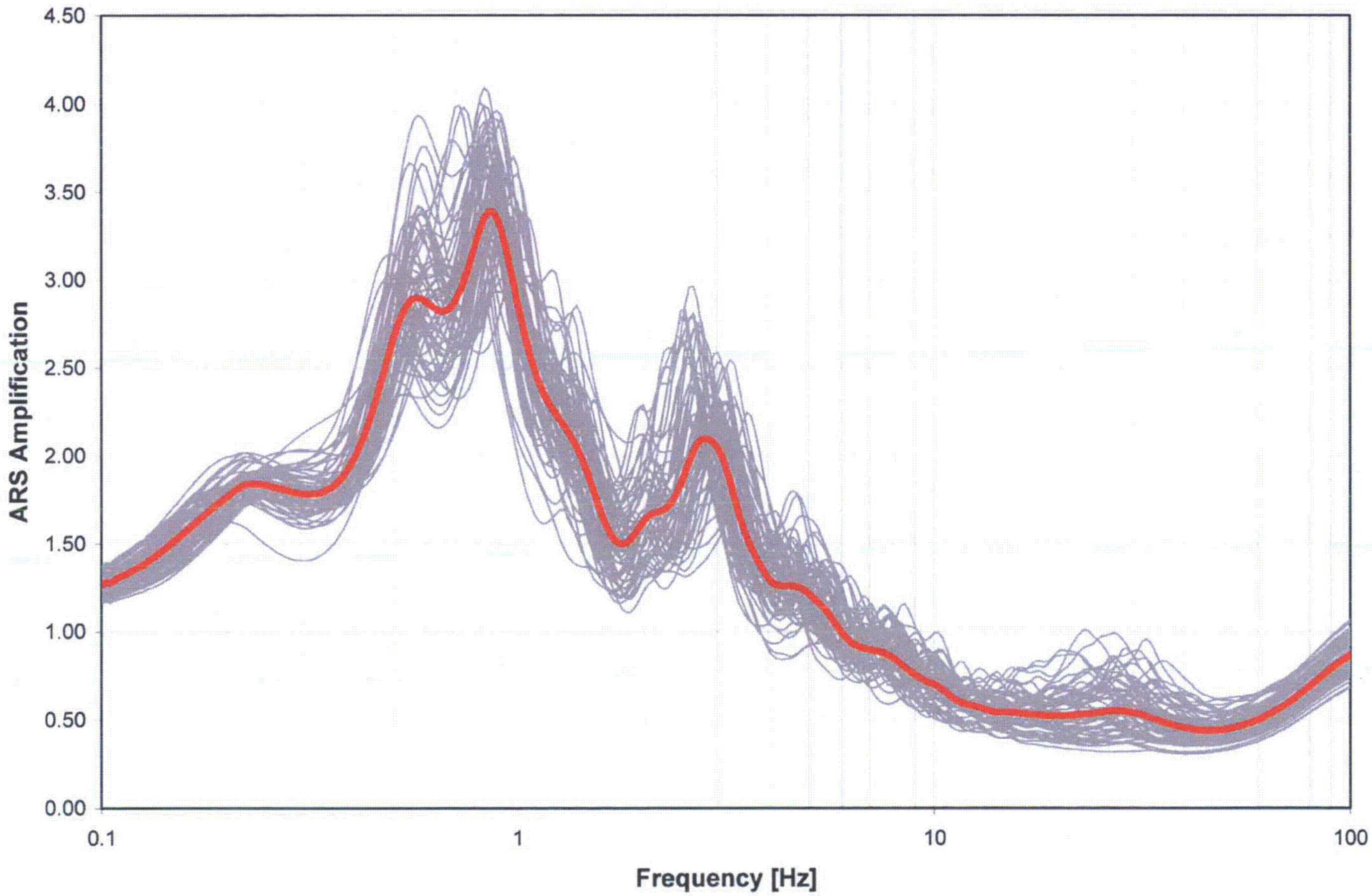

PTN COL 2.5-2

Figure 2.5.2-243 Maximum Strains Versus Depth that are Calculated for the 60 Profiles and their Median (Thick Red Line) with the 1E-04 HF Input Motion

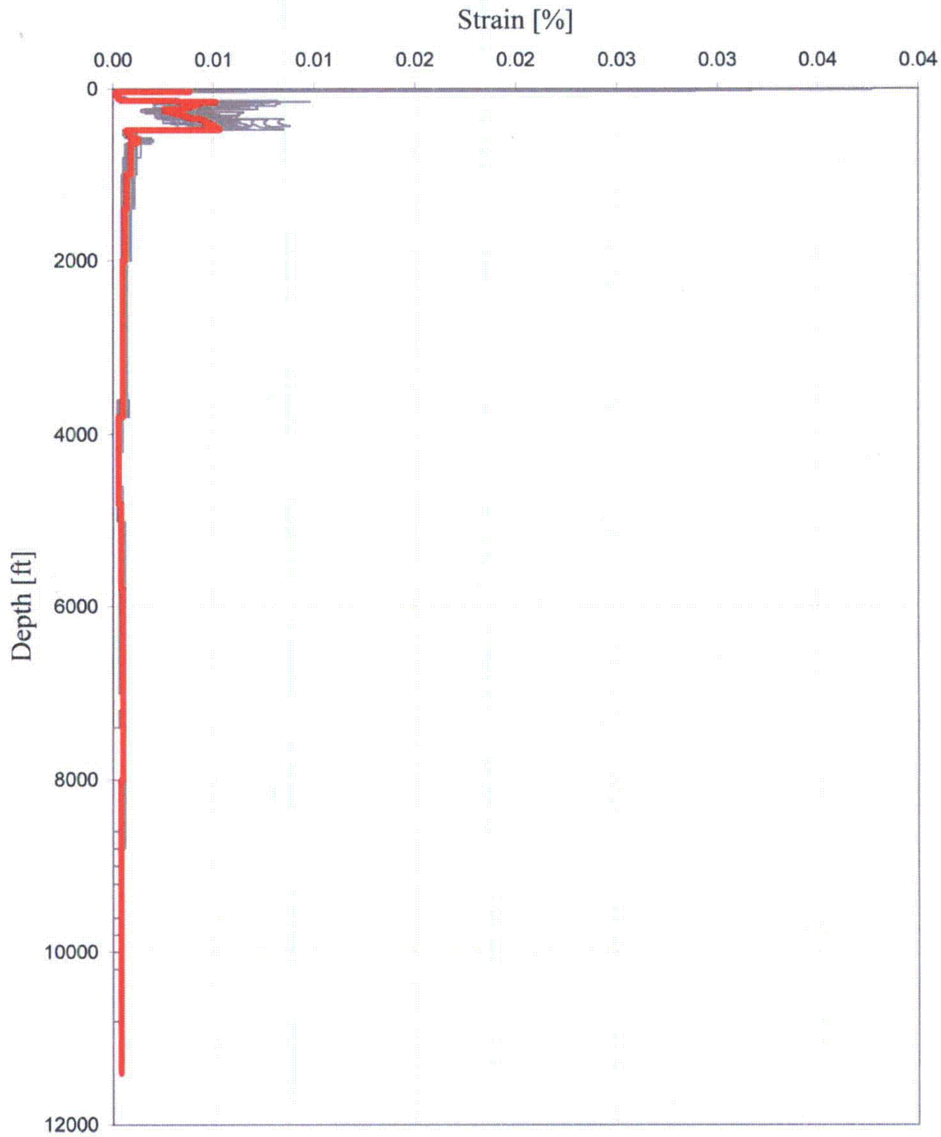

PTN COL 2.5-2

Figure 2.5.2-244 Median of Site Amplification Factors at GMRS Horizon (El. −35 feet) from Analyses of the 60 Random Profiles with the 1E-05 LF Input Motion

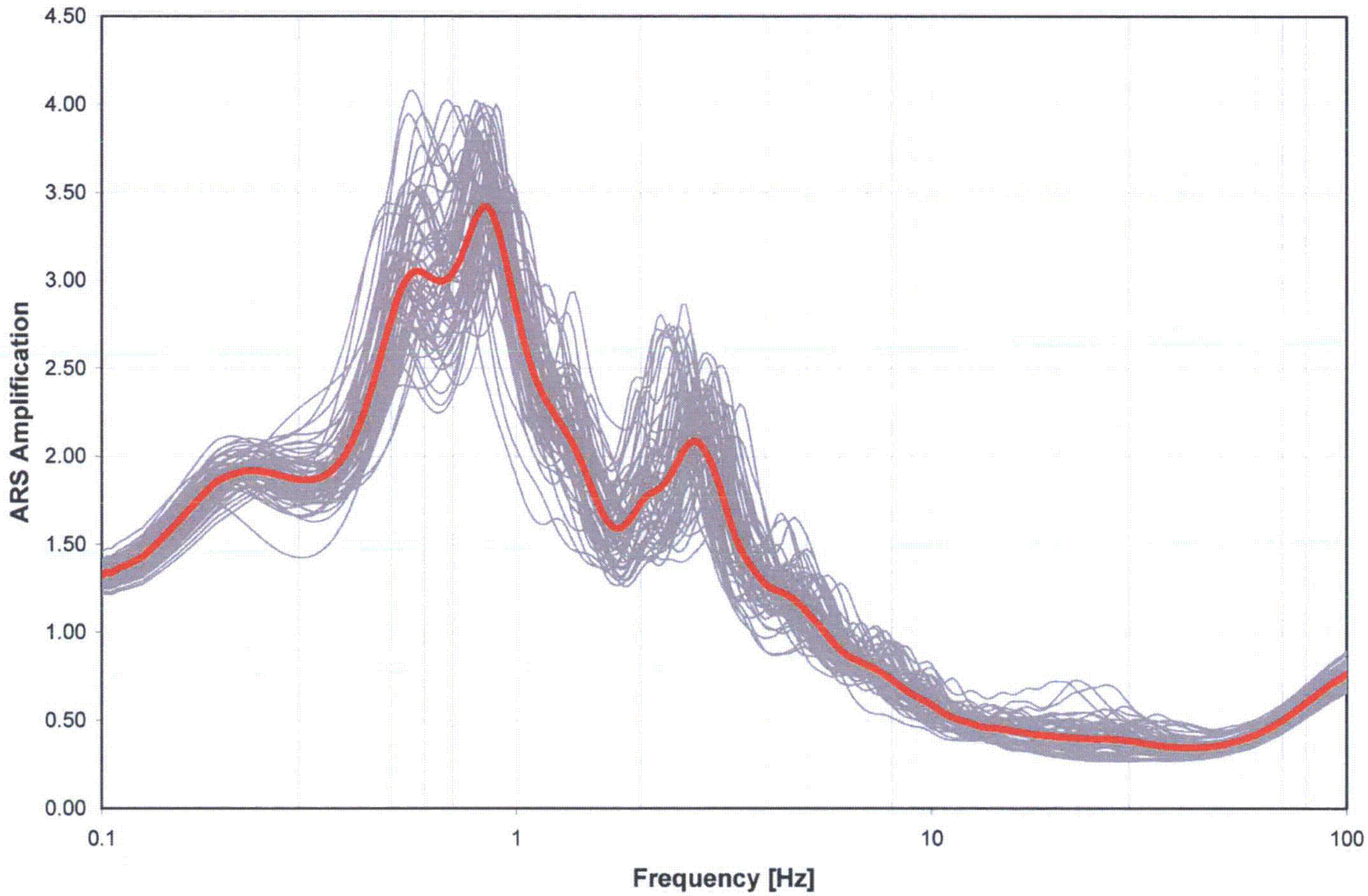

PTN COL 2.5-2

Figure 2.5.2-245 Maximum Strains Versus Depth that are Calculated for the 60 Profiles and their Median (Thick Red Line) with the 1E-05 LF Input Motion

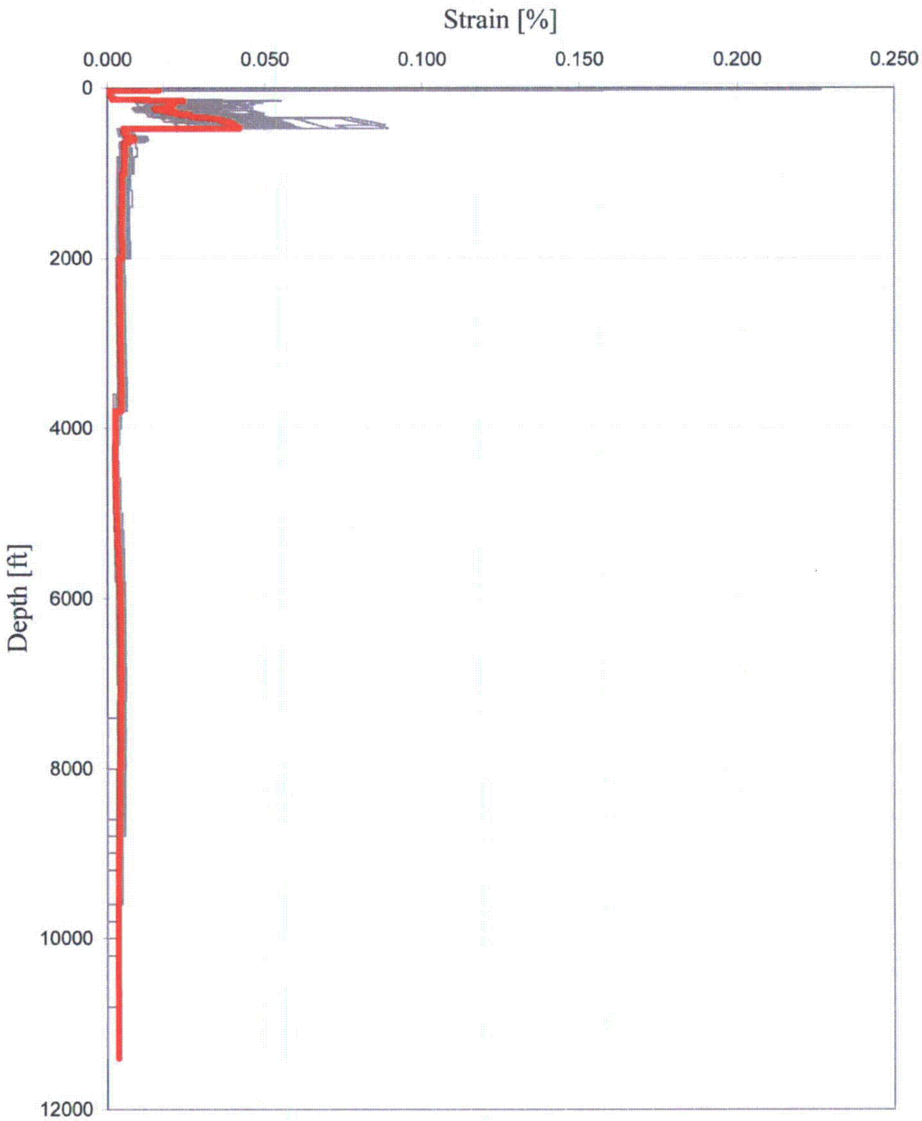

PTN COL 2.5-2

Figure 2.5.2-246 Median of Site Amplification Factors at GMRS Horizon (El. –35 feet) from Analyses of the 60 Random Profiles with the 1E-05 HF Input Motion

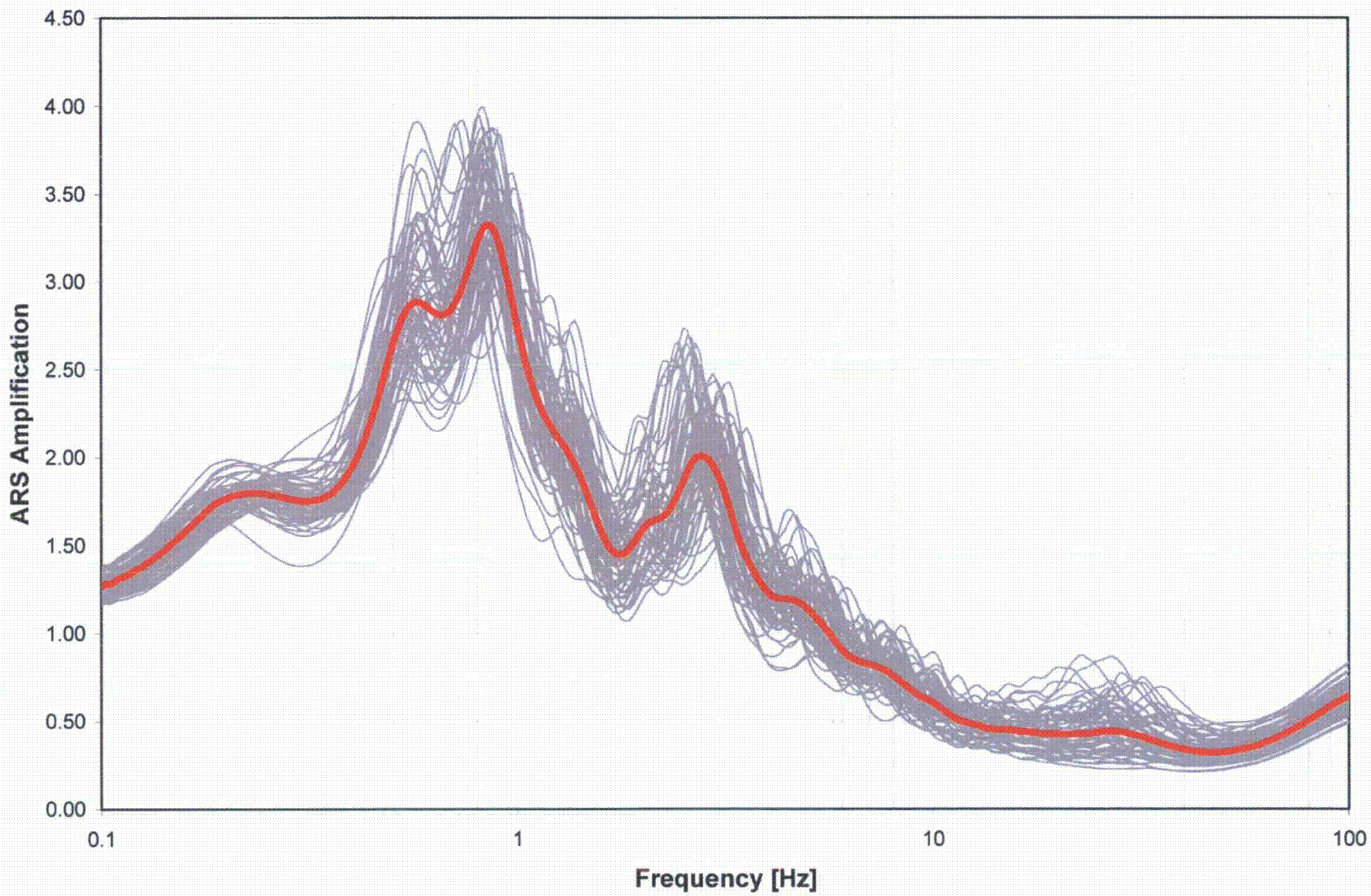

PTN COL 2.5-2

Figure 2.5.2-247 Maximum Strains Versus Depth that are Calculated for the 60 Profiles and their Median (Thick Red Line) with the 1E-05 HF Input Motion

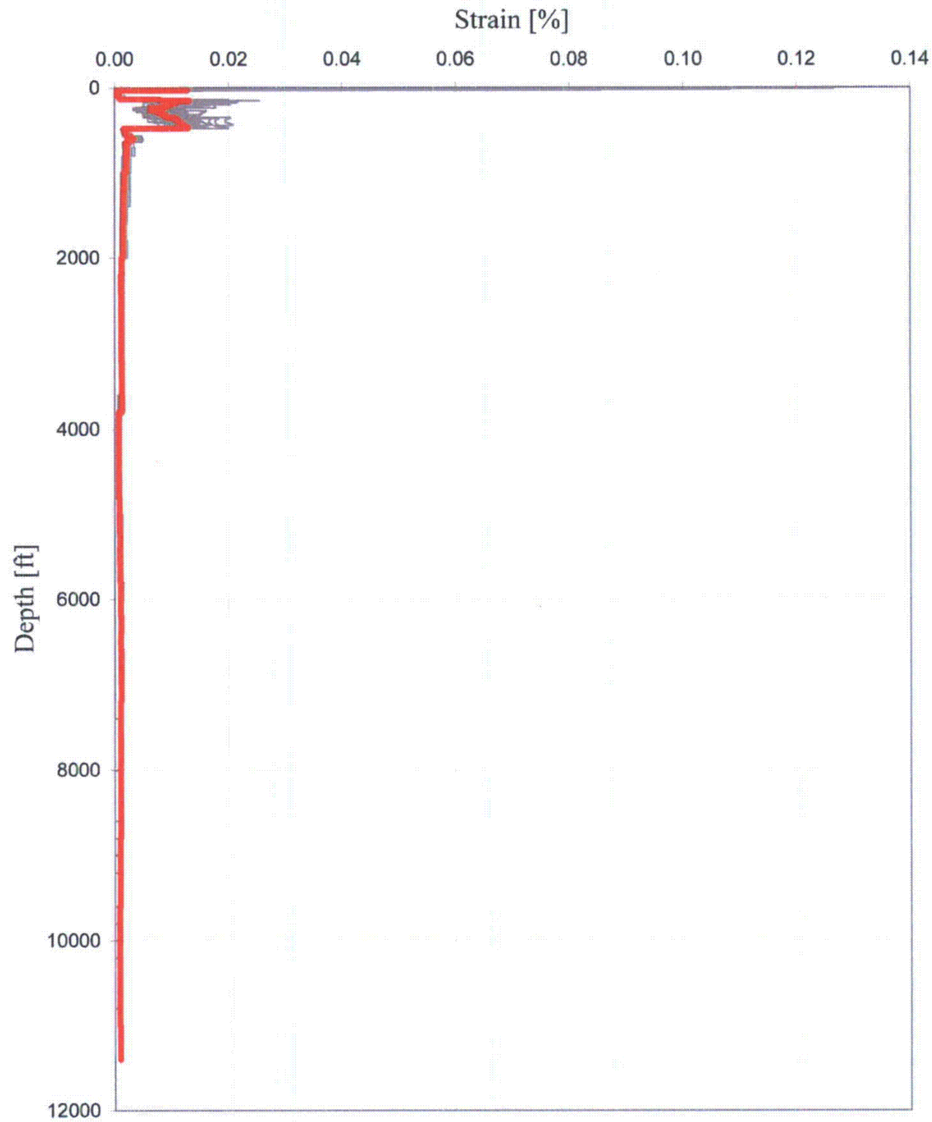

PTN COL 2.5-2

Figure 2.5.2-248 Median Maximum Strain Profiles (Full Soil Column) (Sheet 1 of 2)

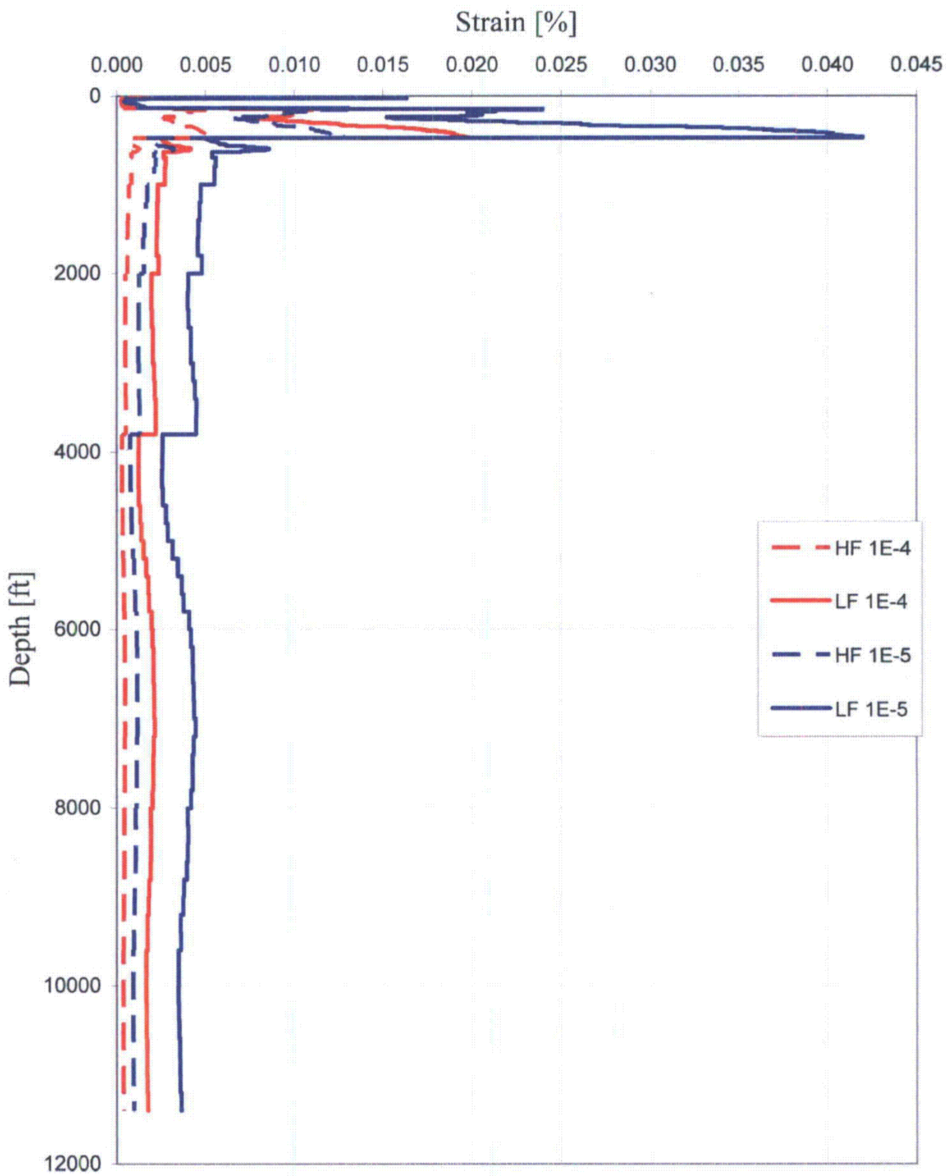

PTN COL 2.5-2

Figure 2.5.2-248 Median Maximum Strain Profiles (Upper 800 feet) (Sheet 2 of 2)

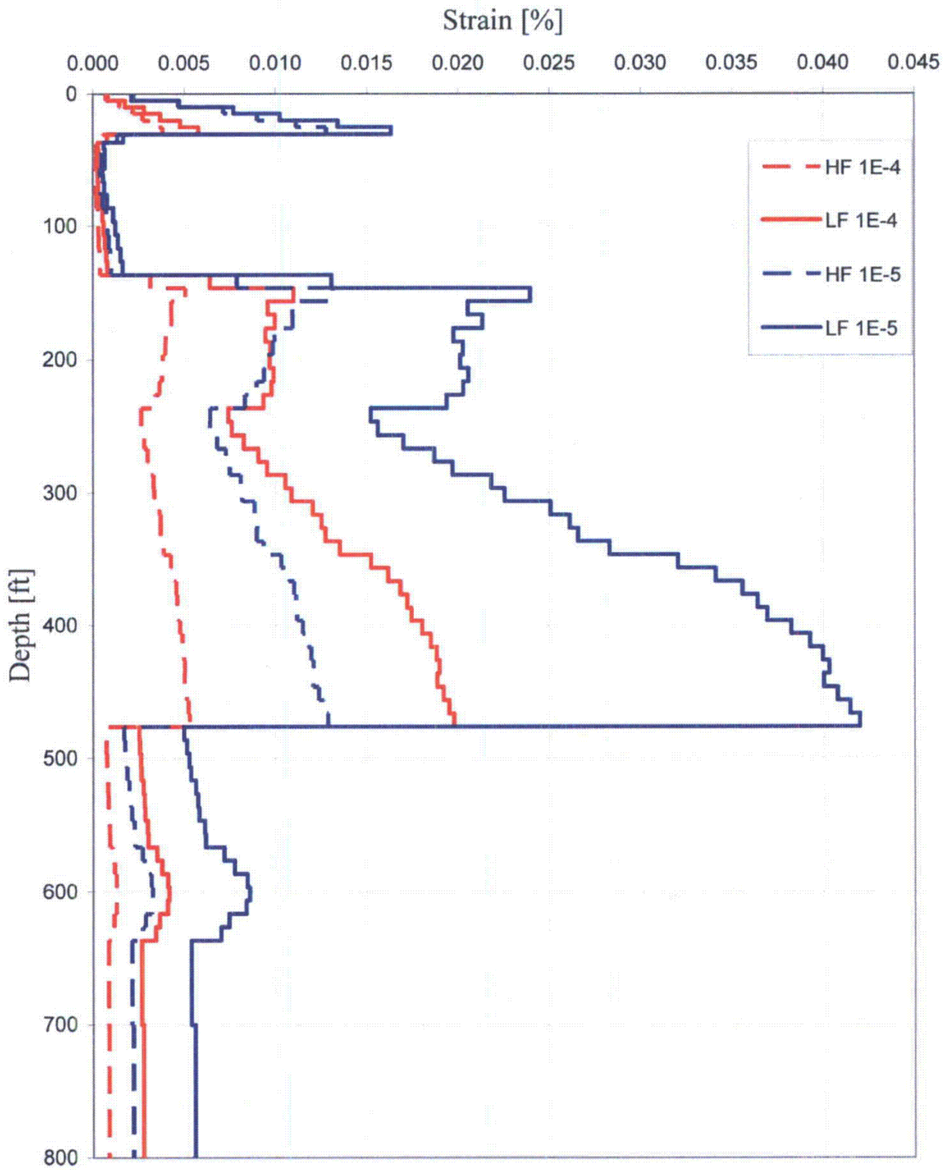

PTN COL 2.5-2

Figure 2.5.2-249 Median Profiles of Strain-Compatible Soil Damping (Full Soil Column) (Sheet 1 of 2)

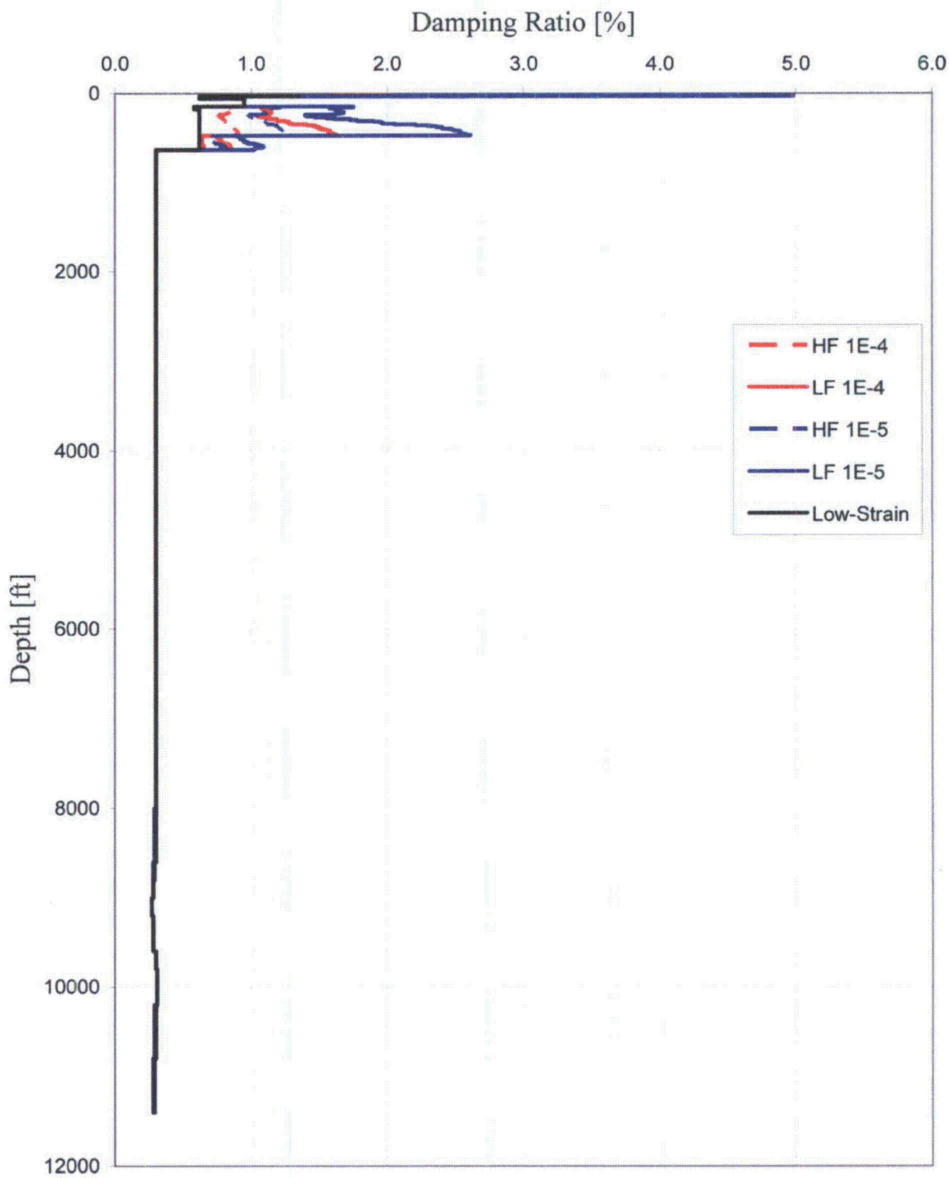

PTN COL 2.5-2

Figure 2.5.2-249 Median Profiles of Strain-Compatible Soil Damping (Upper 800 feet) (Sheet 2 of 2)

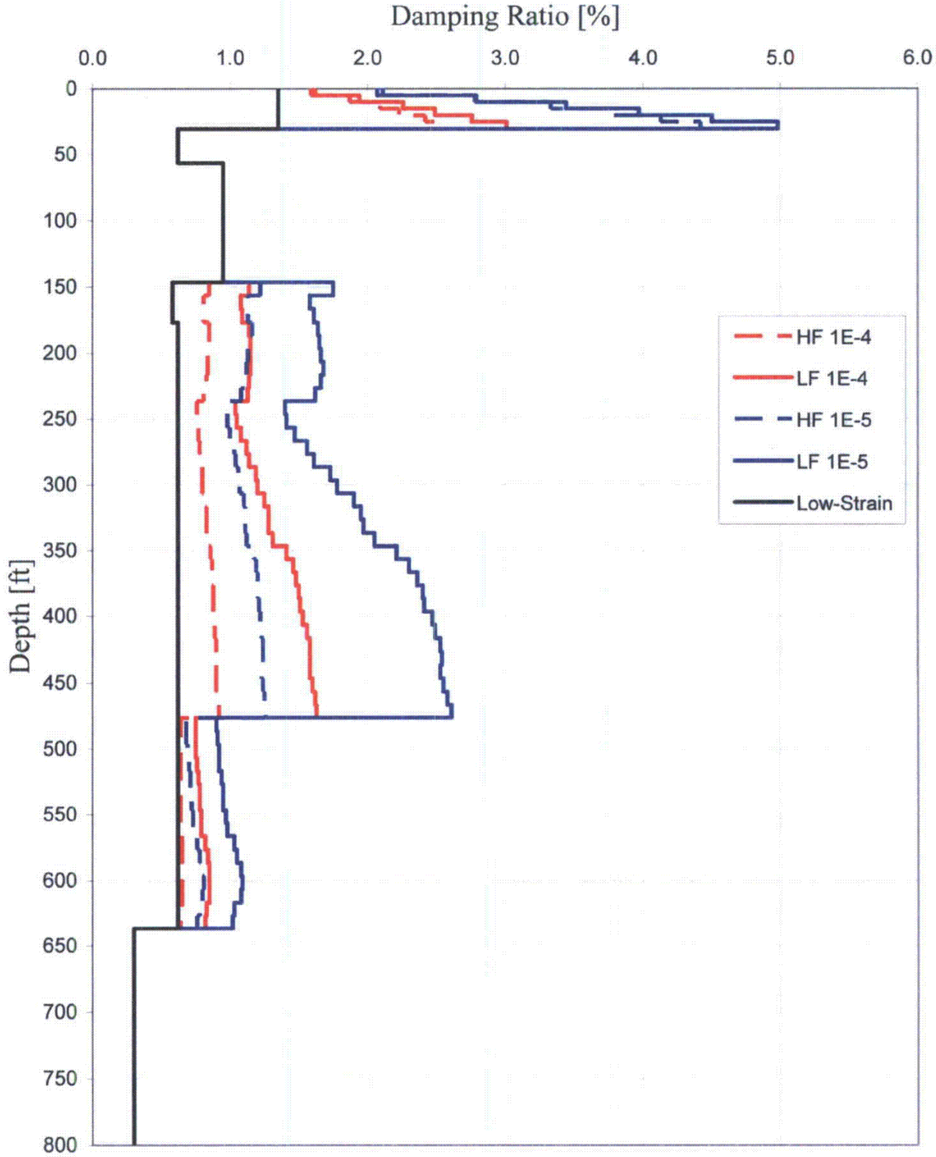

PTN COL 2.5-2

Figure 2.5.2-250 Comparison of Median Soil Amplification Factors at GMRS Horizon for LF and HF 1E-04 and 1E-05 Input Motions

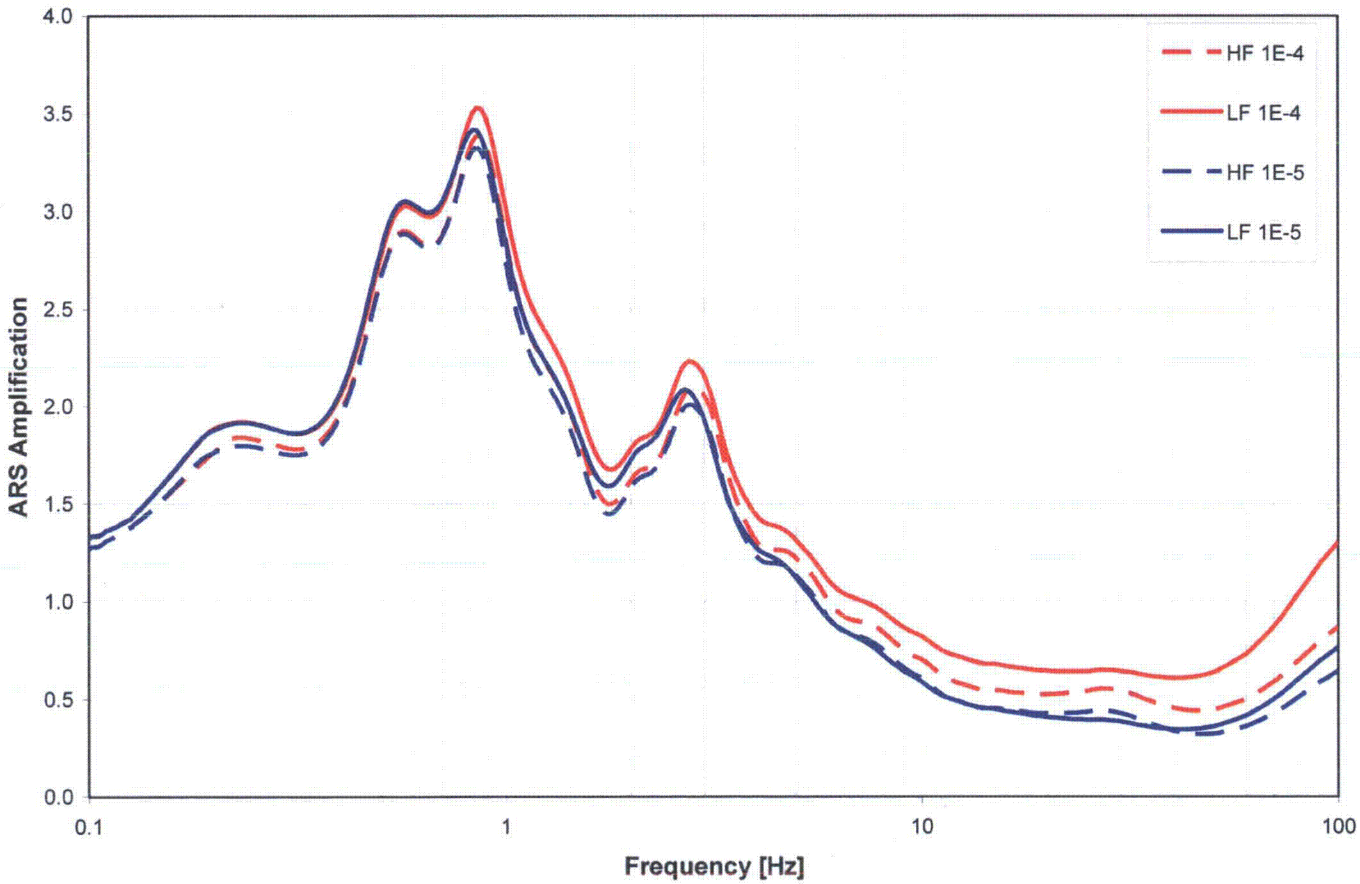

PTN COL 2.5-3

Figure 2.5.2-251 HF and LF Horizontal 1E-04 and 1E-05 Site Spectra

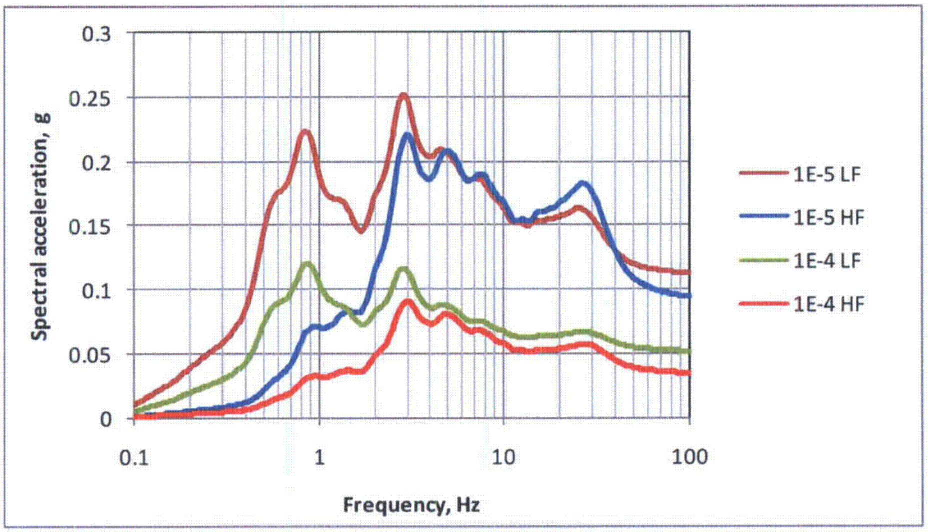

PTN COL 2.5-3

Figure 2.5.2-252 Smoothed Horizontal 1E-04 and 1E-05 Site Spectra

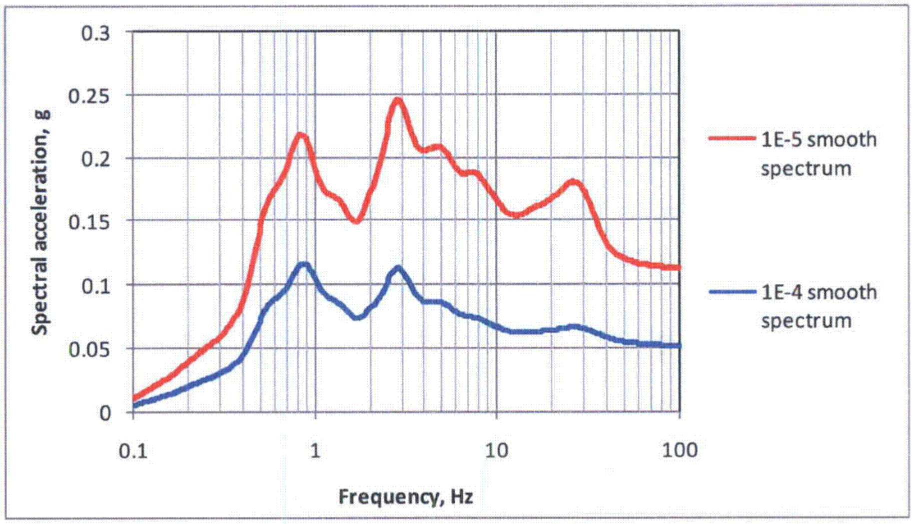

PTN COL 2.5-3

Figure 2.5.2-253 Smoothed Horizontal 1E-04 and 1E-05 Site Spectra and GMRS

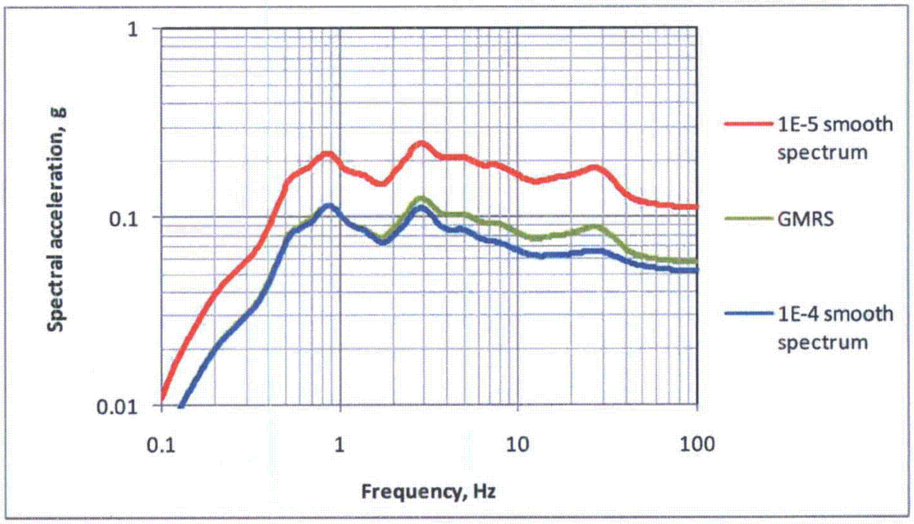

PTN COL 2.5-3

Figure 2.5.2-254 Smoothed Vertical 1E-04 and 1E-05 Site Spectra and GMRS

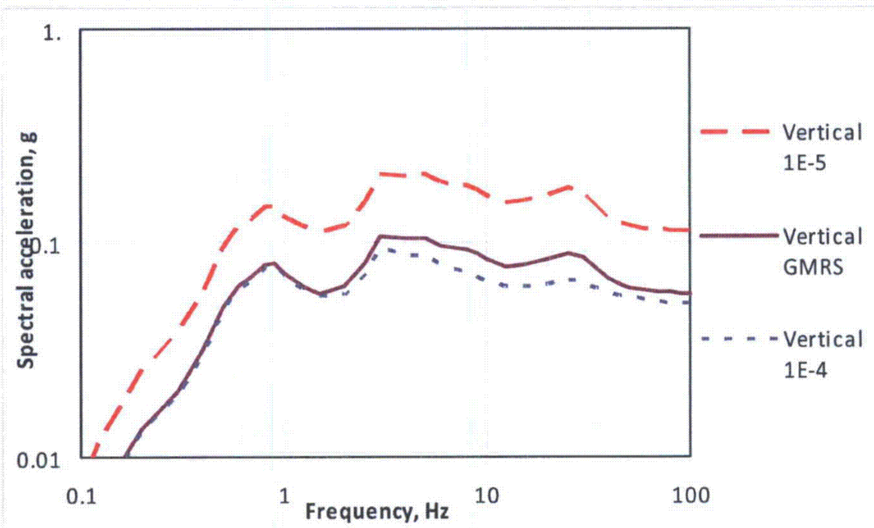

Figure 2.5.2-255 Comparison of PGA Attenuation Curves for the Cuba and Caribbean Region for a Magnitude M_w 7 Earthquake

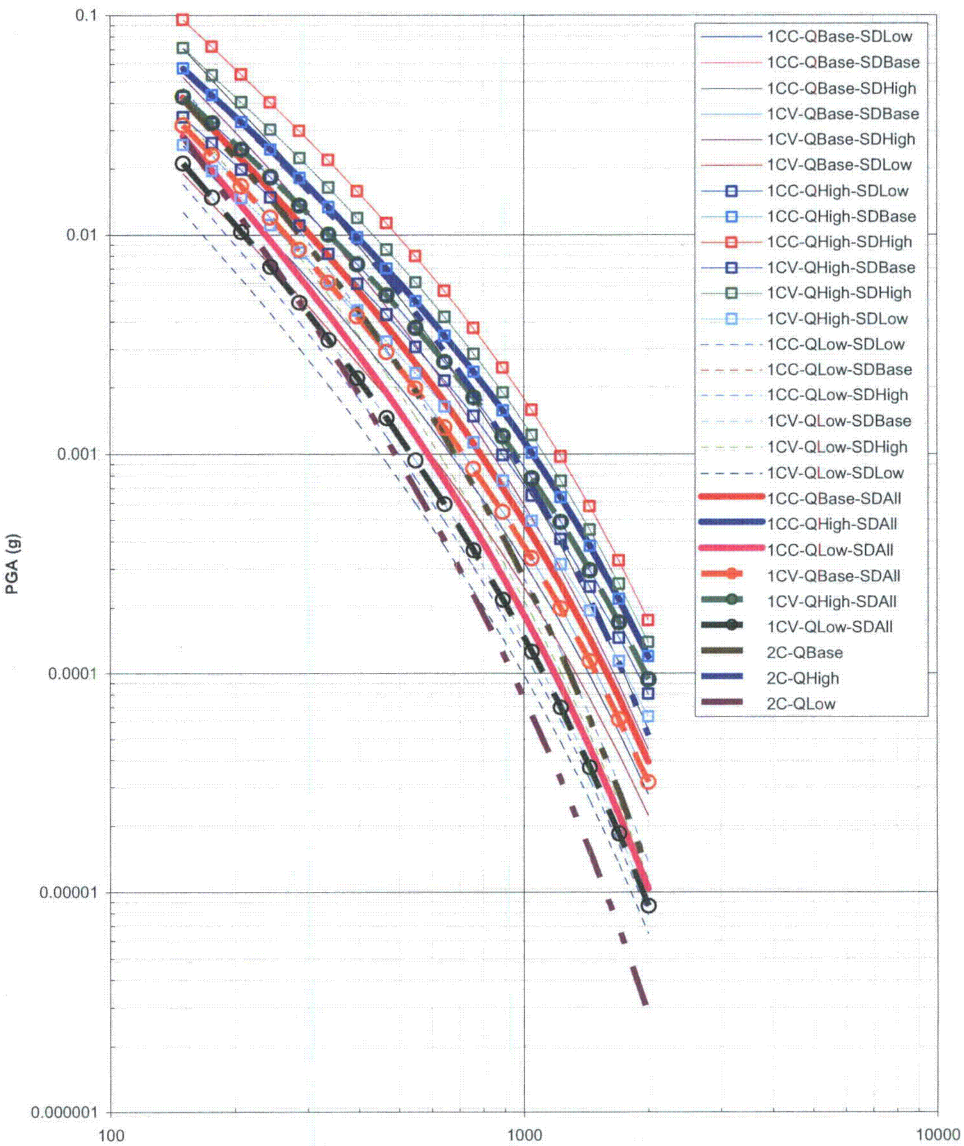

Note: Adopted nine ground motion attenuation models are indicated with thicker lines. Seismic source models are differentiated as 1CC=single corner constant stress parameter, 1CV=single corner variable stress parameter, and 2C=double corner. Stress parameter is indicated in the legend by SD.

Figure 2.5.2-256 Comparison of 10 Hz (T=0.1sec) Attenuation Curves for the Cuba and Caribbean Region for a Magnitude M_w 7 Earthquake

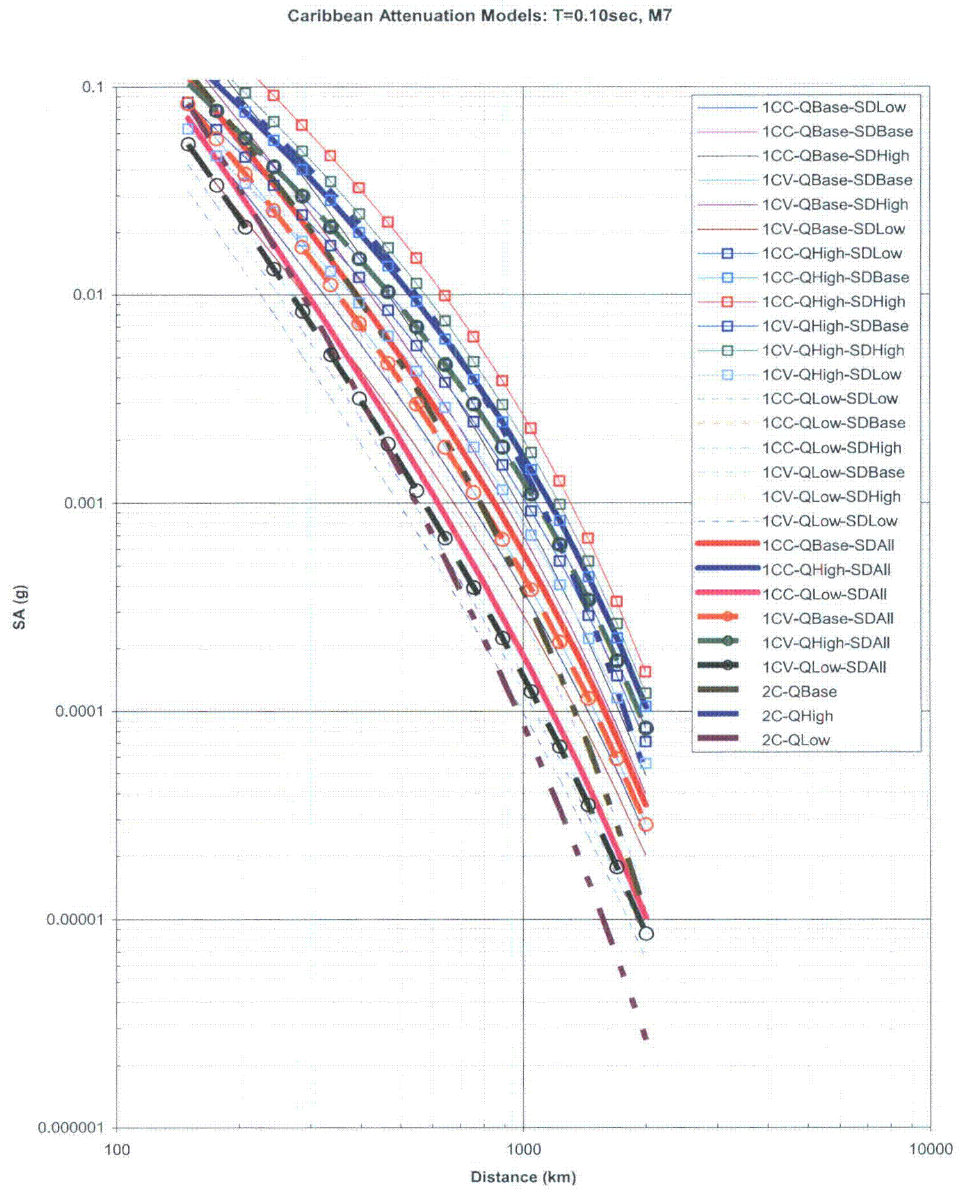

Note: Adopted nine ground motion attenuation models are indicated with thicker lines. Seismic source models are differentiated as 1CC=single corner constant stress parameter, 1CV=single corner variable stress parameter, and 2C=double corner. Stress parameter is indicated in the legend by SD.

Figure 2.5.2-257 Comparison of 1 Hz (T=1.0sec) Attenuation Curves for the Cuba and Caribbean Region for a Magnitude M_w 7 Earthquake

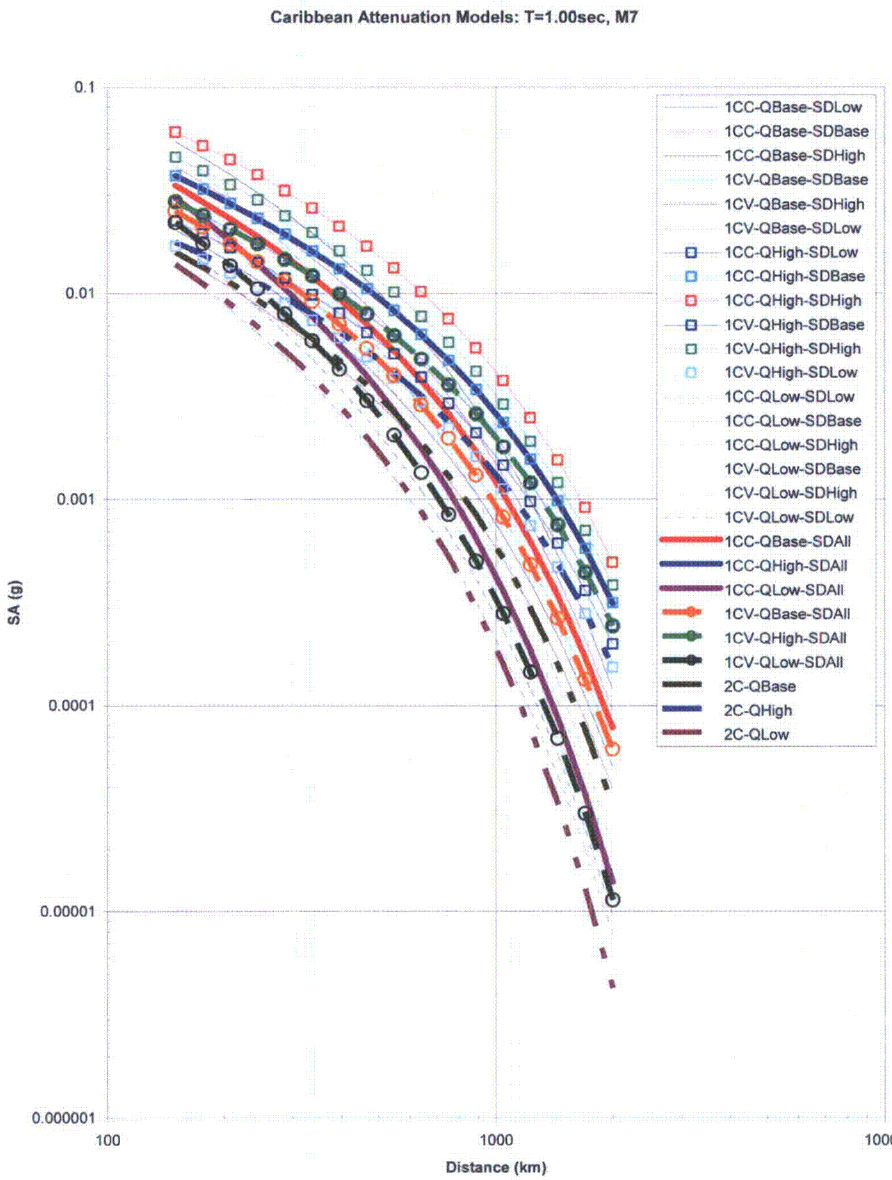

Note: Adopted nine ground motion attenuation models are indicated with thicker lines. Seismic source models are differentiated as 1CC=single corner constant stress parameter, 1CV=single corner variable stress parameter, and 2C=double corner. Stress parameter is indicated in the legend by SD.

PTN RAI 02.05.02-2

Figure 2.5.2-258a Map Showing the Earthquake Location for the 12/14/2004 Caribbean Sea Region Earthquake (M_w 6.8), the IRIS Station Locations Used in the Analysis (Shown as Black Triangles in this and Similar Subsequent Figures), and Turkey Point Units 6 & 7 Site Location

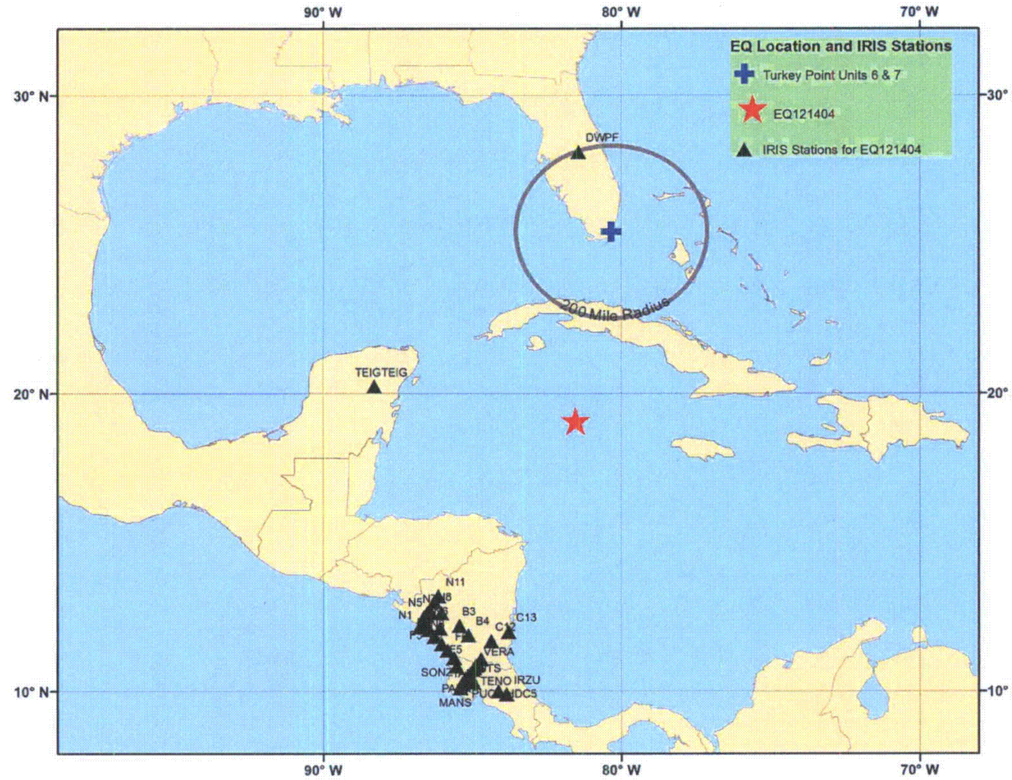

PTN RAI 02.05.02-2

Figure 2.5.2-258b Comparison of Caribbean (Red), EPRI (2004) (Reference 242), Mid-Continent (Blue), and Gulf Coast Region (Green) GMPEs with Raw Empirical IRIS Data (Open Circle), IRIS Data with Atkinson and Boore (2011) (Reference 359) Amplification Factor Corrections (Open Squares) and IRIS Data with Frankel et al. (1996) (Reference 252) Amplification Factor Corrections (Open Diamonds) for a Spectral Frequency of 1 Hz

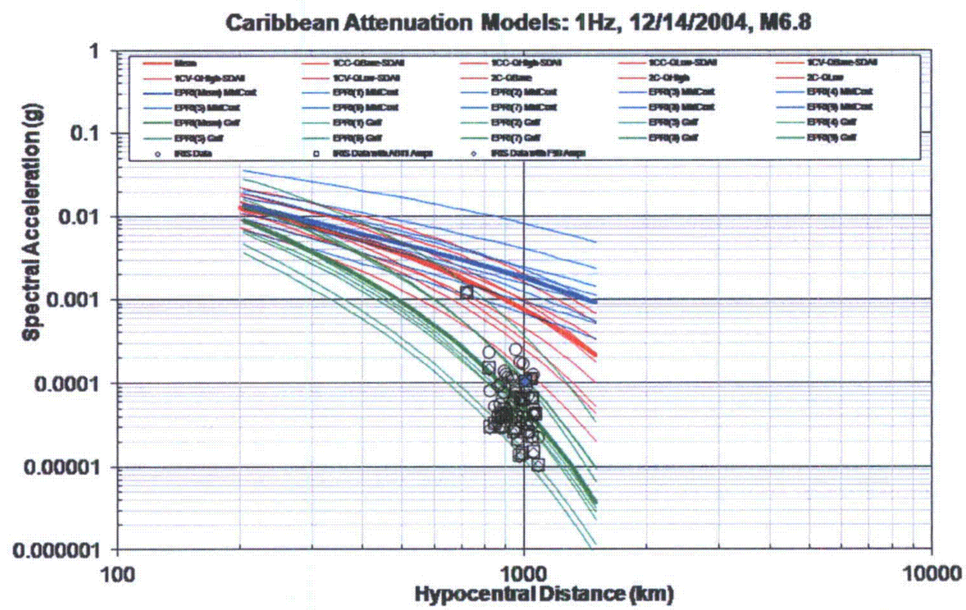

PTN RAI 02.05.02-2

Figure 2.5.2-258c Comparison of Caribbean (Red), EPRI (2004) (Reference 242), Mid-Continent (Blue), and Gulf Coast Region (Green) GMPEs with Raw Empirical IRIS Data (Open Circle), IRIS Data with Atkinson and Boore (2011) (Reference 359) Amplification Factor Corrections (Open Squares) and IRIS Data with Frankel et al. (1996) (Reference 252) Amplification Factor Corrections (Open Diamonds) for a Spectral Frequency of 2.5 Hz

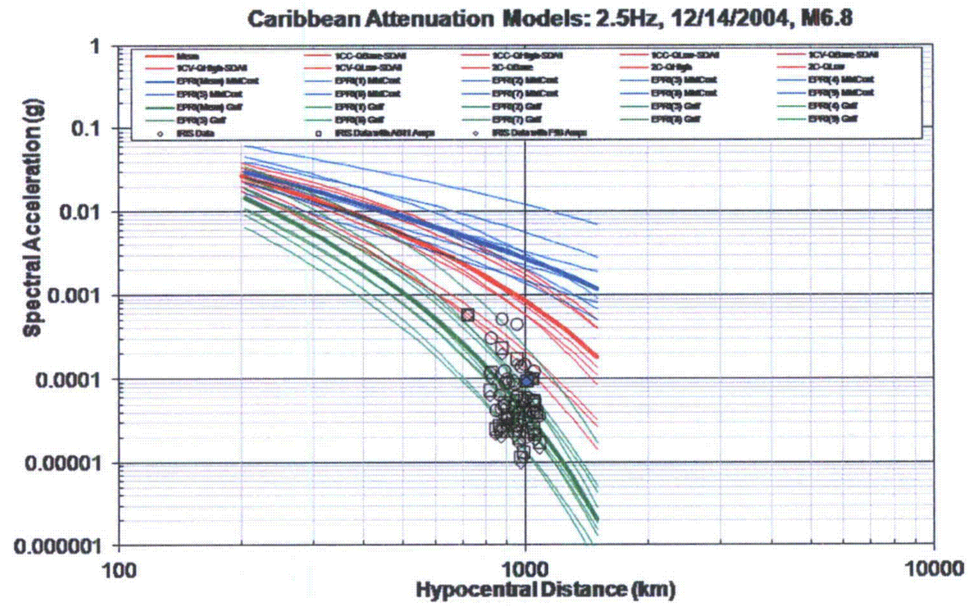

Figure 2.5.2-259a Map Showing the Earthquake Location for the 09/10/2006 Gulf Of Mexico Earthquake (M_w5.9), the IRIS Station Locations Used in the Analysis, and Turkey Point Units 6 & 7 Site Location

PTN RAI 02.05.02-2

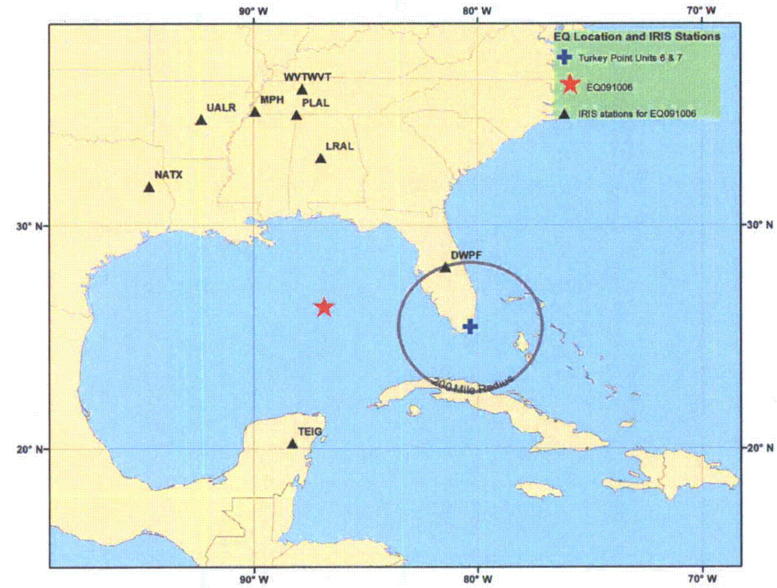

Figure 2.5.2-259b Comparison of Caribbean (Red) EPRI (2004) (Reference 242), Mid-Continent (Blue) and Gulf Coast Region (Green) GMPEs with Raw Empirical IRIS Data (Open Circle), IRIS Data with Atkinson and Boore (2011) (Reference 359) Amplification Factor Corrections (Open Squares) and IRIS Data with Frankel et al. (1996) (Reference 252) Amplification Factor Corrections (Open Diamonds) for a Spectral Frequency of 1 Hz

PTN RAI 02.05.02-2

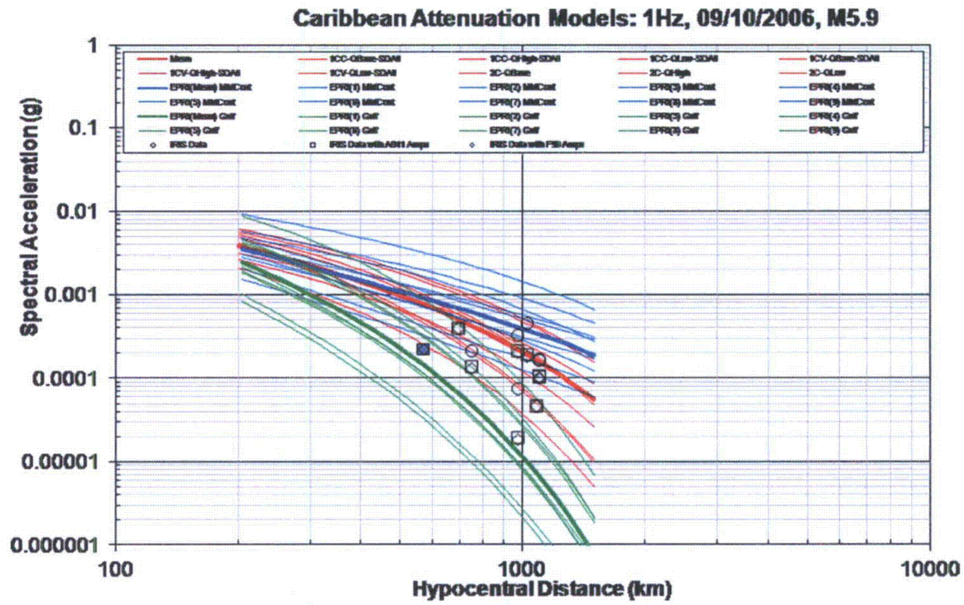

PTN RAI 02.05.02-2

Figure 2.5.2-259c Comparison of Caribbean (Red), EPRI (2004) (Reference 242), Mid-Continent (Blue), and Gulf Coast Region (Green) GMPEs with Raw Empirical IRIS Data (Open Circle), IRIS Data with Atkinson and Boore (2011) (Reference 359) Amplification Factor Corrections (Open Squares) and IRIS Data with Frankel et al. (1996) (Reference 252) Amplification Factor Corrections (Open Diamonds) for a Spectral Frequency of 2.5 Hz.

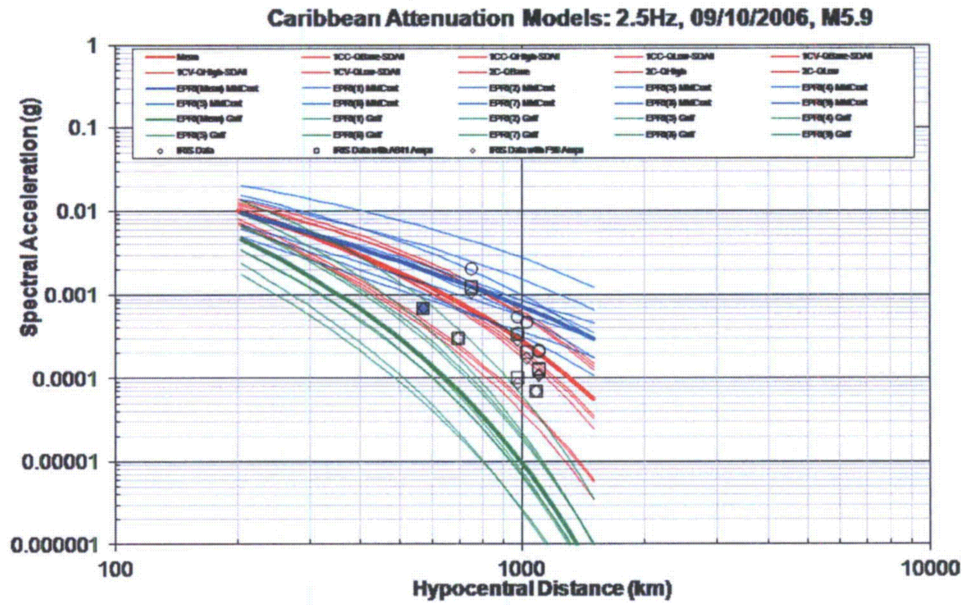

Figure 2.5.2-260a Map Showing the Earthquake Location for the 02/04/2007 Cuba Region Earthquake (M_W 6.2), the IRIS Station Locations Used in the Analysis, and Turkey Point Units 6 & 7 Site Location

PTN RAI 02.05.02-2

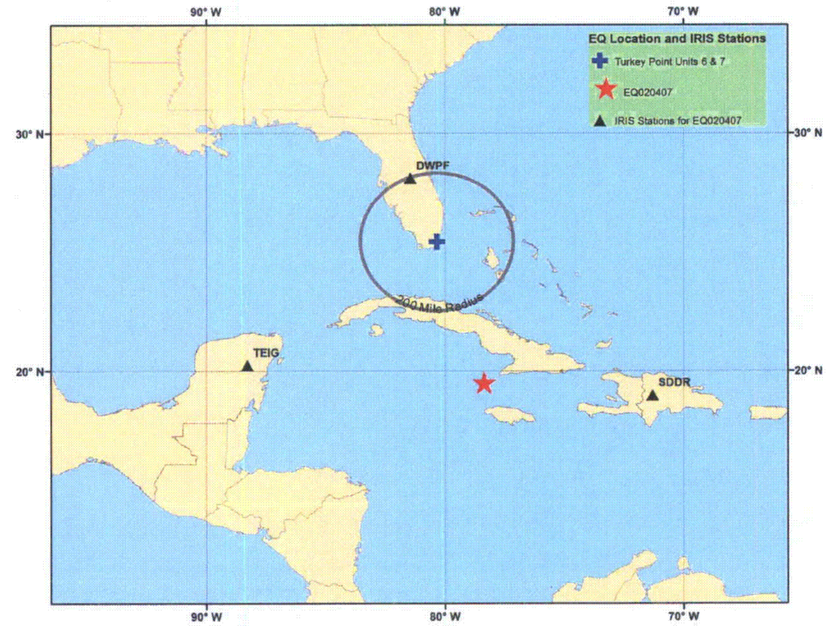

PTN RAI 02.05.02-2

Figure 2.5.2-260b Comparison of Caribbean (Red), EPRI (2004) (Reference 242), Mid-Continent (Blue), and Gulf Coast Region (Green) GMPEs with Raw Empirical IRIS Data (Open Circle), IRIS Data with Atkinson and Boore (2011) (Reference 359) Amplification Factor Corrections (Open Squares) and IRIS Data with Frankel et al. (1996) (Reference 252) Amplification Factor Corrections (Open Diamonds) for a Spectral Frequency of 1 Hz

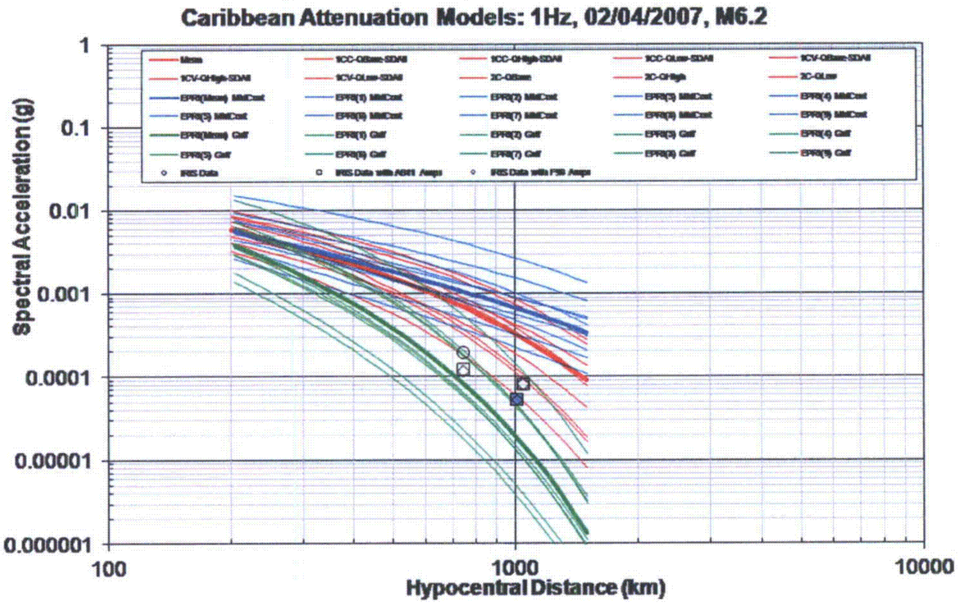

PTN RAI 02.05.02-2

Figure 2.5.2-260c Comparison of Caribbean (Red), EPRI (2004) (Reference 242), Mid-Continent (Blue), and Gulf Coast Region (Green) GMPEs with Raw Empirical IRIS Data (Open Circle), IRIS Data with Atkinson and Boore (2011) (Reference 359) Amplification Factor Corrections (Open Squares) and IRIS Data with Frankel et al. (1996) (Reference 252) Amplification Factor Corrections (Open Diamonds) for a Spectral Frequency of 2.5 Hz

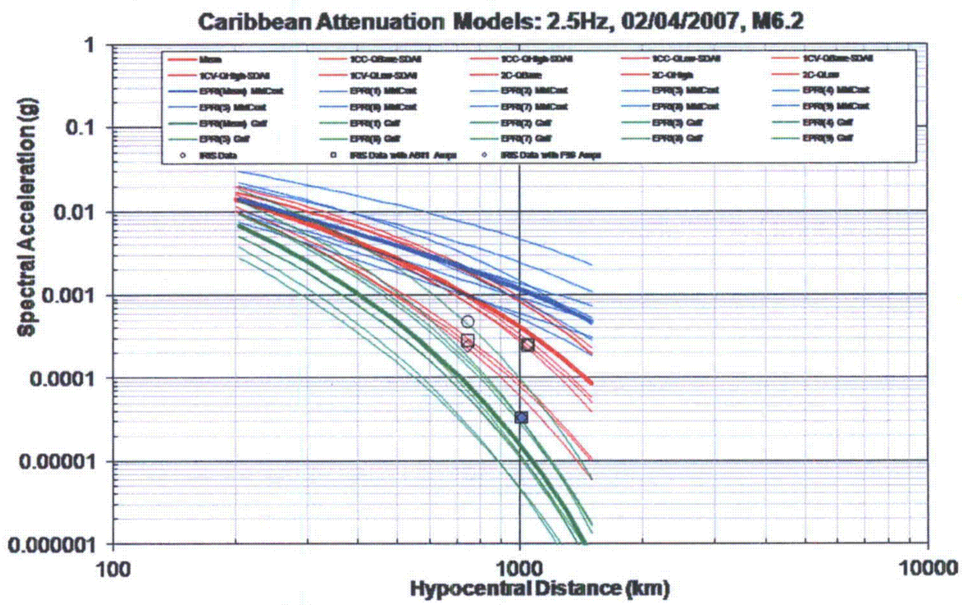

Figure 2.5.2-261a Map Showing the Earthquake Location for the 05/28/2009 North of Honduras Earthquake (M_w 7.3), the IRIS Station Locations Used in the Analysis, and Turkey Point Units 6 & 7 Site Location

PTN RAI 02.05.02-2

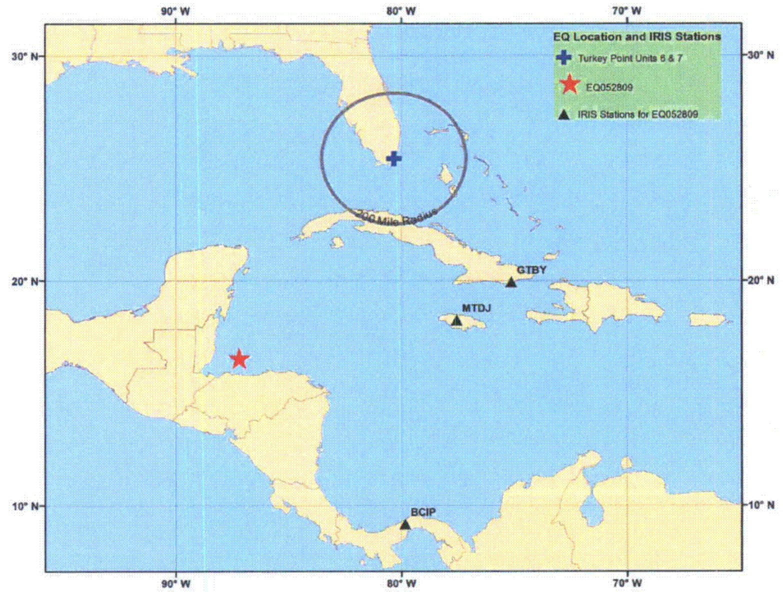

Figure 2.5.2-261b Comparison of Caribbean (Red), EPRI (2004) (Reference 242), Mid-Continent (Blue), and Gulf Coast Region (Green) GMPEs with Raw Empirical IRIS Data (Open Circle), IRIS Data with Atkinson and Boore (2011) (Reference 359) Amplification Factor Corrections (Open Squares) and IRIS Data with Frankel et al. (1996) (Reference 252) Amplification Factor Corrections (Open Diamonds) for a Spectral Frequency of 1 Hz

PTN RAI 02.05.02-2

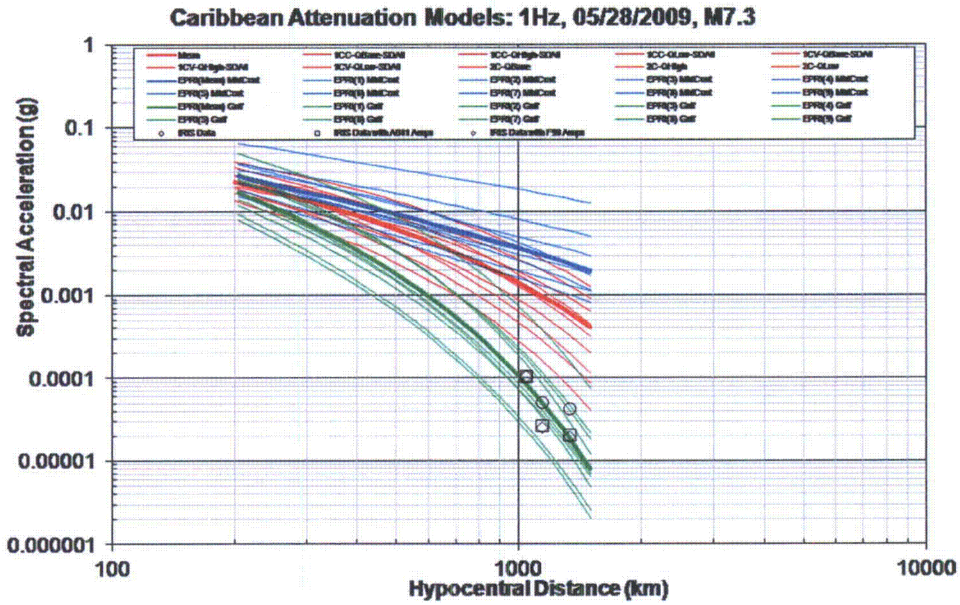

PTN RAI 02.05.02-2

Figure 2.5.2-261c Comparison of Caribbean (Red), EPRI (2004) (Reference 242), Mid-Continent (Blue), and Gulf Coast Region (Green) GMPEs with Raw Empirical IRIS Data (Open Circle) IRIS Data with Atkinson and Boore (2011) (Reference 359) Amplification Factor Corrections (Open Squares) and IRIS Data with Frankel et al. (1996) (Reference 252) Amplification Factor Corrections (Open Diamonds) for a Spectral Frequency of 2.5 Hz

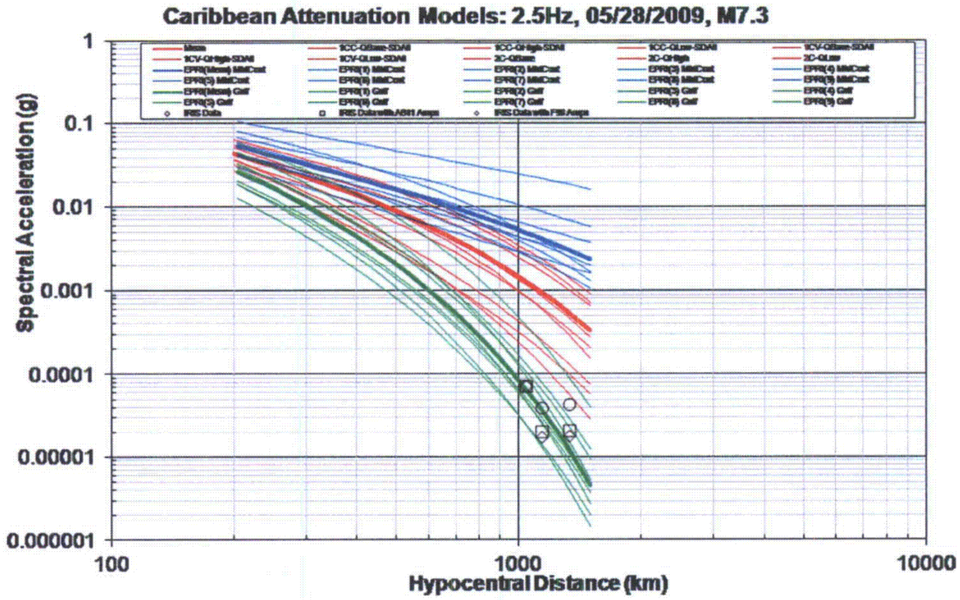

Figure 2.5.2-262a Map Showing the Earthquake Location for the 01/12/2010 Haiti Earthquake (M_W 7.0), the IRIS Station Locations Used in the Analysis, and Turkey Point Units 6 & 7 Site Location

PTN RAI 02.05.02-2

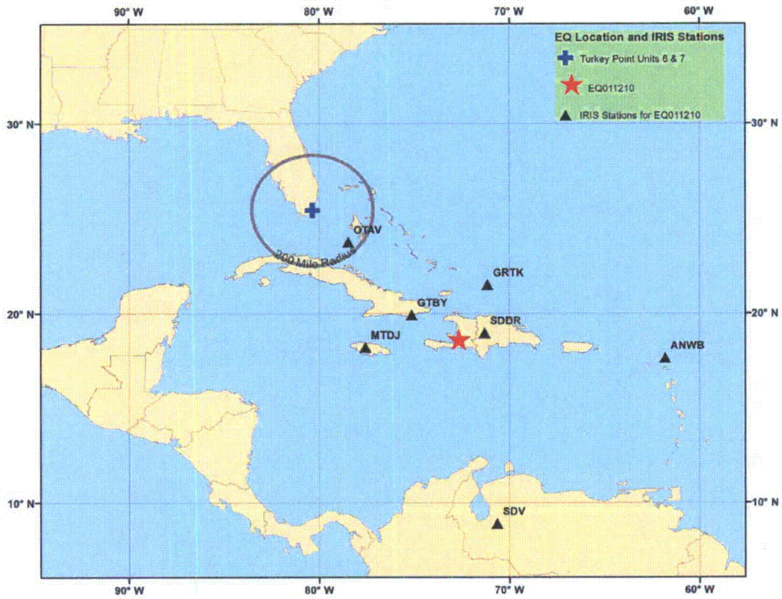

PTN RAI 02.05.02-2

Figure 2.5.2-262b Comparison of Caribbean (Red), EPRI (2004) (Reference 242), Mid-Continent (Blue), and Gulf Coast Region (Green) GMPEs with Raw Empirical IRIS Data (Open Circle), IRIS Data with Atkinson and Boore (2011) (Reference 359) Amplification Factor Corrections (Open Squares) and IRIS Data with Frankel et al. (1996) (Reference 252) Amplification Factor Corrections (Open Diamonds) for a Spectral Frequency of 1 Hz

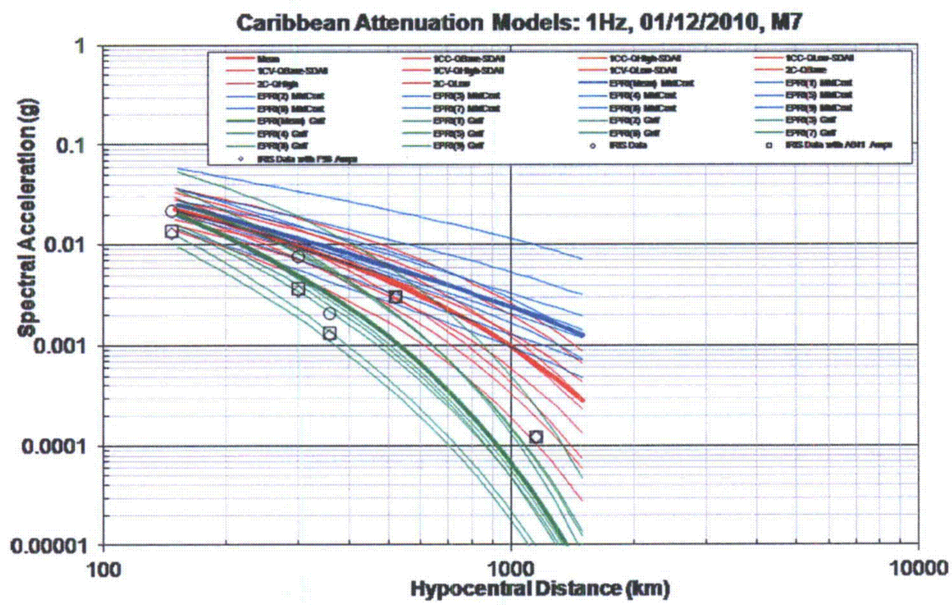

PTN RAI 02.05.02-2

Figure 2.5.2-262c Comparison of Caribbean (Red), EPRI (2004) (Reference 242), Mid-Continent (Blue), and Gulf Coast Region (Green) GMPEs with Raw Empirical IRIS Data (Open Circle), IRIS Data with Atkinson and Boore (2011) (Reference 359) Amplification Factor Corrections (Open Squares) and IRIS Data with Frankel et al. (1996) (Reference 252) Amplification Factor Corrections (Open Diamonds) for a Spectral Frequency of 2.5 Hz

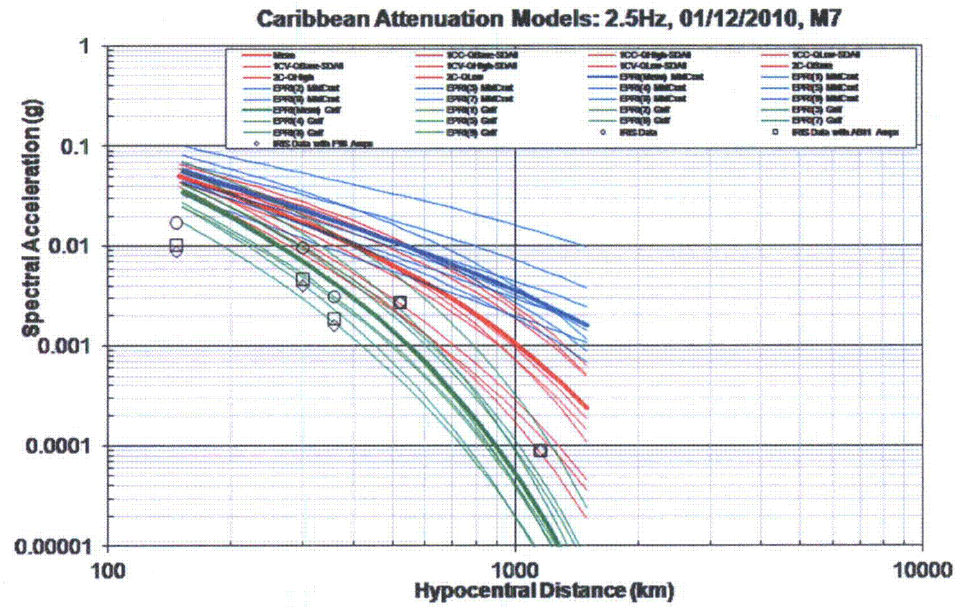

Figure 2.5.2-263 Horizontal GMRS for Caribbean Sources for Five GMPE Models for the Turkey Points Units 6 & 7 Site

PTN RAI 02.05.02-2

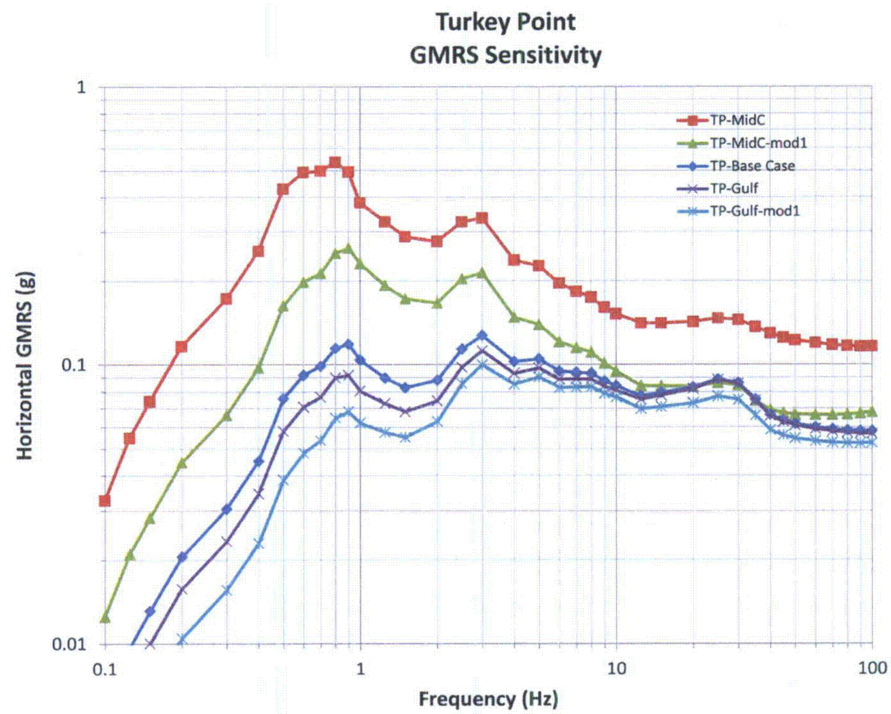

Figure 2.5.2-264 Comparison of EPRI Mid-Continent (Reference 242) Mean (dashed lines) and Caribbean Mean (solid lines) Attenuation Curves for Magnitudes 6, 7, and 8 for PGA

PTN RAI 02.05.02-2

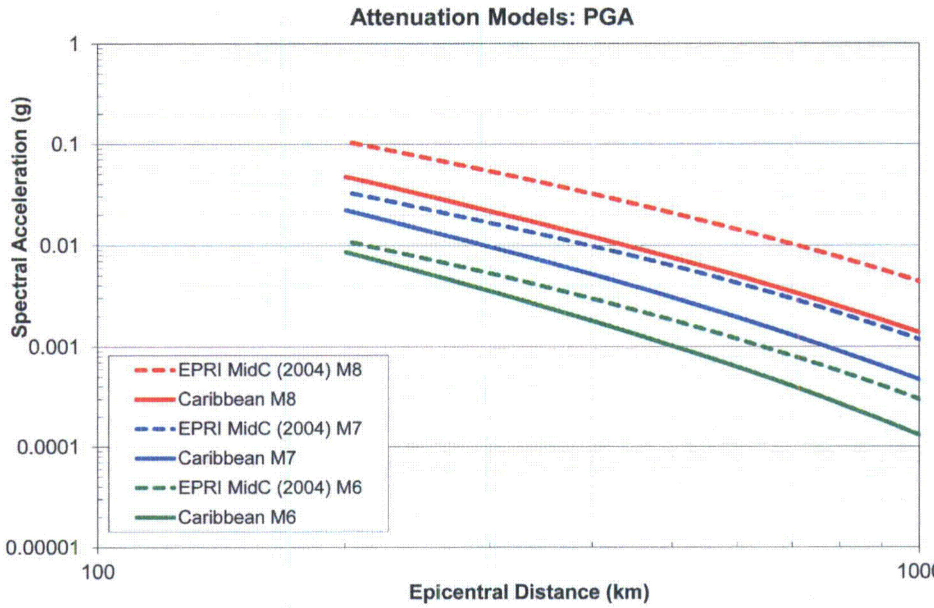

Figure 2.5.2-265 Comparison of EPRI Mid-Continent Mean (dashed lines) and Caribbean Mean (solid lines) Attenuation Curves for Magnitudes 6, 7, and 8 for 25 Hz

PTN RAI 02.05.02-2

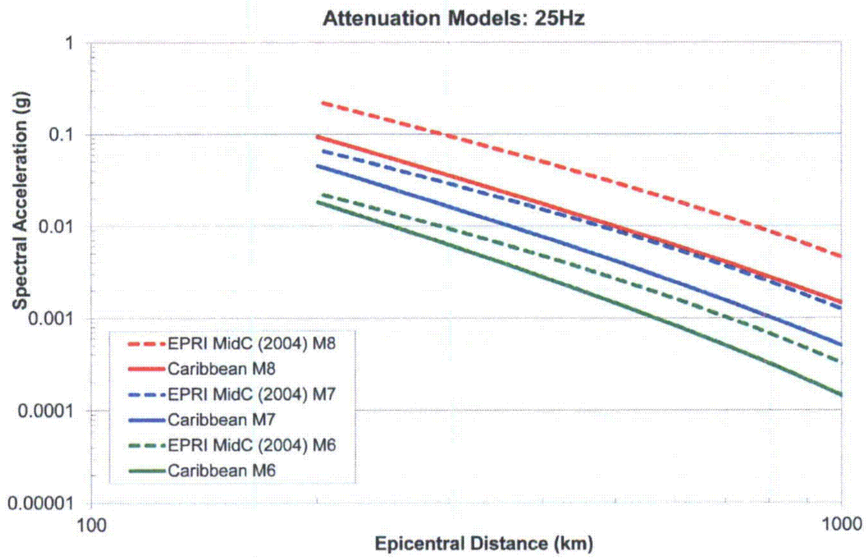

Source: Reference 242

PTN RAI 02.05.02-2

Figure 2.5.2-266 Comparison of EPRI Mid-Continent Mean (dashed lines) and Caribbean Mean (solid lines) Attenuation Curves for Magnitudes 6, 7, and 8 for 10 Hz

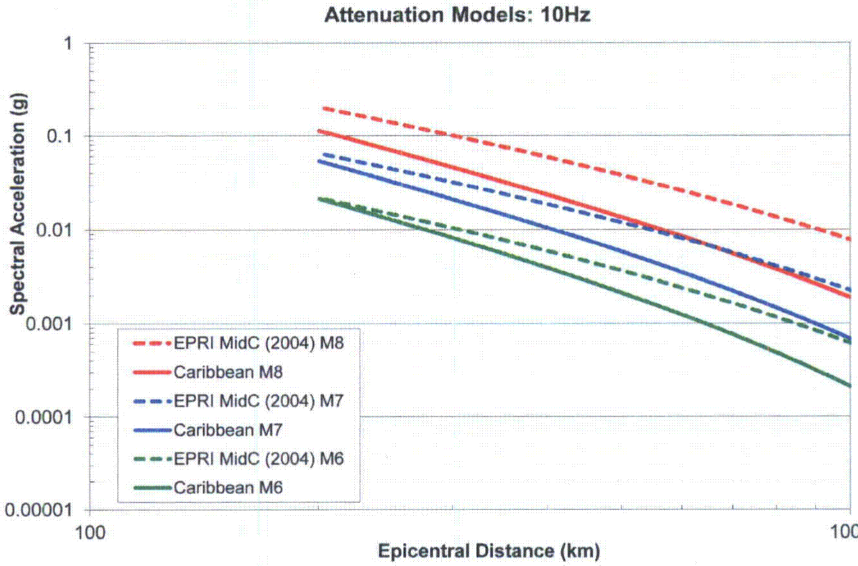

Source: Reference 242

Figure 2.5.2-267 Comparison of EPRI Mid-Continent Mean (dashed lines) and Caribbean Mean (solid lines) Attenuation Curves for Magnitudes 6, 7, and 8 for 5 Hz

PTN RAI 02.05.02-2

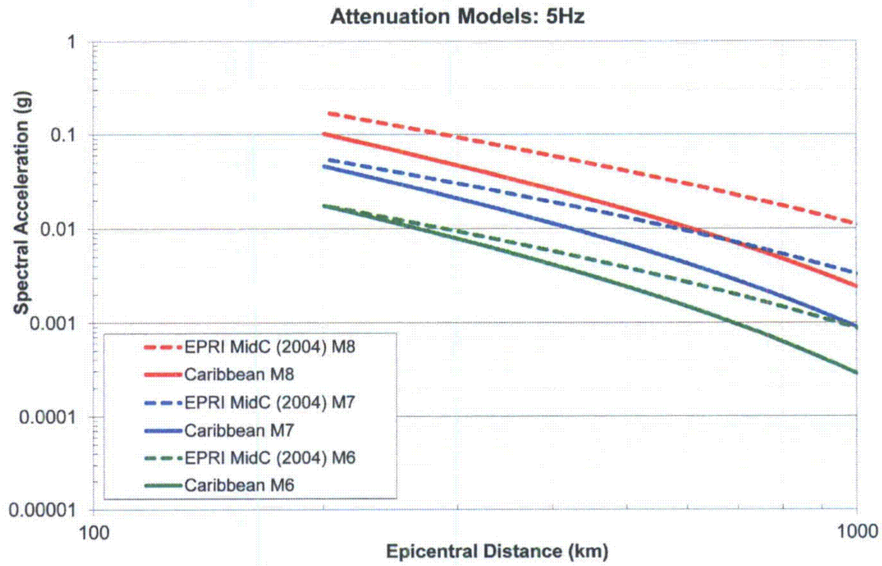

Source: Reference 242

Figure 2.5.2-268 Comparison of EPRI Mid-Continent Mean (dashed lines) and Caribbean Mean (solid lines) Attenuation Curves for Magnitudes 6, 7, and 8 for 2.5 Hz

PTN RAI 02.05.02-2

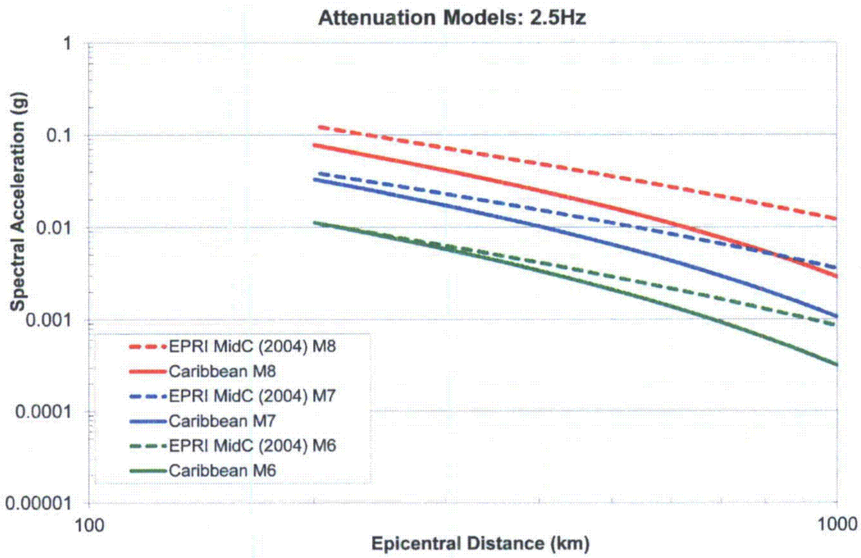

Source: Reference 242

Figure 2.5.2-269 Comparison of EPRI Mid-Continent Mean (dashed lines) and Caribbean Mean (solid lines) Attenuation Curves for Magnitudes 6, 7, and 8 for 1 Hz

PTN RAI 02.05.02-2

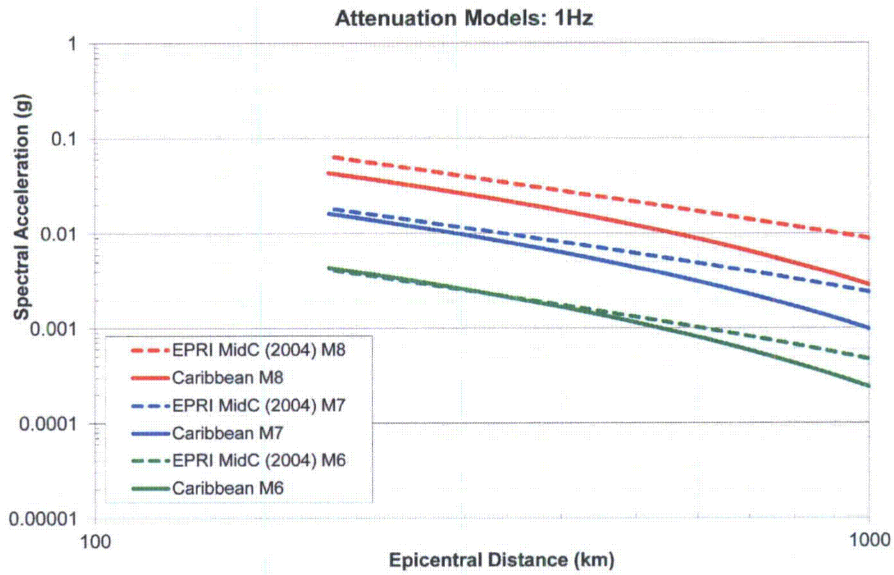

Source: Reference 242

PTN RAI 02.05.02-2

Figure 2.5.2-270 Comparison of EPRI Mid-Continent Mean (dashed lines) and Caribbean Mean (solid lines) Attenuation Curves for Magnitudes 6, 7, and 8 for 0.5 Hz

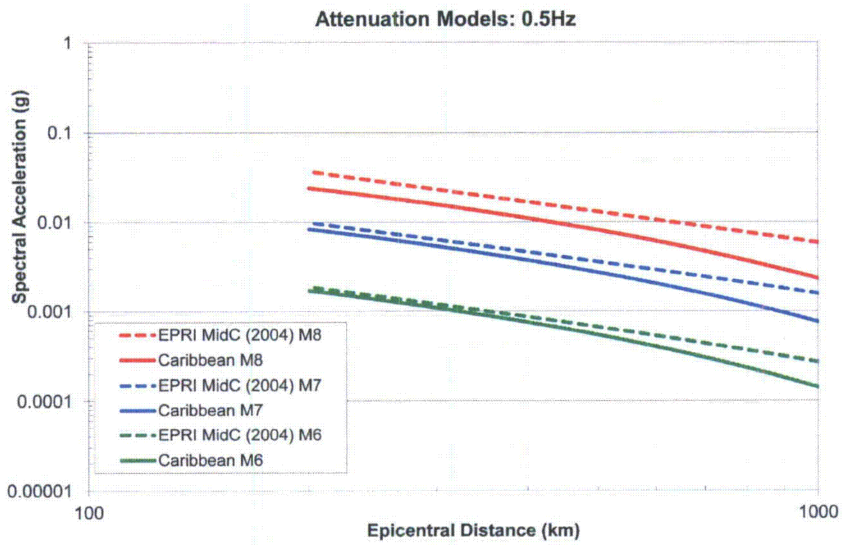

Source: Reference 242

Figure 2.5.2-271 Map Showing Cuba Single Areal Source Zone (solid black line), Six Sensitivity Areal Source Zones (dashed black lines), and Northern Cuba Subzone Used in Hazard Sensitivity Calculation (green shading). Seismicity (blue circles) is from the Phase 2 Earthquake Catalog. Thick Red Lines Show Plate Boundary Fault Sources Included in PSHA.

PTN RAI 02.05.02-4

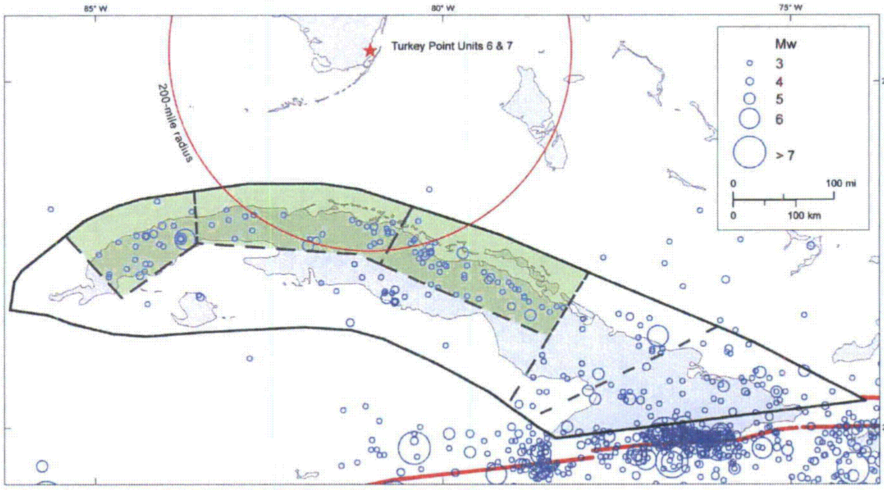

Figure 2.5.2-272 Map of Intraplate Cuba Fault Sources for Hazard Sensitivity Calculation

PTN RAI 02.05.02-4

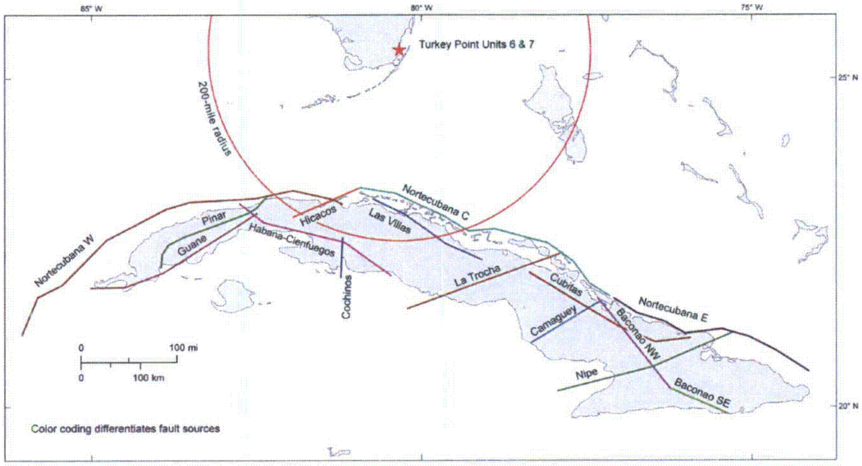

Figure 2.5.2-273 1 Hz Mean Hazard Curves Showing Sensitivity to Cuba Source Scenarios. Lower Panel is Expanded View of Yellow Box in Upper Panel.

PTN RAI 02.05.02-4

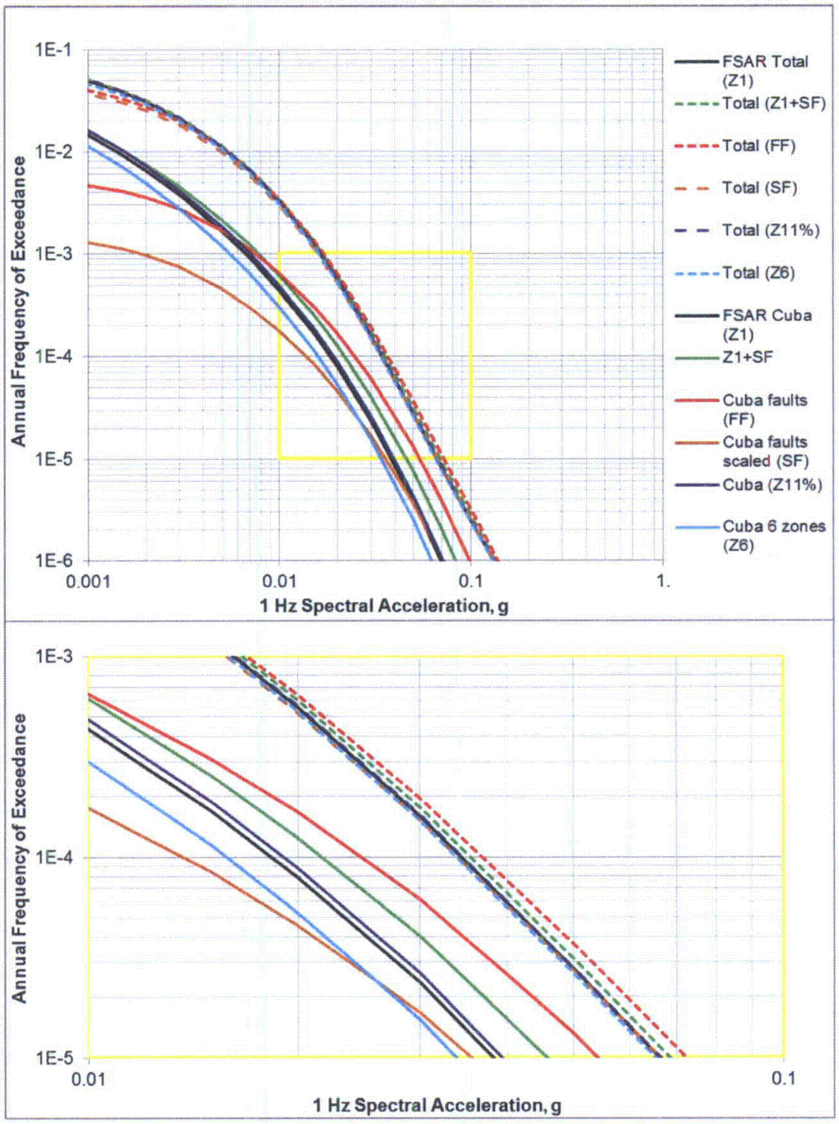

Figure 2.5.2-274 10 Hz Mean Hazard Curves Showing Sensitivity to Cuba Source Scenarios. Lower Panel is Expanded View of Yellow Box in Upper Panel.

PTN RAI 02.05.02-4

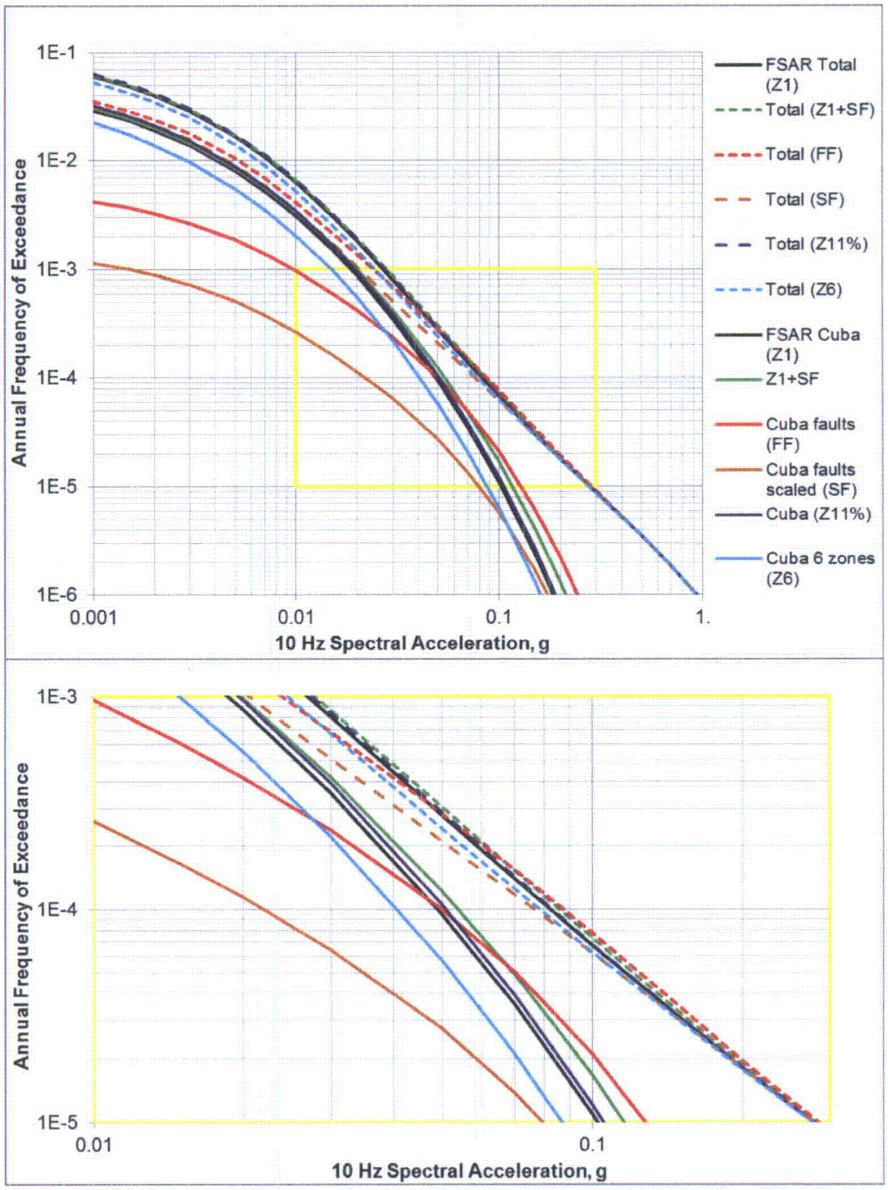

Figure 2.5.2-275 Total Mean Hazard Curves for 1 Hz (Upper) and 10 Hz (Lower) Showing Sensitivity to Four Cuba Source Scenarios

PTN RAI 02.05.02-4

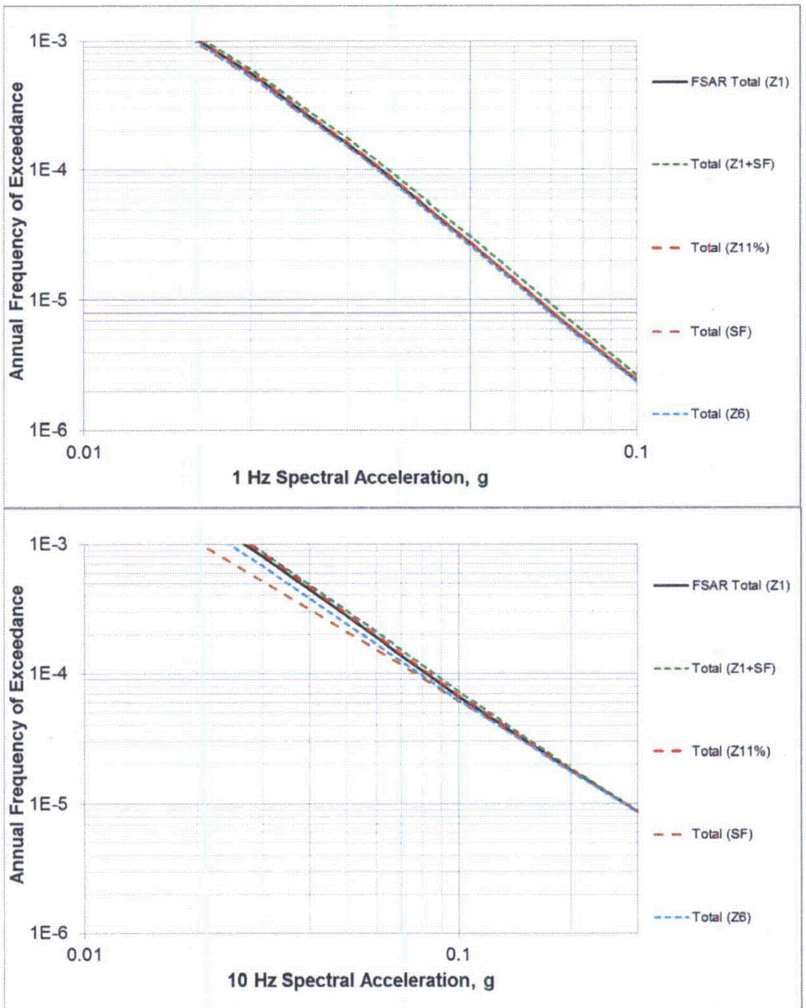

Source: Reference 242

Figure 2.5.2-276 Seismic Sources from the U.S. Geological Survey's 2008 National Seismic Hazard Mapping Project

PTN RAI 02.05.02-13

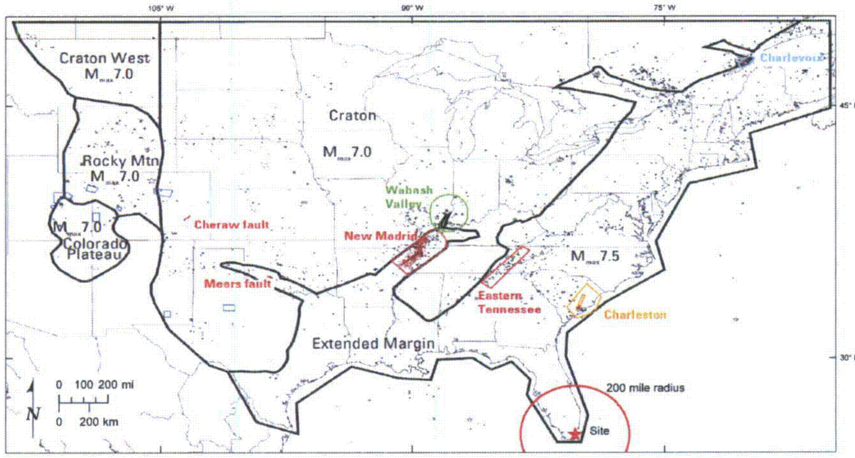

Source: Reference 300

Figure 2.5.2-277 Not Used

Figure 2.5.2-278 Not Used

Figure 2.5.2-279 Not Used

Figure 2.5.2-280 Seismotectonic Source Zones in the CEUS SSC Model

PTN RAI 01.05-1

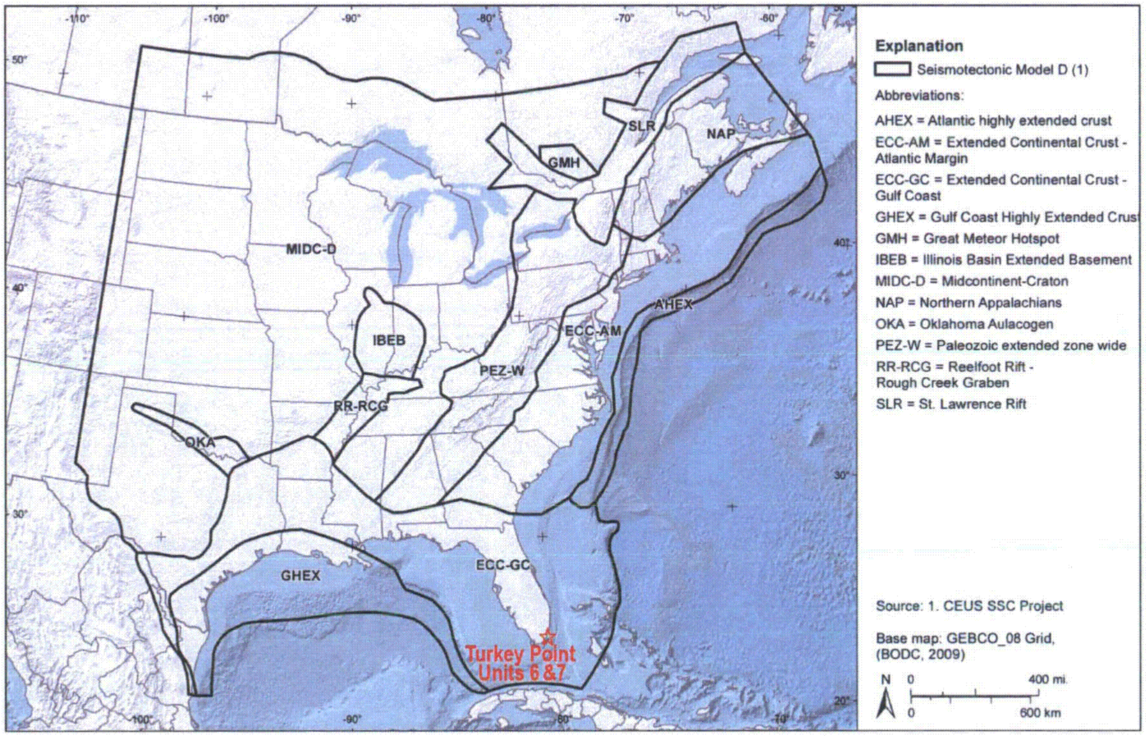

Note: Seismotectonic source zones for the “narrow” interpretation of PEZ and the Rough Creek Graben not included as part of the Reelfoot Rift (RR) source (Figure 4.2.4-2 of NUREG-2115). Approximate location of the Turkey Point Units 6 & 7 site is shown by the red star.

Figure 2.5.2-281 Mmax Source Zones in the CEUS SSC Model

PTN RAI 01.05-1

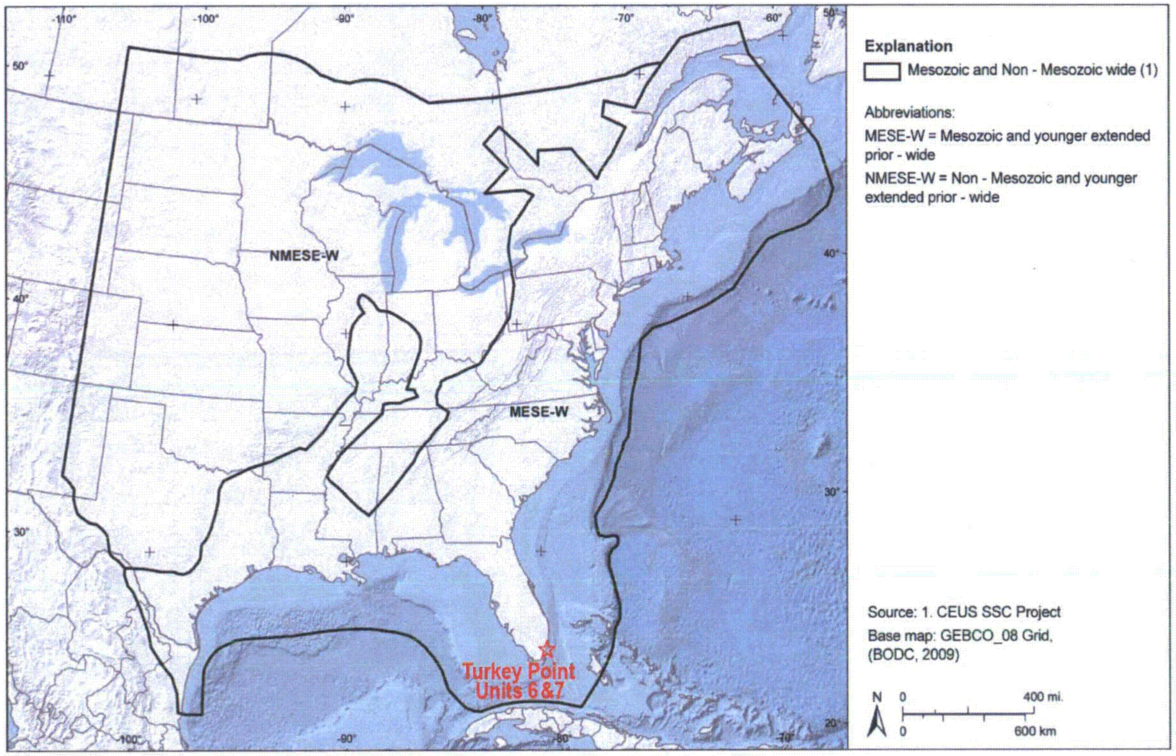

Note: Mmax source zones from the CEUS SSC model for the "narrow" interpretation (Figure 4.2.3-2 of NUREG-2115). Approximate location of the Turkey Point Units 6 & 7 site is shown by the red star.

PTN RAI 01.05-1

Figure 2.5.2-282 RLME Sources in the CEUS SSC Model

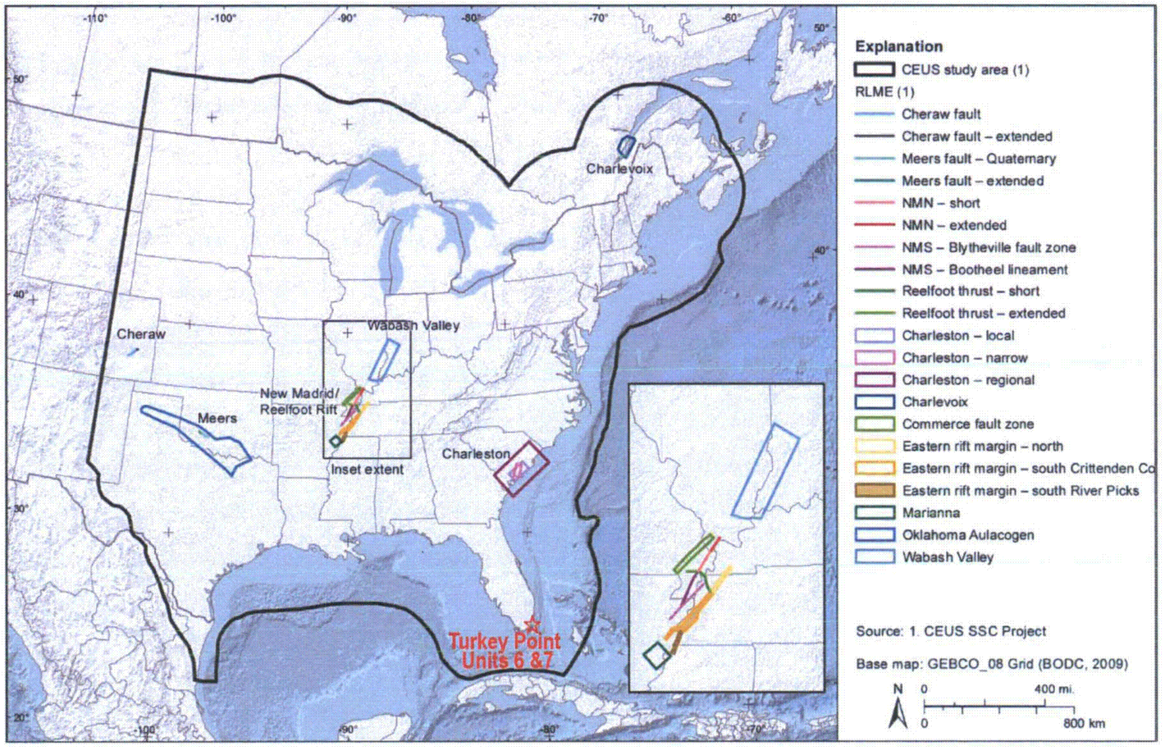

Note: Location of RLME sources in the CEUS SSC model (Figure 4.2.2-2 of NUREG-2115). Approximate location of the turkey Point Units 6 & 7 site is shown by the red star.

Figure 2.5.2-283 Contributions of Various Source Types to Hard Rock Hazard for 10 Hz

PTN RAI 01.05-1

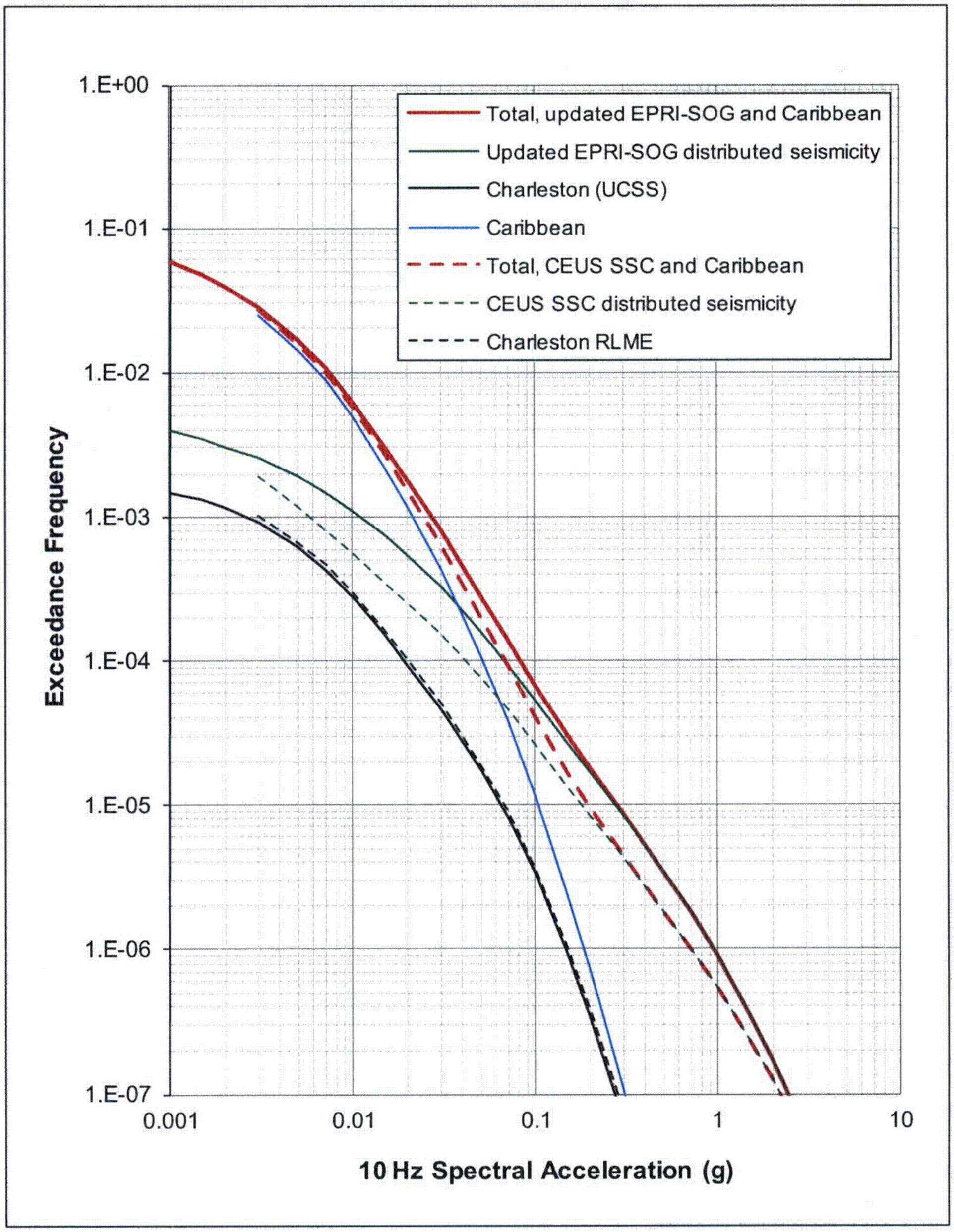

Note: Contributions of various source types to total hazard. Solid curves show hazard based on updated EPRI-SOG. Dashed curves show hazard based on CEUS SSC model.

Figure 2.5.2-284 Contributions of Various Source Types to Hard Rock Hazard for 1 Hz

PTN RAI 01.05-1

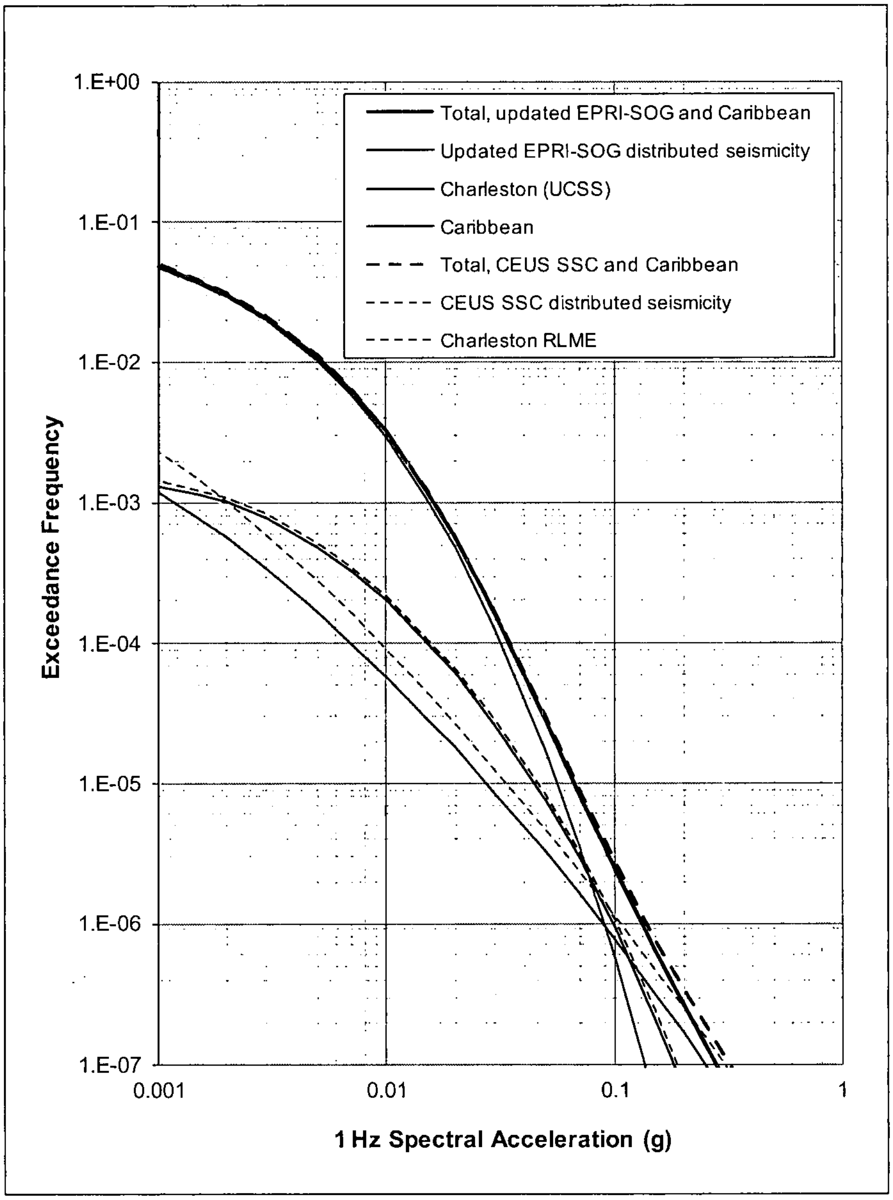

Note: Contributions of various source types to total hazard. Solid curves show hazard based on updated EPRI-SOG model. Dashed curves show hazard based on CEUS SSC model.

Figure 2.5.2-285 Comparison of Hard Rock UHRS

PTN RAI 01.05-1

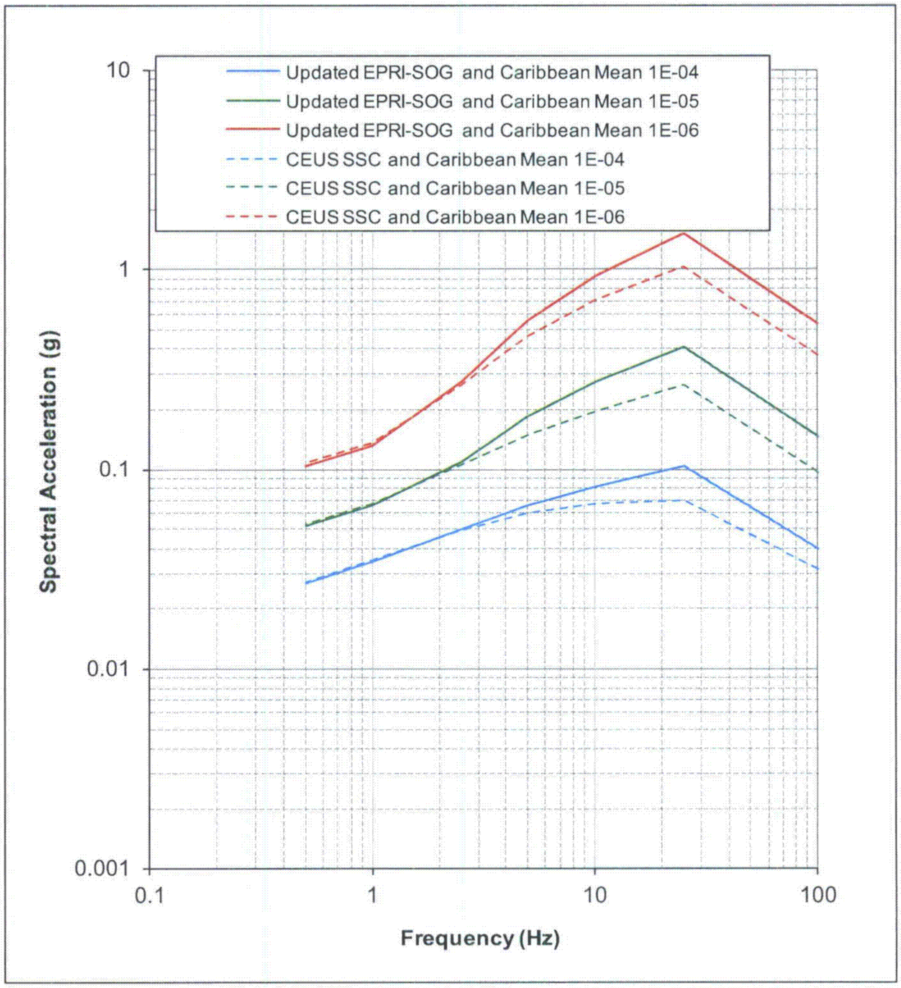

Note: Comparison between the hard rock UHRS based on the updated EPRI-SOG model plus Caribbean Sources, and the UHRS computed using the CEUS SSC model plus Caribbean sources.

Attachment 4

COLA Revision 5 Highlighted Pages for Subsection 2.5.3 RAIs

(Total Pages - 26)

SUBSECTION 2.5.3: SURFACE FAULTING
TABLE OF CONTENTS

SUBSECTION 2.5.3 LIST OF FIGURES

2.5.3 SURFACE FAULTING

PTN COL 2.5-4 This subsection evaluates the potential for tectonic and non-tectonic surface deformation within a 25-mile radius (site vicinity) of Units 6 & 7. Information contained in Subsection 2.5.3 was developed in accordance with RGs 1.165 and 1.208 in order to demonstrate compliance with 10 CFR 100.23(c). RG 1.208 contains guidance on characterizing seismic sources, and it defines a "capable tectonic source" as a tectonic structure that can generate both vibratory ground motion and tectonic surface deformation, such as faulting or folding at or near the earth's surface, in the present seismotectonic regime.

This section contains evaluations of:

- Potential surface deformation associated with capable tectonic sources.
- Potential surface deformation associated with non-tectonic processes, such as collapse structures (karst collapse), subsurface salt migration (salt domes), volcanism, and human-induced deformation (e.g., mining collapse and subsidence due to fluid withdrawal).

The conclusions developed in this subsection as well as Subsections 2.5.1 and 2.5.2 regarding the potential for surface deformation are summarized as follows:

- There are no capable tectonic fault sources or bedrock faults and there is no potential for tectonic fault rupture within the site, site area, or site vicinity.
- There is no evidence of Quaternary tectonic surface faulting or tectonic deformation within the site, site area, or site vicinity.
- There are non-tectonic surface deformation features within the site area and the site. Investigations show that these features are related to surficial dissolution of carbonate strata in the site area.

The following subsections contain the data, observations, evaluations, and references that form the bases for these conclusions.

2.5.3.1 Geological, Seismological, and Geophysical Investigations

Geological, seismological, and geophysical investigations have been performed at the site to characterize the local Quaternary tectonics, structural geology,

stratigraphy, paleoseismology, and geologic history. The results of these investigations, including site and regional geologic maps and profiles that illustrate lithology, stratigraphy, topography, and structure, are presented in Subsections 2.5.1 and 2.5.4. Evaluation of geological, seismological, and geophysical data obtained during investigation for the potential of surface faulting are presented in this subsection.

Information regarding the potential for surface faulting for the site is summarized below from the following investigations and sources:

- Compilation and Review of Existing Data and Literature: The UFSAR for Turkey Point Units 3 & 4 provides information about the stratigraphy and structure within the site area (Reference 209). Consequently, emphasis has been placed on published maps and literature pertaining to the structure, tectonics, and stratigraphy of the region published since the UFSAR (Reference 209). Materials include geologic mapping published by the Florida Geologic Survey and articles published in refereed journals and field trip guidebooks.

- Interpretation of Aerial Photography: Aerial photographs taken pre- and post-construction of Turkey Point Units 3 & 4 were obtained from the U. S. Geological Survey and Florida Department of Environmental Protection. Coverage includes black and white, color infrared, and true color photographs and stereo-pairs. The photographs cover the entire onshore portion of the site area and beyond and were examined specifically for evidence of tectonic or non-tectonic (e.g., karst or dissolution feature) surface deformation. This analysis included mapping and identifying lineaments, or linear features, in the site vicinity. No lineaments were identified within the site area.

- Review of Seismicity Data: A comprehensive catalog of instrumental and historical earthquakes was compiled and analyzed (Subsection 2.5.2.1). Based on the catalog, no earthquakes with estimated body wave magnitude (Emb) $\geq$ 3.0 have occurred within the Turkey Point site vicinity.

- Field and Aerial Reconnaissance: Geologic field reconnaissance was conducted as part of the Units 6 & 7 characterization activities. Field reconnaissance included visiting type localities for geologic units, performing detailed geologic mapping of the site, and visiting geomorphic features and outcrops of interest in the region. Aerial reconnaissance was focused on features closest to the site area but included assessment of lineations identified from the aerial photography study as well as two potential

geomorphic features described in the literature. No evidence of faulting or seismic activity (such as paleoliquefaction features) was found.

- Geologic reconnaissance and aerial photo analysis: Numerous ellipsoidal or circular features with a higher concentration of vegetation as well as water-filled areas that are generally less than 1 foot lower in elevation than the surrounding areas within the site and site area were identified; however, these surficial depressions observed on pre-construction photographs were both small and confined to the near-surface. Many surficial depressions have been removed by construction of the Turkey Point Units 3 & 4 cooling canals.

- Integrated Multi-method Geophysical Survey: An integrated, multi-method geophysical investigation program was conducted on and around the area of Units 6 & 7. The geophysical investigation program was focused on identifying the potential for subsurface dissolution features. Geophysical techniques deployed consisted of high-resolution microgravimetric, seismic refraction, and multichannel analysis of surface waves techniques obtained in collocated lines. The results of this survey found no evidence of cover-subsidence or cover-collapse hazards in the site area (Subsection 2.5.4.4.5).

2.5.3.1.1 Previous Site Investigations

The results of previous geologic and seismologic investigations are presented in the UFSAR for Turkey Point Units 3 & 4 (Reference 209) and in a more detailed study of the 5-mile radius site area (Reference 215). Both studies conclude that no tectonic or non-tectonic surface deformation hazards exist at the site. In addition, the UFSAR states that “local depressions, some of which attain depths as great as 16 feet, are occasionally encountered in the surface of the limestone bedrock at the site. Such depressions are not sinkholes associated with collapse above an underground solution channel, but rather potholes, which are surficial erosion or solution features” (Reference 209). The UFSAR further explains that the Miami Limestone and Fort Thompson Formation have been susceptible to solution activity from groundwater during periods of low sea level (Pleistocene glacial advances), but that the “bedrock beneath the site is competent with respect to foundation conditions and is capable of supporting heavy loads” (Reference 209) (Subsection 2.5.4.4.5).

2.5.3.1.2 Regional and Local Geological Studies

Regional and local geologic mapping by the Florida Geologic Survey and other researchers does not indicate any faults at the surface on the Florida peninsula

within the 200-mile radius site region (References 213, 214, 226, 212, and 234) (Figures 2.5.1-201 and 2.5.1-331). Mapping indicates that the Miami Limestone, a Pleistocene unit approximately 20 feet thick, is exposed over an area greater than 50 miles wide in southern Florida (Reference 226). The outcrop pattern indicates that less than 20 feet of offset or differential erosion has occurred over a wide area and is evidence for the lack of geologic deformation in the region. Well data along a greater than 30-mile east-west transect indicate a maximum relief on the base of the Miami Limestone of 10 feet (References 213 and 214) and this variability is due to sedimentary variations in unit thickness. All geologic contacts within the site area and site are sedimentary in nature (Figures 2.5.1-335, 2.5.1-334, and 2.5.1-337).

In addition to the geologic mapping described above, the U.S. Geological Survey has published a compilation of all known or suggested Quaternary faults, liquefaction features, and possible tectonic features in the Central and Eastern United States (References 203 and 235) (Figure 2.5.3-201). These compilations did not extend into the Bahamas or Cuba, and therefore do not depict faults in these regions. Within the boundaries of these compilations, no Quaternary tectonic faults or tectonic features are identified in the site region or site area. However, one potential Quaternary feature, Grossman's Hammock, is located approximately 20 miles northwest of the site, but a ground-penetrating radar study provides evidence that the feature has no tectonic offset (Reference 217); Subsection 2.5.3.2 describes this feature in detail. The U.S. Geological Survey studies (References 203 and 235) classify Grossman's Hammock as a non-tectonic feature (Figure 2.5.3-201).

The United States Army Corps of Engineers (USACE) used Landsat satellite data, supplemented locally with digital orthophoto quadrangles, to identify possible linear features across central and southern Florida (Reference 232) (Figure 2.5.3-204). This study identifies more than 500 lineaments, or linear patterns, in sinkholes and solution depressions, ponds or lakes, streams, and tonal changes. The features have dominantly a northwest trend (~305°) with a secondary northeast (~40°) trend. While the USACE notes that the northwest trend is similar to the trend of previously hypothesized basement structures, e.g., the Bahamas fracture zone, no offsets along any of these lineaments are reported, nor are any designated as faults (Reference 232). The northwest and northeast orientations exhibited by the mapped lineaments are typical for all of Florida, and are recognized as reflecting joint or fracture patterns in the limestone, which are enhanced by karstic dissolution (e.g., Reference 221). The density of mapped lineaments appears to be directly proportional to karst density (Figure 2.5.1-222).

2.5.3.1.3 Seismicity Data

The Florida peninsula is an area of low seismic activity. The original EPRI earthquake catalog (Reference 205) does not contain any earthquakes within the Turkey Point site vicinity. Only three earthquakes in the original EPRI catalog (Reference 205) occur within the 200-mile radius site region. However, the original EPRI catalog did not cover Cuba and large parts of the Gulf of Mexico (Subsection 2.5.2.1.2).

As described in Subsection 2.5.2.1.2, the EPRI earthquake catalog for this COL investigation was updated to include earthquakes that have occurred after the publication of the EPRI catalog. Moreover, this updated earthquake catalog extends south of the original EPRI catalog to include the entire site region and beyond to a latitude of 15° N.

The updated earthquake catalog for the Phase 1 seismicity investigation region (22° to 35° N, 100° to 65° W) contains a total of about 700 earthquakes with Rmb ≥ 3.0 or intensity $I_0 \geq$ IV for all years through mid-February 2008 (Figure 2.5.3-201). Approximately 66 out of about 700 earthquakes are located within the 200-mile radius site region. Most of these earthquakes are concentrated in a zone of seismicity in and near Cuba, which is greater than about 160 miles south of the Units 6 &7 site. Figure 2.5.3-203 shows that there are no earthquakes from the updated Phase 1 earthquake catalog inside the 25-mile radius site vicinity.

2.5.3.1.4 Current Field and Aerial Reconnaissance

Aerial photography, satellite imagery, and topographic maps of varying scales and vintages reveal no evidence of geomorphic features indicative of the potential for tectonic surface deformation (e.g., faulting or folding) within the site area. Imagery reviewed as part of this COL investigation includes:

- 1:40,000-scale, black and white, stereo aerial photographs acquired in 1940 by the U.S. Geological Survey covering the entire site area (pre-construction).
- 1:40,000-scale, color infrared photographs acquired in 1999 by the Florida Department of Environmental Protection covering the entire site area and much of southern Florida.
- 1:40,000-scale, true color photographs acquired in 2004 by the Florida Department of Environmental Protection covering the entire site area and much of southern Florida.

- 1:20,000-scale, black and white photographs (1944) near Ft. Myers, Florida from the archives of the University of Florida.
- 1:40,000-scale, color infrared photographs acquired in 2004 by the U.S. Geological Survey near the Shark River in Everglades National Park.

Southern Florida is characterized by extremely subdued topography. In general, the only features on topographic maps with elevations greater than 5 feet within the site and site area are man-made roads or levees. To the north, the Atlantic Coastal Ridge (Subsection 2.5.1.1.1.1.1.1) trends north-northeast to south-southwest; it is up to 50 feet high and extends into the site vicinity (Reference 236). No topographic features within the site vicinity indicate the presence of surface faulting.

Based on an analysis of aerial imagery, three north-south-trending vegetation lineaments were identified more than 5 miles west of the site. These lineaments were investigated during aerial and field reconnaissance; no evidence for surface rupture or geomorphic features indicative of active faulting was found. The lineaments were identified as linear swaths where vegetation had been cleared. Review of published literature in southern Florida identified four other features that were further investigated during fieldwork:

- Grossman's Hammock, a rock reef in Everglades National Park, approximately 20 miles northwest of the site (Reference 231).
- Tree lineaments reported near the intersection of Flamingo Road and Ingram Highway in Everglades National Park, located 18 miles west of the site (Reference 236).
- A linear segment of the Shark River channel in Everglades National Park, approximately 34 miles west of the site (Reference 236), beyond the site vicinity.
- Faults postulated from borehole data in the McGregor Isles area near Ft. Myers, 120 miles northwest of the site (Reference 230), beyond the site vicinity.

Subsection 2.5.3.2 provides additional description of these four features. Based on the geologic field reconnaissance, no geomorphic or other evidence for faulting or surface deformation is associated with any of these features. In addition, field and aerial reconnaissance did not identify any evidence for surface rupture,

warping, or offset of geomorphic features indicative of active faulting within the site or site area. Field and aerial reconnaissance did identify several vegetated and some water-filled depressions (Figures 2.5.1-333 and 2.5.3-202) within the site and site area, which are interpreted to be related to a process of surficial dissolution (Subsection 2.5.4.4.5). Analysis of 1:40,000 scale aerial photos that were taken in the 1940s prior to construction at the Turkey Point site indicates that many of these surficial depressions have been obliterated by the construction of Turkey Point Units 3 & 4 cooling canals.

2.5.3.2 Geological Evidence, or Absence of Evidence, for Surface Deformation

Field reconnaissance, review and interpretation of aerial photography, and review of published literature did not reveal any evidence for active tectonic deformation within the site vicinity or site area. No active faults or geomorphic features relating to active faulting have been mapped in the site vicinity, site area, or the site (Figures 2.5.1-334, 2.5.1-336, 2.5.1-337, 2.5.1-338, 2.5.1-339, 2.5.1-340, 2.5.1-341, and 2.5.1-342). Although a basement fault has been interpreted to exist within the site vicinity (Figure 2.5.1-253), there is no evidence to suggest that this buried pre-Cretaceous fault is active or represents a surface faulting hazard (Figures 2.5.1-261 and 2.5.1-263) (Subsection 2.5.1.1.1.3.2.1). Therefore, no capable faults are known to exist within the site vicinity. In addition, no seismic activity has been reported within the site vicinity (Subsection 2.5.2), and bedding is horizontal and undisturbed (Subsection 2.5.1.2.3). No salt domes, Quaternary volcanic features, or glacial sources of deformation occur in the site vicinity (Figures 2.5.1-201 and 2.5.1-237) (Subsections 2.5.3.8.2.1, 2.5.1.1.2.1.1, 2.5.1.1.1.2.1.1, 2.5.1.2.4, and 2.5.1.2.3). Non-tectonic deformation features in the site area are interpreted to be "potholes" caused by surficial dissolution (Subsections 2.5.1.2.4 and 2.5.4.4.5). PTN RAI 02.05.03-3

The site vicinity is located on the Florida carbonate platform, a tectonically stable region (Reference 219) that is characterized by extremely low rates of seismicity. The updated earthquake catalog includes no seismicity within the site vicinity (Subsection 2.5.2.1). Historical and late Holocene sea level data collected in central and southern Florida show tectonic quiescence during this period (Reference 211). Published geologic mapping at a range of scales show no bedrock faults mapped within the site vicinity (References 211, 213, 214, and 226). Regional high-resolution bathymetry and seismic data give no indication of faulting in shallow sediments offshore along the Florida Keys (References 237 and 238) or onshore in Dade county (Reference 239).

Within the site vicinity, Grossman's Hammock is the only geomorphic feature that has been speculated to be related to faulting (Figure 2.5.3-201). Grossman's Hammock (sometimes referred to as "rock reef") is 8 miles long and is similar to eight other ridges in southern Florida that have widths of approximately 300 feet and vertical relief of 1-5 feet. Steinen et al. (Reference 231) interpret a fault to account for the apparent offset of a buried Quaternary erosion surface identified in a limited number of boreholes beneath Grossman's Hammock. However, more recent work, including a ground-penetrating radar study showing no offset on the underlying Quaternary surface, documents that there is no faulting associated with this feature (Reference 217). Consequently, Crone and Wheeler (Reference 203) classify Grossman's Hammock as a Class D feature; that is, geologic evidence demonstrates that the feature is not a tectonic fault or structure (Figure 2.5.3-201). Other postulated explanations for Grossman's Hammock include fracture-related preferential cementation, and preservation of paleoshorelines or paleo-mud banks. While its origin is unresolved, tectonic faulting has been effectively ruled out as a hazard associated with this feature (Reference 235).

Also within the site vicinity, White (Reference 236) indicates that trees in the Everglades National Park form a local alignment near the intersection of the Main Park Road (previously called Flamingo Road) and Ingram Highway. Although a geologic cause for such an alignment is improbable, this feature was investigated as part of geologic field reconnaissance. Ground-based observations as well as satellite imagery and aerial reconnaissance photographs did not reveal the presence of an alignment of trees nor any linear features that would be subject to further examination.

No geomorphic features or lineaments associated with faulting within the site area were identified during analysis of aerial imagery. The lineament analysis did identify numerous linear and ellipsoidal/circular features associated with changes in vegetation within 5 and 0.6 miles of Units 6 & 7 (Figures 2.5.1-333 and 2.5.3-202). These ellipsoidal or circular features are loci of more highly concentrated vegetation. These features are interpreted to be the result of the surficial dissolution of the limestone bedrock and are described in detail in Subsection 2.5.3.8.2. The linear features associated with these vegetated patches within the site area generally are characterized by an alignment of two to three vegetated patches connected by short, narrow drainage features. These features are oriented perpendicular to the coastline (oriented roughly east-west to northeast-southwest). The linear channels between the vegetated patches are interpreted to be tidally influenced (Reference 236). Fieldwork following the aerial

imagery analysis indicated that the three north-south trending vegetation lineaments located 5-6 miles west of the site are simply areas where the vegetation has been cut down in wide swaths. There is no geomorphic expression of these features or other evidence that would indicate tectonic faulting associated with these vegetation lineaments.

Two features beyond the site vicinity were investigated as part of the geologic field reconnaissance. The first of these is a linear segment of the Shark River channel in Everglades National Park, approximately 34 miles west of the site. This linear segment was identified by White (Reference 236) and is within the Shark River slough, the dominant path of surface-water flow from anthropologically routed water discharge sites in central Florida to the southwest Gulf coast of Florida. The channel system in the Shark River slough is developed on limestone bedrock, with peat, organic debris, and shells forming mounds or levees that separate the channels. Based on field reconnaissance and review of aerial photography, there is no evidence to suggest that this linear segment is tectonic in origin. Instead, tides, joints in the limestone bedrock, and human-controlled water flow likely influence its linearity.

The second feature beyond the site vicinity investigated as part of geologic field reconnaissance includes possible faults identified from borehole data in the McGregor Isles area near Ft. Myers, 120 miles northwest of the site. Based on gamma-ray logs from several wells, Sproul et al. (Reference 230) interpret faulting of pre-upper Hawthorn (Miocene) strata. In spite of their interpretation that overlying upper Hawthorn and younger strata are unfaulted, Sproul et al. (Reference 230) suggest possible geomorphic indicators of faulting. Sproul et al. (Reference 230) noted a bend in the coastline near the westward projection of a few of the subsurface faults and that a stream between two of the faults is aligned subparallel to the faults. However, despite the landscape being heavily modified by urban development, field reconnaissance and inspection of aerial photography reveal no evidence for faulting at the surface, and published studies identified no surficial faulting in the area (Reference 240).

PTN RAI 02.05.03-4 LDP-CS564

PTN RAI 02.05.03-4

2.5.3.3 Correlation of Earthquakes with Capable Tectonic Sources

The original EPRI earthquake catalog was updated to incorporate earthquakes that occurred between 1985 and mid February 2008 (Subsection 2.5.2.1.2). The updated Phase 1 earthquake catalog contains no earthquakes within the site vicinity (Table 2.5.2-201). No seismicity or capable tectonic sources exist within the site vicinity or site area; therefore, there is no spatial correlation of earthquake epicenters or capable tectonic sources (Figure 2.5.3-203).

2.5.3.4 Ages of Most Recent Deformation

Field reconnaissance, review and interpretation of aerial photography, and review of published literature do not reveal any evidence for tectonic deformation within the site vicinity. In addition, results of the subsurface exploration program at the site indicate continuous, horizontal stratigraphy that precludes the presence of faults, folds, or structures related to tectonic deformation (Figure 2.5.1-335). Therefore, there is no correlation of geologic structures to ages of recent deformation (Figures 2.5.1-338, 2.5.1-339, 2.5.1-340, and 2.5.1-341) (Subsection 2.5.1.2.5.3).

2.5.3.5 Relationship of Tectonic Structures in the Site Area to Regional Tectonic Structures

Field reconnaissance, review and interpretation of aerial photography, and review of published literature do not reveal any evidence for tectonic deformation within the site area. In addition, results of the subsurface exploration program at the site indicate continuous, horizontal stratigraphy that precludes the presence of faults, folds, or structures related to tectonic deformation (Figures 2.5.1-338, 2.5.1-339, 2.5.1-340, 2.5.1-341). Therefore, there is no correlation of geologic structures in the site area to regional, capable tectonic structures (Subsection 2.5.1.2.5.3).

2.5.3.6 Characterization of Capable Tectonic Sources

Field reconnaissance, review and interpretation of aerial photography, and review of published literature, do not reveal any evidence for tectonic deformation within the site vicinity. In addition, results of the subsurface exploration program at the site indicate continuous, horizontal stratigraphy that precludes the presence of faults, folds, or structures related to tectonic deformation (Figure 2.5.1-335) (Subsections 2.5.1.2, 2.5.1.2.2, and 2.5.1.2.3). Based on the above data and analyses, there are no capable tectonic sources within the site vicinity or site area.

2.5.3.7 Designation of Zones of Quaternary Deformation in the Site Region

Results of the subsurface exploration program at the site indicate continuous, horizontal stratigraphy that precludes the presence of Quaternary faults, folds, or structures related to tectonic deformation at the site (Figure 2.5.1-335). There are no zones of Quaternary deformation associated with tectonic faults requiring detailed investigation within the site area (Figure 2.5.1-335). Field reconnaissance, review, and interpretation of aerial photography, and review of published literature performed, do not reveal any evidence for Quaternary tectonic deformation, including paleoliquefaction, within the site, site area, or site vicinity.

Within the site region, seismicity and potential Quaternary deformation are restricted to the faults within the Cuba areal source zone, approximately 140 miles south of the site, and possible deformation associated with the Walkers Cay fault and Santaren anticline (Figure 2.5.3-205). No sand blows or paleoliquefaction features have been identified in the published literature for the site region. Karstic dissolution of limestone is a source of non-tectonic Quaternary deformation found in Florida and the Bahamas within the site region (Subsection 2.5.3.8.2.1 and 2.5.4.4.5). PTN RAI 02.05.03-2 LDP-CS561

2.5.3.8 Potential for Tectonic or Non-Tectonic Deformation at the Site

There are no sources for potential tectonic deformation at the site. The only evidence for non-tectonic deformation at the site is "potholes" that appear to be caused by surficial dissolution (Subsection 2.5.1.2.4). The potential for carbonate dissolution and karst development at the site is discussed in Appendix 2.5AA. LDP-CS561

2.5.3.8.1 Potential for Tectonic Deformation at the Site

Field reconnaissance, review and interpretation of aerial photography, and review of published literature do not reveal any evidence for tectonic deformation at the site (Subsections 2.5.1.2, 2.5.1.2.2, and 2.5.1.2.3). In addition, results of the subsurface exploration program at the site indicates continuous, horizontal stratigraphy that precludes the presence of faults, folds, or structures related to tectonic deformation (Figure 2.5.1-335). Therefore, there is no potential for tectonic surface deformation at the site, nor are there any capable tectonic faults within the site vicinity. The subsurface exploration program shows no evidence of folding or warping related to Quaternary tectonic activity (Figures 2.5.1-335 and 2.5.3-201).

Quaternary volcanic activity has not been mapped in the site region (Figure 2.5.1-201). The field reconnaissance and review of published literature indicate no sand blows or paleoliquefaction features are identified in the site area.

2.5.3.8.2 Potential for Non-Tectonic Deformation

No salt domes, Quaternary volcanic features, or glacial sources of deformation occur in the site vicinity (Figures 2.5.1-201 and 2.5.1-237). No human activities occurring in the site area pose a hazard for surface deformation. The only evidence for non-tectonic deformation at the site is "potholes" caused by surficial dissolution (Subsection 2.5.4.4.5). The potential for carbonate dissolution and karst development at the site is discussed in Appendix 2.5AA. LDP-CS561

2.5.3.8.2.1 Potential Sources of Non-Tectonic, Geologic Deformation

There is no evidence of non-tectonic deformation within the site in the form of glacially induced faulting or salt migration. Pleistocene continental glaciers did not extend as far south as the site region, and there are no documented examples of glacially induced faulting in the site region. No piercement-type salt domes are located within the site vicinity. The nearest salt dome is approximately 220 miles southeast of Units 6 & 7 along Cuba's northern coast. The Florida coastal plain is part of a stable continental region, and no Tertiary or Quaternary volcanic activity is found within the site vicinity. The nearest Cenozoic volcanic activity is recorded in early Tertiary tuffs located 400 miles southeast of Units 6 & 7 in southeastern Cuba (Reference 218). The subdued topography indicates that no slopes are steep enough within the site area to pose a slope-stability hazard. However, deformation related to karst is noted in southern Florida (Reference 223), and limestone dissolution is evident in stratigraphic units, such as the Miami and Key Largo Limestones, which underlie the site (References 222 and 225). These are not expected to pose a significant surface deformation hazard at the Units 6 & 7 site. The potential for carbonate dissolution and karst development at the site is discussed in Appendix 2.5AA. LDP-CS561

Quaternary limestones in the region, including the Key Largo Limestone, the Miami Limestone, and portions of the Fort Thompson Formation, are documented as exhibiting vugs and high permeability related to soluble, karstic limestone (References 204, 215, 209, and 216) (Subsections 2.5.1.2.4, 2.5.1.1.1.2.1.1, and 2.5.4.1.2.1). In addition, an offshore U.S. Geological Survey study just southeast of the site vicinity has documented the presence of a 600-meter-diameter sinkhole southeast of Key Largo (Reference 228). Furthermore, the UFSAR indicates that "local depressions, some of which attain depths as great as 16 feet, are occasionally encountered in the surface of the limestone bedrock at the site" (Reference 209). However, the UFSAR concludes that these features are "not sinkholes associated with collapse above an underground solution channel, but rather potholes, which are surficial erosion or solution features" (Reference 209). The conclusion has been substantiated by an integrated geophysical investigation (Subsections 2.5.4.4.5 and 2.5.1.2.4).

Geologic reconnaissance and aerial photo analysis identified numerous ellipsoidal or circular features. These features consist of vegetation and water-filled areas that are generally less than 1 foot lower in elevation than the surrounding areas within the site and site area. Many of these surficial depressions observed on pre-construction photographs have been obliterated by construction of the Turkey Point Units 3 & 4 cooling canals (Figures 2.5.1-333 and 2.5.3-202). The

underlying Miami Limestone is covered by recent deposits of organic-rich mud and silt approximately 0.6 to 1.8 meters (2 to 6 feet thick) (Subsection 2.5.1.2.2). In these vegetated areas, field and geotechnical work investigations have confirmed that the deposits of mud and silt reach thicknesses exceeding 1.8 meters (6 feet) and appear to be wetter than the surrounding areas. These karst features were formed after the deposition of the Pleistocene Miami Limestone, but their exact timing is not known. The formation and significance of the vegetated depressions are discussed further in Appendix 2.5AA. PTN RAI 02.05.01-17

The Florida Geological Survey generally assigns a low hazard to karst features that form when limestone is exposed at the surface or beneath a thin veneer of permeable sediment, as is the case within the site area (Reference 229) (Figure 2.5.1-222). In these cases, such solution potholes are generally expected to be shallow and broad and to develop gradually, rather than in a single, sudden collapse event. Additionally, these solution potholes are not expected to form large voids beneath the surface that would pose a hazard to the site (Reference 229). Based on information developed in this subsection and in Subsection 2.5.1.2.5.2, the possibility of dissolution features similar to the one reported southeast of Key Largo (Reference 228) existing at depth beneath this site area is unlikely (Subsection 2.5.4.4.5). No collapse or settlement problems associated with karst-type dissolution of underlying limestones have been associated with Turkey Point Units 3 & 4 (Reference 209). An integrated geophysical survey focused on the Units 6 & 7 power block area and several of the surficial depressions identified within the site was conducted as part of this application and is discussed in Subsection 2.5.4.4.5. Although subject to spatial resolution and detection limits inherent in a subsurface investigation, the available borehole and geophysical data indicate there is minimal hazard posed by sinkholes and no evidence for potential surface collapse due to the presence of large underground openings at the site. LDP-CS561

2.5.3.8.2.2 Potential Sources of Non-Tectonic, Human-Related Deformation

There is no human-related, permanent ground deformation hazard at the site. There are no underground mining activities within the site area that may produce man-induced surface collapse. The closest quarrying activities are located 8 miles from the site and include localized blasting and excavation. This surficial excavation is not expected to impact the site area. No oil or gas production-related activities occur within the site or site area. Some oil and gas exploration has been performed in southern Florida, and approximately six dry holes were drilled within the site vicinity (Reference 208). No ground-shaking or subsidence hazard is expected from these activities (Subsection 2.5.1.2.5.4).

2.5.3.8.3 Summary of Potential Deformation at the Site

There is no evidence of potential tectonic faulting or tectonic deformation at the site. The only potential non-tectonic, geologic hazard at the site is surficial limestone dissolution. No apparent indicators of collapse or settlement problems exist at the site, and the geotechnical investigation found no evidence for subsurface dissolution features that would cause such problems. This conclusion is partly confirmed by the results of an integrated geophysical investigation focused on identification of subsurface dissolution features at the site (Subsection 2.5.4.4.5). No human-related deformation hazard exists at the site. To address uncertainties in the resolution of the geophysical data away from survey lines and at depth beneath the foundation, a microgravity survey will be conducted at the base of the Unit 6 and Unit 7 nuclear island excavations (Subsection 2.5.4.4.5.5).

PTN RAI 03.08.05-1

PTN RAI 03.08.05-1

PTN RAI 03.08.05-1

2.5.3.9 References

201. British Oceanographic Data Centre, Centenary Edition of the GEBCO Digital Atlas, Global One Arc-Minute Bathymetric Grid, *General Bathymetric Chart of the Oceans*. Available at http://www.bodc.ac.uk/data/online_delivery/gebco/, accessed November 18, 2008.

202. Scott, T., K. Campbell, F. Rupert, J. Arthur, T. Missimer, J. Lloyd, W. Yon, and J. Duncan, *Geologic Map of the State of Florida*, Map Series 146, Florida Department of Environmental Protection, Florida Geologic Survey, 2001 (Revised April 15, 2006 by David Anderson).

203. Crone, A. and R. Wheeler, *Data for Quaternary Faults, Liquefaction Features, and Possible Tectonic Features in the Central and Eastern United States, East of the Rocky Mountain Front*, U.S. Geological Survey, Open-File Report 00-260, 2000.

204. Cunningham, K., R. Renken, M. Wacker, M. Zygnerski, E. Robinson, A. Shapiro, and G. Wingard, *Application of Carbonate Cyclostratigraphy and Borehole Geophysics to Delineate Porosity and Preferential Flow in the Karst Limestone of the Biscayne Aquifer, SE Florida*, Perspectives on Karst Geomorphology, Hydrology, and Geochemistry, Special Paper, Vol. 404, pp. 191–208, Geological Society of America, 2006.

205. Electric Power Research Institute, *Seismic Hazard Methodology for the Central and Eastern United States*, Document No. NP 4726, 1986.

206. Not Used.

207. Florida Department of Environmental Protection, *RGB Aerial Photography*, 2004.

208. Florida Geological Survey, *Regional Oil and Gas Well Location Maps*, Map Series 6, Sheet 13 of 26, 2002.

209. Florida Power & Light Company, *Updated Final Safety Analysis Report for Turkey Point Units 3 & 4*, Docket Nos. 50-250 and 50-251, Miami-Dade County, Florida, 1992.

210. French, C. and C. Schenk, (digital compilers), *Map Showing Geology, Oil and Gas Fields, and Geologic Provinces of the Caribbean Region*, U.S. Geological Society, Open-File Report 97-470-K, 2004. Available at http://pubs.usgs.gov/of/1997/ofr-97-470/of97-470k/graphic/data.html, accessed June 5, 2008.

211. Gornitz, V. and L. Seeber, *Vertical Crustal Movements along the East Coast, North America, from Historic and Late-Holocene Sea Level Data, Tectonophysics*, Vol. 178, pp. 127–150, 1990.

212. Green, R. and K. Campbell, *Surficial Sediments of the Western Portion of the USGS 1:100000 Scale Homestead Quadrangle,* Florida Geological Survey, Open-File Map Series 83-09, 1996.

213. Green, R, K. Campbell, and T. Scott, *Bedrock Geology of the Eastern Portion of the USGS 1:100000 Scale Homestead Quadrangle*, Florida Geological Survey, Open-File Map Series 83-01, 1995.

214. Green, R, K. Campbell, and T. Scott, *Surficial Sediment Map of the Eastern Portion of the USGS 1:100000 Scale Homestead Quadrangle*, Florida Geological Survey, Open-File Map Series 83-02, 1995.

215. Gupton, C. and S. Berry, *Mat Foundations on Miami Limestone*, presented to the Florida Section of American Society of Civil Engineers, Orlando, Florida, Meeting, September 24, 1976.

216. Halley, R. and C. Evans, *The Miami Limestone: A Guide to Selected Outcrops and Their Interpretation*, p. 63, Miami Geological Society, 1983.

217. Kruse, S., J. Schneider, D. Campagna, J. Inman, and T. Hickey, *Ground Penetrating Radar Imaging of Cap Rock, Caliche and Carbonate Strata*, Journal of Applied Geophysics, Vol. 43, pp. 239–249, 2000.

218. Lewis, J. and G. Draper, *Geology and Tectonic Evolution of the Northern Caribbean Margin*, The Geology of North America, Vol. H, The Caribbean Region, Geological Society of America, 1990.

219. Ludwig, K., D. Muhs, K. Simmons, R. Halley, and E. Shinn, *Sea-Level Records at ~80 ka from Tectonically Stable Platforms: Florida and Bermuda*, Geology, Vol. 24, pp. 211–214, 1996.

220. National Oceanic and Atmospheric Administration, *National Geophysical Data Center Coastal Relief Model*. Available at http://www.ngdc.noaa.gov/mgg/coastal/startcrm.htm, accessed March 19, 2008.

221. Paull, C., F. Spiess, J. Curray, and D. Twichell, *Origin of Florida Canyon and the Role of Spring Sapping on the Formation of Submarine Box Canyon*, Geological Society of America Bulletin, Vol. 102, pp. 502–515, 1990.

222. Parker, G. and C. Cooke, *Late Cenozoic Geology of Southern Florida with a Discussion of the Ground Water*, Florida Geological Survey, Bulletin 27, p. 119, 1944.

223. Parker, G., G. Ferguson, S. Love, et al., *Water Resources of Southeastern Florida, with Special Reference to the Geology and Ground Water of the Miami Area*, U.S. Geological Survey, Water Supply Paper 1255, p. 965, 1955.

224. Puri, H. and R. Vernon, *Summary of the Geology of Florida*, Florida Geological Survey, Special Publication 5, p. 312, 1964.

225. Schroeder, M. and H. Klein, *Geology of the Western Everglades Area, Southern Florida*, U.S. Geological Survey, Circular 314, 1954.

226. Scott, T., K. Campbell, R. Rupert, J. Arthur, T. Missimer, J. Lloyd, J. Yon, and J. Duncan, *The Geologic Map of Florida*, Scale 1:750,000, Florida Geological Survey, 2001.

227. Scott, T., *Text to Accompany the Geologic Map of Florida*, Florida Geological Survey, Open-File Report 80, 2001.

228. Shinn, E., C. Reich, S. Locker, and A. Hine, *A Giant Sediment Trap in the Florida Keys*, Journal of Coastal Research, Vol. 12, No. 4, pp. 953–959, 1996.

229. Sinclair, W. and J. Stewart, *Sinkhole Type, Development, and Distribution in Florida*, U.S. Geological Survey, Map Series 110, 1985.

230. Sproul, C., D. Boggess, and H. Woodard, *Saline-Water Intrusion from Deep Artesian Sources in the McGregor Isles Area of Lee County, Florida*, U.S. Geological Survey and the Florida Department of Natural Resources, Information Circular 75, 1972.

231. Steinen, R., E. Shinn, and R. Halley, *Hypothesized Fault Origin for the Rock Reefs of South Florida, (abstract)*, Geological Society of America Abstracts with Programs, Vol. 27, No. 6, p. A-229, 1995.

232. U.S. Army Corps of Engineers, *Lineament Analysis South Florida Region: Aquifer Storage and Recovery Regional Study*, Draft Technical Memorandum, p. 59, 2004.

233. U.S. Geological Survey, *Historical Aerial Photography for the Greater Everglades of South Florida: The 1940, 1:40,000 Photoset,* Open-File Report 02-327, 2003. Available at http://sofia.usgs.gov/publications/ofr/02-327/htm/intro.htm, accessed November 25, 2008.

234. Vernon, R. and H. Puri, *Geologic Map of Florida*, Map Series 18, Florida Bureau of Geology, 1964.

235. Wheeler, R., Quaternary *Tectonic Faulting in the Eastern United States,* Engineering Geology, Vol. 82, pp. 165–186, 2006.

236. White, W., *The Geomorphology of the Florida Peninsula*, Geological Bulletin 51, Florida Bureau of Geology, Florida Department of Natural Resources, 1970.

237. Banks, K., B. Riegl, E. Shinn, W. Piller, and R. Dodge, *Geomorphology of the Southeast Florida Continental Reef Tract (Miami-Dade, Broward, and Palm Beach Counties, USA),* Coral Reefs, Vol. 26, pp. 617–633, 2007.

238. Kramer, P., F. Anselmetti, and R. Curry, *Geophysical Characterization of Pre-Holocene Limestone Bedrock Underlying the Biscayne National Park Reef Tract, Florida,* E. Kuniansky (ed.), USGS Karst Interest Group

Proceedings, Water-Resources Investigations Report 01-4011, pp. 128–133, 2001.

239. Kindinger, J., *Lake Belt Study Area: High Resolution Seismic Reflection Survey*, Miami-Dade County, Florida, U.S. Geological Survey, Open-File Report 02-325, 2002.

240. Scott, T. and T. Missimer, *The Surficial Geology of Lee County and the Caloosahatchee Basin*, Florida Geological Survey, Special Publication, Issue 49, pp. 17–20, 2001. PTN RAI 02.05.03-4 LDP-CS536

241. Masaferro, J., *Interplay of Tectonism and Carbonate Sedimentation in the Bahamas Foreland Basin*, (Ph.D dissertation), p.146, University of Miami 1997.

242. Kerr, A., M. Iturralde-Vinent, A. Saunders, T. Babbs, and J. Tarney, *A New Plate Tectonic Model for the Caribbean: Implications from a Geochemical Reconnaissance of Cuban Mesozoic Volcanic Rocks*, Geological Society of America Bulletin, Vol. 111, pp. 1581–1599, 1999.

243. Hall, C., S. Kesler, N. Russell, E. Pinero, R. Sanchez, M. Perez, J. Moreira, and M. Borges, *Age and Tectonic Setting of the Camaguey Volcanic-Intrusive Arc, Cuba: Late Cretaceous Extension and Uplift in the Western Greater Antilles*, Journal of Geology, Vol. 112, pp. 521–542, 2004.

244. Cotilla-Rodríguez, M., H. Franzke, and D. Cordoba-Barba, *Seismicity and Seismoactive Faults of Cuba*, Russian Geology and Geophysics, Vol. 48, pp. 505–522, 2007.

245. Tait, J., Y. Rojas-Agramonte, D. Garcia-Delgado, A. Kroner, and R. Perez-Aragon, *Paleomagnetism of the Central Cuban Cretaceous Arc Sequences and Geodynamic Implications*, Tectonophysics, Vol. 470, pp. 284–297, 2009.

246. Mullins, H. and H. Van Buren, *Walkers Cay Fault, Bahamas; Evidence for Cenozoic Faulting*, Geo-Marine Letters, Vol. 1, No. 3-4, pp. 225–231, 1981.

247. Pardo, G., *The Geology of Cuba*, Studies in Geology Series 58, American Association of Petroleum Geologists, 2009.

Figure 2.5.3-201 Potential Quaternary Features and Seismicity

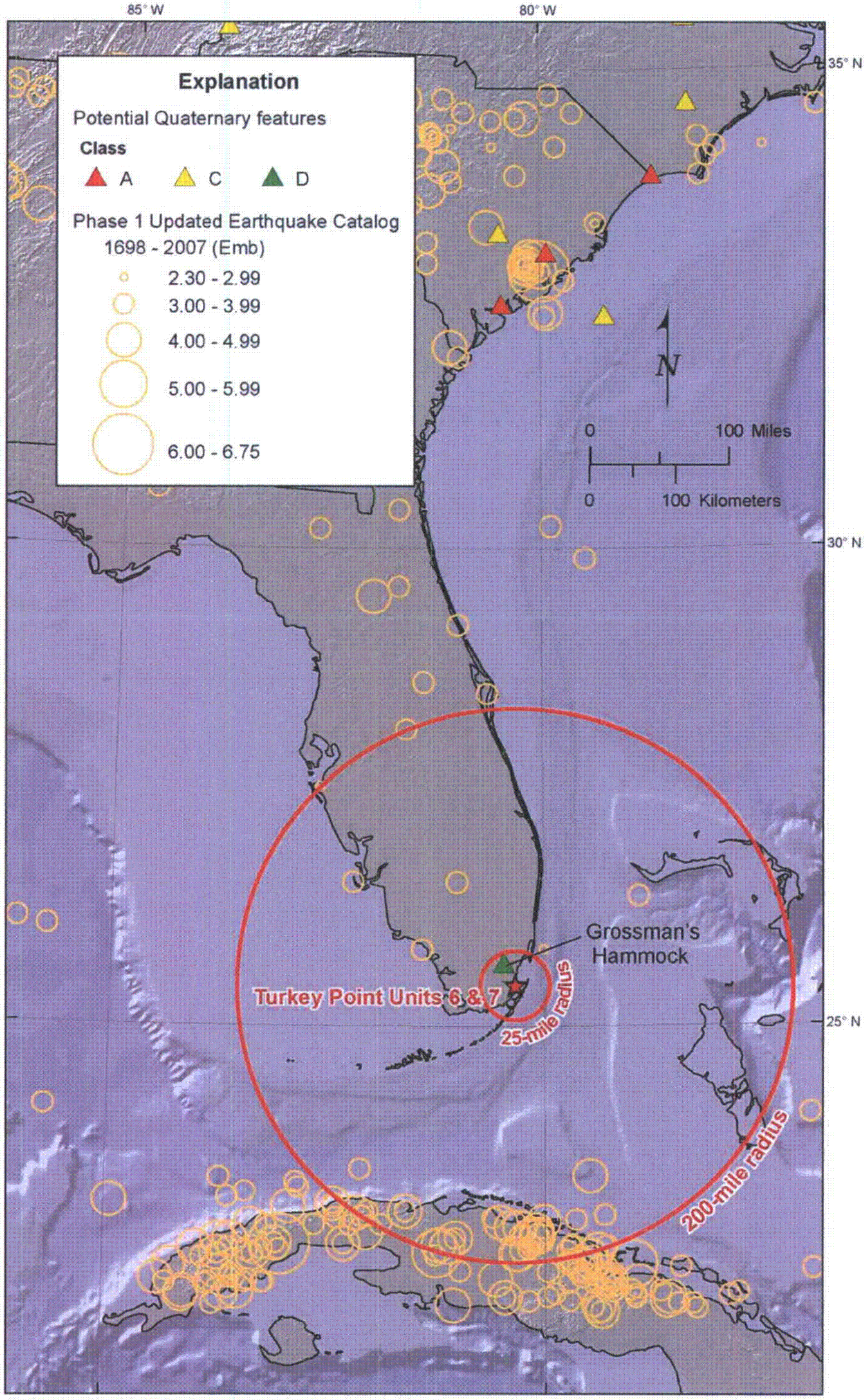

Base source: Reference 201
Source of Quaternary features: Reference 203

Figure 2.5.3-202 Vegetated Depressions Identified Within Site Area from Photographs Taken Before Construction of the Cooling Canals

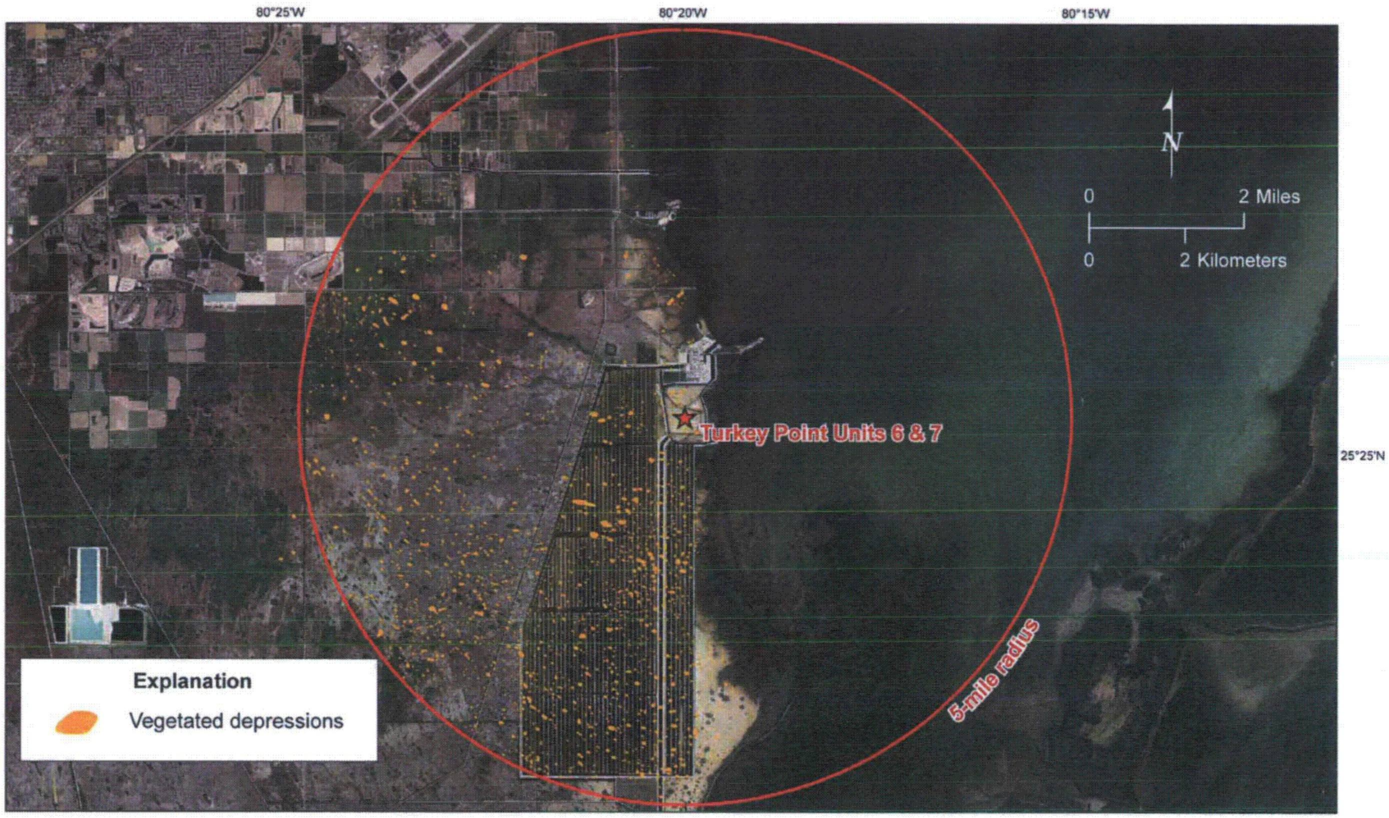

Note: Reconnaissance mapping performed using 1940s 1:40,000 scale panchromatic stereo aerial photography (Reference 233), but shown on 2004 imagery (Reference 207) of the Units 6 & 7 Site for reference.

Figure 2.5.3-203 Site Region Seismicity

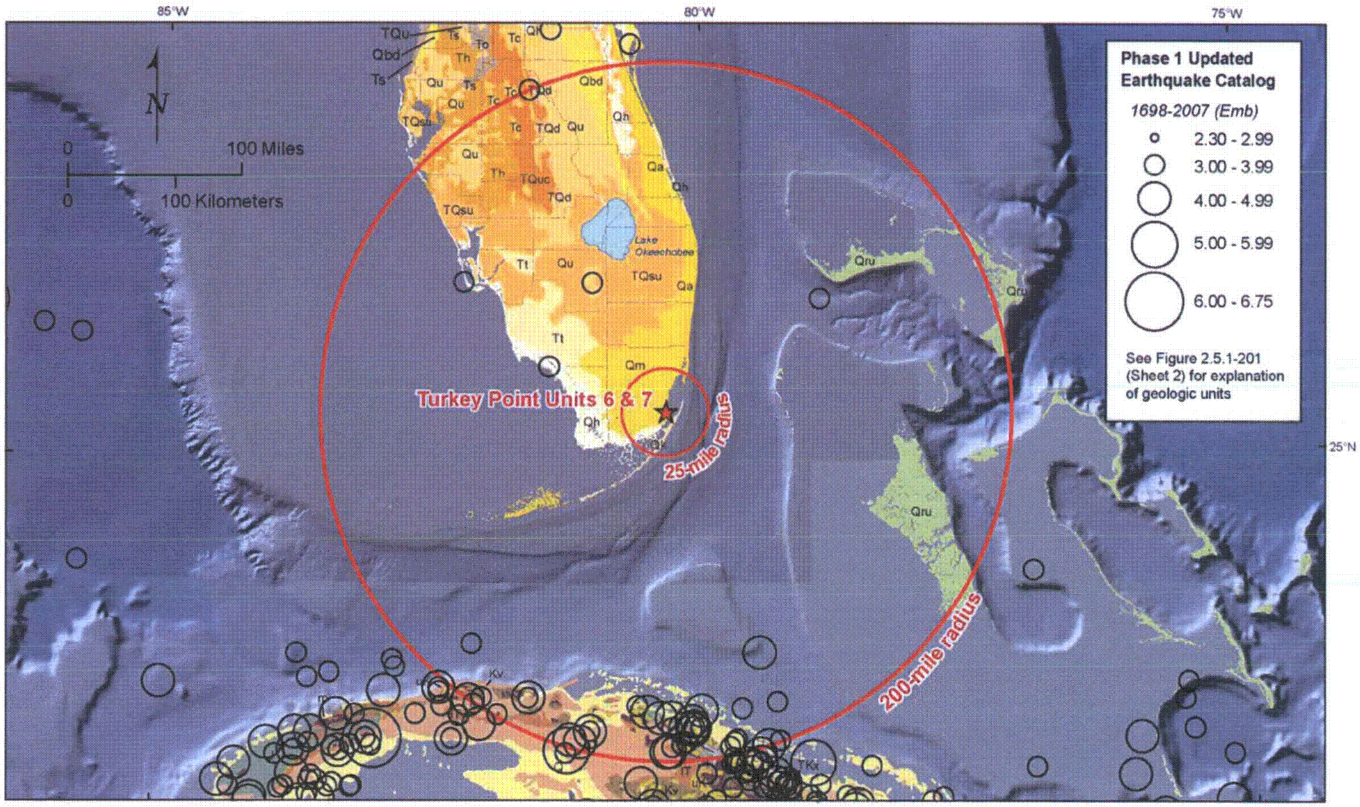

Base sources: References 201 and 220
Geologic information sources: References 210, 202, and 227

Figure 2.5.3-204 Lineament Analysis of South Florida for ASR Regional Study

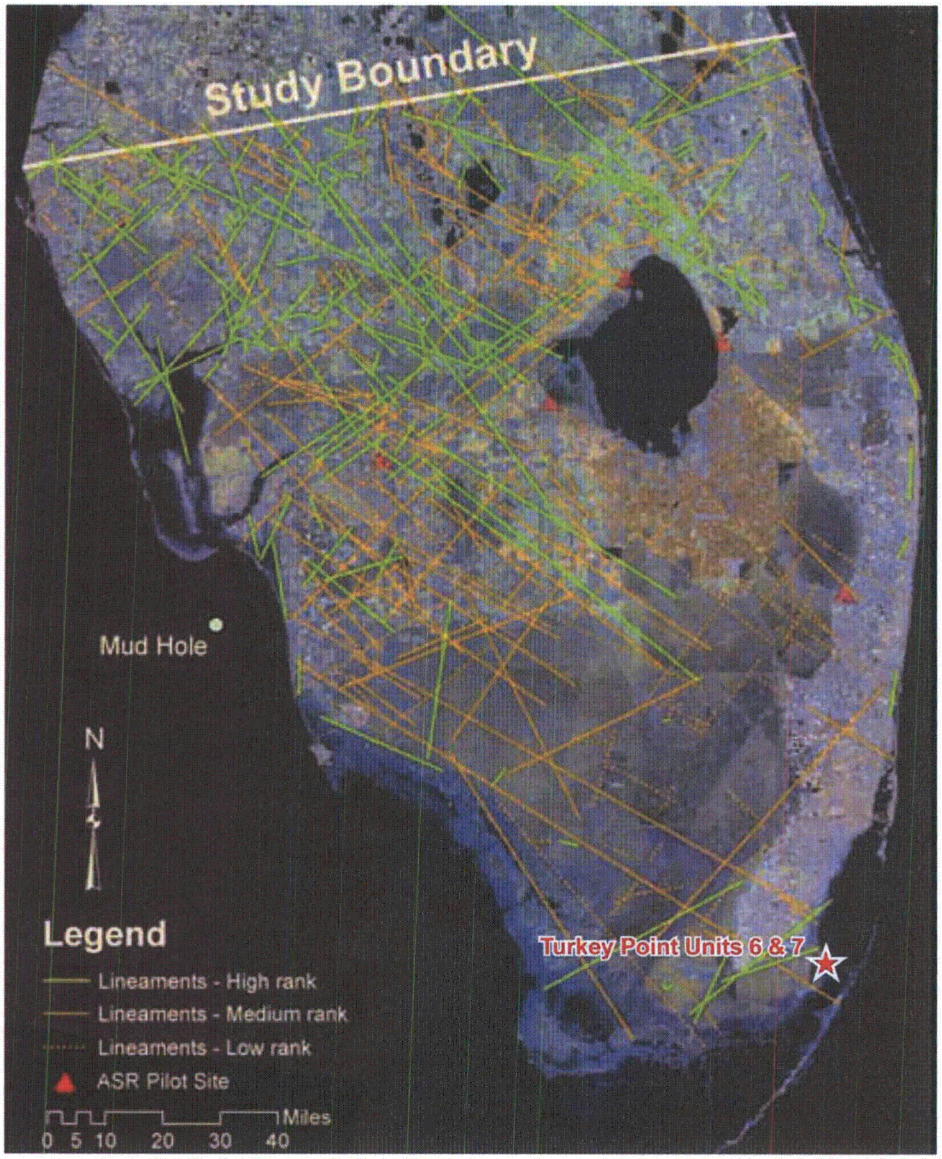

Source: Reference 232

Figure 2.5.3-205 Potential Quaternary Tectonic Structures within the Site Region

PTN RAI
02.05.03-2